A Knowledge-based Energy-saving Approach to PWM Control of a Novel Integrated Pneumatic Valve

by

Hanieh Aghighi

A thesis
presented to the University of Waterloo
in fulfillment of the
thesis requirement for the degree of
Master of Applied Science
in
Mechanical Engineering

Waterloo, Ontario, Canada, 2008

I hereby declare that I am the sole author of this thesis. This is a true copy of the thesis, including any required final revisions, as accepted by my examiners.

I understand that my thesis may be made electronically available to the public.

Abstract

As manufacturers, the automotive industry, and many other sectors face an increasingly competitive global business environment; they seek opportunities to reduce production costs by reducing energy consumption. Energy costs have become one of the fastest-rising expenses of doing business, and the industrial sector is rushing to implement new energy conservation initiatives. Pressurized air, as an important source of energy, has been widely used by various industries, providing simple solutions for automated lines.

In this project, an Accumulator-Based Equalization (ABE) strategy was combined with a knowledge-based PWM (Pulse Width Modulation) protocol, and then incorporated into an integrated solenoid valve to increase the energy efficiency of pneumatic systems through the optimization of flow consumption. Modeling and simulation of the proposed system was carried out to assess the proposed ideas and reduce the cost of system developments. An experimental setup was constructed to assess the performance of the proposed strategy when implemented on configured pneumatic control valves.

Equalization was performed at home positions of a typical linear actuator, where the chambers of the pneumatic actuators were momentarily connected to each other. Furthermore, during the extension and retraction, a knowledge-based PWM signal was applied to the valves to maintain the actuator dynamics in an acceptable posture. To obtain the knowledge-based PWM signal, an expert-fuzzy controller was designed to control the speed of the actuator.

This knowledge-based protocol was based on fuzzy structures, which were implemented on the configured pneumatic valves in an open-loop fashion to decrease the amount of flow consumption without compromising the dynamic performance of the pneumatic actuators. The identified duty cycles profiles from the expert fuzzy controller were implemented on an open-loop system. It was observed that, while an open-loop system is used, the pressurized air can be saved about 20% under 50 N load and almost 10% under 150 N load.

"Smoothness index" was defined as a measure of the piston motion smoothness when applying the proposed strategies. In addition to smoothness of the motion in the closed-loop control methods, the energy-saving results were compared to the results of the open-loop system and the performance under different conditions was evaluated.

Acknowledgements

I gratefully acknowledge the advice of Professor Ehsan Toyserkani, whose guidance shaped this research and whose supervision led this project. This research would not have been possible without the contributions of Ash Charles, whose ideas, hard work, encouragements and dedicated efforts were significant in this accomplishment. I also thank Mihaela Vlasea for her contribution in the valve design phase of this project.

I want to express my gratitude to Ernie Lynch, President and CEO of Lynch Companies, for his generous support in the advancement of pneumatics within the university.

It is a pleasure to convey my gratitude to Mr. Raj Soundararajan, the manager of the department of Instrumentation and Control (I&C) in SNC Lavalin Nuclear Inc., for all his kind support during the last year of my study. I also thank Professor William Melek for his support at the beginning of my study.

I would like to give special thanks to Dr. Sina Valadkhan, Dr. Siamak Arzanpour, Hamid Bolandhemmat, and Yusof Ganji for the abundantly helpful detailed discussions we had in the area of my research.

This thesis is the result of a two-year-long endeavor. While it has been a great adventure and a remarkable experience for me to work with industrial pneumatic tools, I had the companionship, help, and support of many people in this journey, which will be always kept in my mind as a pleasant memory. I wish to thank my friends Nasim Paryab, Azadeh Mohebbi, Atefeh Mashatan, Negar Rasti, Shahrzad Towfighian, Hajar Sharif, Mehrdad Iravani, and Seyed Hamidreza Alemohammad, for being there when I needed them.

I thank my family, my parents and my lovely sisters, Homa, Hiva, and Yasaman, whose constant love has always encouraged me to move forward. Words fail me to express my appreciation to my gifted partner Yusof Ganji, whose company, steadfast support, and inspiration in various ways, made my life worth living.

Dedication

This thesis is dedicated to

my parents

for their unconditional love and affection.

Contents

List of Tables

List of Figures

Chapter 1

Introduction

1.1 Pneumatic Systems

Pneumatic systems are one of the major types of actuation for industrial and automation purposes. The similar dynamic characteristics of pneumatic and electrical systems have been confirmed [1] and have made pneumatic systems popular to be utilized in many automation and manufacturing applications at reasonable costs.

Although pneumatic systems are popular in many applications, because of their simple construction, easy maintenance, low cost, cleanness, etc., several issues including low efficiency, friction, losses and time delays in cylinders, valves and transmission lines create complexities and nonlinearities in such systems. The mentioned drawbacks have created a strong motivation for researchers to improve the performance of pneumatic systems.

1.2 Energy-Saving Concept: The Motivation

Recently, many research programs have been performed on pneumatic systems and their control elements. Given the fact that compressed air is an available source in many manufacturing sectors, and can improve safety in hazardous environments,

these systems have a good potential to compete with most of their electric counterparts.

Nowadays, in the global economy, compressed air is not an inexpensive source of motive force. Pressurized air, as a safe and reliable sources of energy, has become the continual supply of pneumatic systems in process industries. The price of energy has increased dramatically over the last five years. This means that in today's industrial environment, energy should be used efficiently. From ecological and economical points of view, it is time to find methods to achieve less air consumption in operating pneumatic systems. Manufacturers, the automotive industry, and many other sectors also facing an increasingly competitive global business environment, seek opportunities to reduce production costs by reducing energy consumption.

Preventing the air leakage, using the exhaust air effectively, reducing the pressure of supplying sources, sizing the actuators carefully based on the load conditions, controlling the pressure drop (considering the serious impact of pressure losses on the efficiency of pneumatic equipment), and shortening the distance in distribution systems are some of the solutions which can be applied to pneumatic systems to achieve energy saving; therefore, all the techniques and methods related to the production of compressed air, air storage, distribution and control modules in pneumatic systems should be investigated carefully to find methodologies for acceptable energy consumption.

When pneumatic systems are evaluated in production equipment, any cost reduction is translated directly into profit and any contribution will have a positive impact on the global warming issue.

1.3 Objective

This thesis describes novel approaches to pulse width modulation control of an integrated pneumatic valve, to reduce the consumption of compressed air without compromising their normal performance.

To achieve these objectives, an integrated pneumatic valve is considered and different strategies are proposed and experimentally assessed by the integrated pneumatic valve. These strategies are: Accumulator-Based Equalization (ABE) Strategy, PWM Strategy, Expert Fuzzy Controller, and Error-Based Fuzzy Controller.

1.4 Looking Ahead

Background and literature survey will be presented In Chapter 2. In Chapter 3, PWM and and an accumulator-based system for saving energy will be discussed in detail. In order to assess the proposed ideas and reduce the cost of system developments, the model of the system was simulated in Simulink® and the results are provided in Chapter 4. Chapter 5 is about the development of the proposed methods on the test rig. In this Chapter the effect of the different parameters on saving energy will be evaluated. Furthermore, the smoothness of the movement will be determined by a defined criteria call "Smoothness Index". Finally, the conclusion will be provided in Chapter 6.

Chapter 2

Literature Review and Background

2.1 Introduction

This chapter presents the background information related to pneumatic systems. Different methodologies utilized to control pneumatic systems, and applied strategies in order to optimize energy consumption, will be presented as well.

2.2 Structure of a Basic Pneumatic System

The basic structure of a pneumatic control system is schematically shown in Figure 2.1. The load is rigidly connected to the piston and the valve is an on/off solenoid valve. The command input to the valve can be voltage or current. Changing the input command of the valve controls the air flow by charging one side or discharging the other side of the cylinder. The air pressure on the left side of the cylinder forces the piston to move to the right. If the air in the right side of the cylinder cannot be exhausted out of the system, the trapped air prevents the movement of the piston. In such a condition the cylinder is "jammed". As a result, the air on the right side

should be exhausted to the atmosphere; thus, controlling the rate of the exhaust air will result in controlling the velocity and position of the piston in the system. The pressure in both sides of the cylinder changes according to the movement of the piston and the load.

A position sensor is often used to get feedback from the motion of the cylinder. Two types of valves can be used in pneumatic applications: proportional or servo valves, and solenoid or on/off valves. Although servo valves have been the most popular valves for position control, solenoid valves have drawn the attention of the industry again because of their fast switching characteristics and their low cost. This type of valve will be covered in the subsequent sections.

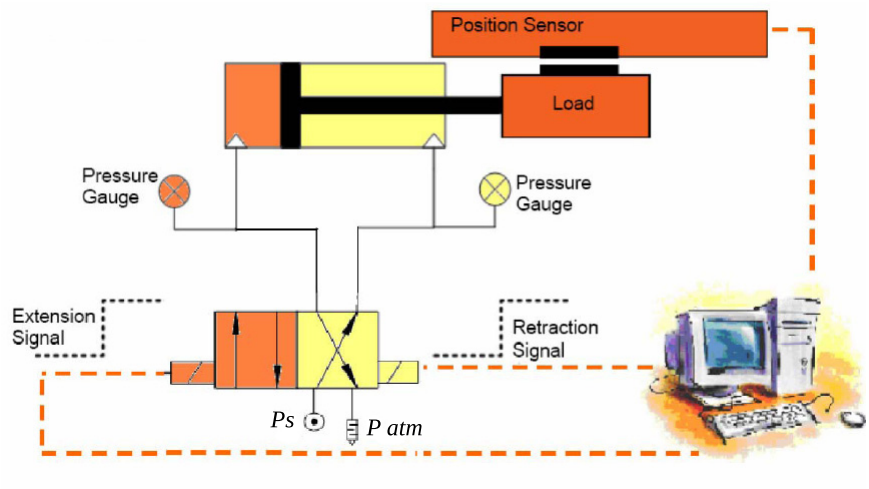

Figure 2.1: A typical pneumatic system.

2.3 Pneumatic Control Systems Review

Many efforts have been conducted in modeling and feedback control of pneumatic actuation systems by Shearer [2][3][4], in the 1950's. Shearer studied the dynamic behavior of air in the chambers of actuators and derived a mathematical model, including characteristics of airflow through the control valve. His model is still the basis of many pneumatic systems used in spacecraft and missile engine controls.

Mannetje [5] investigated the stability of a pneumatic control system based on a different control strategy from Shearer's, considering the effect of time delay, air compression, load and valve connections. Mannetje used a high gain differential pressure feedback as the command to a valve, and increased the closed loop bandwidth of the control system for a specific valve and cylinder size.

Liu and Bobrow [6] created a linearized mathematical model of a pneumatic servo system in the state-space domain. They extended the linearized model over a series of invariant operation points. However, no reference to the variable operating points could be found. Ben-Dov and Salcudean [7] used a linearized pneumatic actuator model, considering the dynamics of a flapper valve and air flow , in order to implement a force controlled actuator. They selected a glass cylinder with a graphite piston, in order to reduce the complexity caused by friction. The cylinder pressure was considered equal to supply pressure, when one side of the cylinder was pressurized, and equal to atmosphere when the other side was discharged. By applying a lead-lag compensator in conjunction with a low pass filter, they demonstrated that for stationary loads, the frequency response of 16 Hz at 2 N load is achievable by force control, using pressure feedback.

Bobrow and McDonell [8] extended the control algorithms of a pneumatic manipulator, to handle the nonlinear flow characteristics caused by the compressibility of air. They designed a nonlinear control law based on the stability of hierarchical systems and implemented it on a multiple-degree-of-freedom robot. Wang et al. [9] derived a model for pneumatic cylinder actuator systems, including a dynamic model of a pneumatic cylinder, dynamic relationship within the control chambers, and flow relationships between the control valves and load dynamics. Based on the model, they proposed a robust servo control strategy. However, this method required full-state feedback, which definitely increases the cost of the whole system.

Karpenko and Sepehri [10] developed and experimentally evaluated a practical nonlinear position controller for a typical industrial pneumatic actuator. They improved the relative stability of the closed loop system, by using a simple fixed-

gain PI controller, to minimize the effects of the nonlinearities in the system.

2.4 PID and Sliding Mode Controllers

As mentioned earlier, pneumatic systems have been widely used in different applications of automation industry, such as "pick and place" and pressing workpieces. The nonlinear characteristics of such systems associated with air compressibility, friction, etc., make them difficult to control and to use in accurate positioning applications. Therefore, researchers in this field focused on the development of various motion and force control strategies, utilizing mathematical process models and classical control methodologies, such as sliding mode and PID controllers.

Wang et al. [11] developed a PID controller with acceleration feedback, instead of pressure feedback, for a servo-controlled pneumatic actuator, which can compensate for nonlinearities due to air compressibility in the system. They showed that the improved PID controller increased the stability of the pneumatic actuator system. This strategy can be used in industrial applications because of its simple structure and lower cost compared to conventional control strategies due to the elimination of pressure feedback.

Guvenc [12] showed that a "discrete time model regulation" has the effect of sensitivity reduction in systems with significant uncertainties like pneumatic systems, although their results only cover a simulation study with no experimental validation. Hamdan and Gao [13] developed a modified PID (MPID) controller to control and to minimize the effect of hysteresis in pneumatic proportional valves. They added a nonlinear mechanism to their PID controller and improved the step response of the system.

Sliding mode controllers are generally well-suited for pneumatic servo actuators, with highly non-linear behavior and uncertainties [14], and many researchers have designed sliding mode controllers to overcome the uncertainties in their pneumatic systems. In 1994, Paul et al. [15] proved the applicability of sliding mode

control theory in pneumatics. They presented a nonlinear"reduced- order" technique without any pressure loop, achieving stability and robustness in the system. Although they did not consider the nonlinear behavior of compressed air in the cylinder chambers, the motion of the plant was observed to be smooth.

Richer and Hurmuzlu [16][17] provided an accurate model of a pneumatic actuator system controlled by a proportional control valve. For this purpose, they considered the friction in the piston seals, the difference in active areas of the piston due to the rod, inactive volume at the ends of the piston stroke, leakage between chambers, valve dynamics, flow nonlinearities through the valve orifice, time delay and flow amplitude attenuation in valve-cylinder connecting tubes. Then they developed a new force controller based on sliding mode control theory for proportional-valve pneumatic actuators using the detailed mathematical model developed. They also developed a reduced order controller which neglected the valve dynamics and the time delay effect in order to evaluate the advantages and disadvantages of the system.

Acarman and Hatipoglu [18] used the robustness implications of the sliding mode control theory, and the structural properties of pneumatically actuated systems, to design a nonlinear controller. They drove the output tracking error to zero, in a finite time.

2.5 Pressure Observers

Nowadays, pressure sensors are very expensive and a typical high-precision pressure sensor can be more costly than the actuator itself. In addition, the use of pressure sensors increases the cost, size, weight, energy consumption, and complexity of the overall system and reduces its reliability [19]. Thus, some researchers have attempted to eliminate the pressure sensors from pneumatic systems, in order to reduce their cost and their complexity.

Bigras and Khayati [20] devised a nonlinear pressure observer for a pneumatic

cylinder system. They considered a "non-negligible restriction" in the connection ports of the actuator. In their systems, the pressure inside the chamber was difficult to control because it could not be measured directly. The pressure could also not be calculated as a function of pressure provided by the sensor, which was connected before the connection port. Hence, their observer estimated the pressure in the chamber, using the measured pressure outside the cylinder. They used the Linear Matrix Inequality (LMI) approach to calculate the observer gains and to ensure the stability of the system. However, no further experimental values were shown to demonstrate the validity of the simulation results. In addition, the observer was based on the measurement of actual pressure outside the cylinder, hence pressure sensors could not be eliminated from the system.

Pandian et al. [19] presented two methods for observing pressure considering the fact that the cylinder dynamics and the pressures of both chambers are not observable completely and simultaneously . In the first method, a continuous gain observer proposed in which the pressure on one side of the cylinder was measured and the pressure on the other side was estimated. In the second method, a sliding-mode observer was proposed where a numerically estimated acceleration was used in order to observe both pressure values. However, the accuracy of their system was limited due to the existing friction in the cylinder and control valves.

Wu et al. [21] investigated the possibility of eliminating pressure sensors in a pneumatic servo actuator by a nonlinear state observer. A nonlinear observability analysis demonstrated that observation of pressure from the measurement of motion is not possible in a pneumatic servo system.

Gulati and Barth [14] developed two Lyapunov-based pressure observers for a pneumatic servo actuator system. In "energy-based Lyapunov observer" design, a Lyapunov function was chosen based on the energy of the system and in "force-error based Lyapunov observer" design, the function was based on the error between actual and estimated pressures of the cylinder. In the latter method, the output error was used to control the convergence of the observed pressures. Their results

showed uncertainties in the observed values of the pressure. The authors continued their work [22] by design and implementation of a robust observer-based controller. They applied sliding mode control theory to the controller design.

2.6 Pulse Width Modulation (PWM) Control Systems with On/Off Pneumatic Valves

The preceding control methodologies were based on the control of proportional valves. The high cost of proportional valves has been a motivation for many researchers to use inexpensive on/off valves. Utilizing these types of valves in conjunction with Pulse Width Modulation (PWM) method has provided lower cost and to some extent, the same quality in terms of the system performance.

In the PWM controlled systems, the power delivered to the valve is completely on, or completely off. If the system is connected to the source in specific time intervals, the system response will be very similar to the continuous case and an average mass flow rate, related to the average input signal value, goes into or out of a cylinder. A considerable volume of research work has been devoted to the development of PWM-based pneumatic controllers.

One of the first attempts in the development of a PWM-based control technique in pneumatic systems, returns back to 1986 by Noritsugu [23][24], who constructed a PWM-mode, electro-pneumatic servo mechanism utilizing automobile-type fuel injection valves. The PWM signal was generated by a proportional controller, which acted based on the speed or position tracking error.

Kunt and Singh [25] applied a control theory method on the Linear Time Varying (LTV) model. Their goal was to predict the dynamic behavior of an open-loop pneumatic actuator controlled by solenoid valves. Ye et al. [26] presented two models for the pneumatic PWM solenoid valves. They considered valves as solenoid devices with opening and closing delays and compared the static characteristics and

the dynamic behavior of the system experimentally. The accuracy of their models was demonstrated with simulation results.

Shih and Hwang [27] designed a fuzzy PWM controller for the position control of a pneumatic cylinder of a robot. They proposed "modified differential PWM" or DPWM method and combined it with the fuzzy control concept to improve the performance of their system.

The above-mentioned works, utilized specific heuristic methods, and they did not establish the performance or stability of their methodology analytically. Some other researchers provided linear control methods to control PWM-based pneumatic systems.

Van Varseveld et al. [28] implemented a PID controller with position feedback and friction compensation to control a PWM-based pneumatic system. The performance and robustness were indicated in experiments. One of the PWM schemes suggested by Varseveld et al [28] was later used by Gentile et al. [29], who were able to tune the controller by using a heuristic method. They performed some experimental tests on position control of a PWM-based pneumatic actuator and developed two different PWM algorithms. All the control algorithms were coded in LabView® software.

Ahn et al. [30] developed a switching algorithm using Learning Vector Quantization Neural Network (LVQNN) approach to estimate the external loads of a pneumatic actuator and to perform position control. The method was based on "Modified PWM (MPWM)" and "gain selecting" technique. In their strategy, the amount of the external load was recognized and suitable gains for each load situation were selected. Eight two-way on/off solenoid valves were used in their experiments. They found the best performance for the designed neural network system, when the number of inputs were 30, and when the number of the hidden layers were 40.

Messina et al. [31] proposed the mathematical model for a PWM-based pneumatic system. The model was developed and tested for position control of their system, including two 3/2 solenoid valves. They also validated their model analyt-

ically and experimentally in different applications. Although their model was able to provide the accuracy of less than 2 mm, this accuracy was not repeatable for more than five cycles.

Barth et al. [32] utilized a state-space averaging approach to provide an analytic method for a PWM-based pneumatic system. Applying this approach, they were able to remove the discontinuities associated with switching and to transform it into a continuous model . They designed a sliding mode controller, where the actuator was able to track sinusoidal inputs at maximum frequency of 1.25 Hz. One year later, they [33] presented "loop-shaping" method and proposed a control methodology which transformed a discontinuous switching model into an equivalent linear continuous model. Although they demonstrated an equivalent linear model, prescribed degree of stability robustness, and good tracking performance, a nonlinear control approach was more effective because of the nonlinear nature of compressed air.

Shen et al. [34] [35] extended Barth's averaging techniques to nonlinear systems and presented a method for nonlinear model-based PWM control of a pneumatic servo actuator. The controller was implemented on a single degree-of-freedom pneumatic servo system and the effectiveness of the method was verified by experimental trajectory tracking data. The control valves were two 3-way solenoid valves operating at a PWM frequency of 25 Hz. Because of the limited switching response time and the dynamic limitations of the valves, the closed-loop system bandwidth was reduced to approximately an order of magnitude below the PWM switching frequency and could not track frequencies greater than 2 Hz.

Topcu et al. [36] investigated a simple and fast switching pneumatic PWM-controlled valve for position-control applications. Using their method, the opening time of the valve was as fast as 3 ms, and the closing time of the valve was 6 ms under 7.105 N/m^2 of supply pressure and their PWM-controlled valve provided a linearity up to 33 Hz. Although they claimed that their valve, as a single stage valve with simple construction, achieved higher flow rates than conventional servo

valves, they did not provide a clear numerical comparison.

2.7 Fuzzy Controllers in Pneumatic Systems

One of the most important issues that researchers faced in the control of pneumatic systems has been the use of complex mathematical models of these systems in addition to the uncertainties and nonlinearities involved in different parameters. The nonlinearities can come from supply pressure, chamber pressure, rod position, velocity, and even the particular kind of valves used in a system [37].

The quality of the manufacturing process of a cylinder, the sealing mechanism such as band sealing or split sealing, friction, load force, and temperature are among the parameters that induce nonlinearities in a pneumatic system [38].

Fuzzy logic controllers have the advantage that they do not require precise modeling of the system, hence uncertainties which can happen during the operation cannot affect the performance of the controller directly. Specifically, when the relationship between the inputs and outputs, like duty cycle for switching valves, is defined carefully and if the obtained behavior of the system under different conditions is investigated precisely, fuzzy logic controllers can provide an acceptably high performance. Unlike sliding mode controllers, which can perform successfully only if the system is correctly modeled, these controllers have robust capabilities while they can accept a lower level of information related to the system model or system identification [39][40][41].

In 1993, Sano et al. [39] and Raparelli et al. [42] presented different tuning methods of fuzzy controllers in pneumatic servo systems. Investigation on position control of pneumatic systems by fuzzy controllers was provided by Scavarda [40] and by Matsui [41]. Shih and Wang [27] developed a position controller for a pneumatic robot cylinder using PWM-driven digital valves, and fuzzy control. Parnichkun and Ngaecharoenkul [43] showed that by utilizing a hybrid fuzzy-PID control strategy, reasonable accuracy is achievable in a specific pneumatic system with PWM-driven

valves.

Situm et al. [44] proposed a precise position control of a pneumatic system. In their controller structure, a conventional controller performed the direct control of the process. For adjustment of the conventional controller parameters, a correction signal obtained from the fuzzy logic inference procedure was used. The conventional controller was a PID controller tuned to achieve optimum damping. Applying a friction compensation and stabilization algorithm, they could achieve a precise position control with accuracy of 1 mm.

Chillari et al. [45] presented an experimental comparison between six different control algorithms to control the position of pneumatic actuators. The methods considered were PID, fuzzy-logic, PID with pressure feedback, fuzzy with pressure feedback, sliding mode, and neuro-fuzzy control. They used PWM signals to control four solenoid valves in their model and concluded that fuzzy control, with the adoption of pressure feedback, was the best controller tested for most of the reference signals.

2.8 Energy-saving Systems

Currently global warming has become one of the most important issues in the world. In 1997, an anti-global warming conference was held in Kyoto. United Nations Environment Programme stated that "Japan and 160 other countries reached agreement on a legally binding protocol under which industrialized countries would reduce their collective emissions of greenhouse gases by 5.2%" [46].

"On December 17, 2002, Canada ratified the treaty that came into force in February 2005, requiring it to reduce emissions to 6% below 1990 levels during the 2008-2012 commitment period." [47] Therefore, energy saving has become an important issue, specially in the industry. In addition, in a competitive global market, the production cost should be decreased and energy cost associated with a product should be reduced to satisfy this goal.

Farmington in the 59th issue of Hydraulics and Pneumatics magazine (August 2006) [48] said that "According to different estimates provided by the U.S. Department of Energy, the automotive industry, and pneumatic equipment distributors, the cost of air ranges from \$0.16 to \$0.30 per 1000 ft^3. Buying electricity accounts for 76% of the cost. Equipment and maintenance are also factors in increasing the cost of air, as illustrated in Figure 2.2. Therefore, the generation of compressed air requires a huge amount of energy and cost."

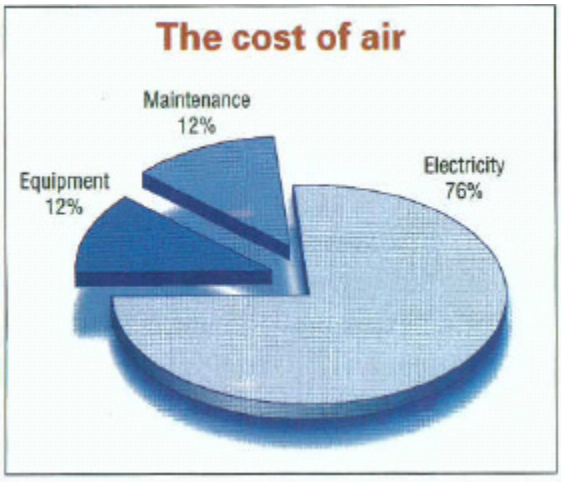

Figure 2.2: Breakdown of the cost of pressurized air, courtesy of H.W. Wilson Company.

According to an article published in Machine Design magazine in February 2006 [49], "Cylinders running 5 days per week and 50 weeks per year will operate 120,000 minutes per year. In the above application, that equates to 32.65 scfm [1] × 120,000 min = 3,918,000 scf [2] of compressed air consumed by this single cylinder annually. If the average cost of compressed air is \$0.25/1000 scf, operating the 4-inch-bore cylinder costs \$979.50 per year. For the 5-inch-bore cylinder, that figure jumps to \$1,549.22 per year." With an assumption of just 15% saving, the annual air consumption of one single 4-inch-bore cylinder will be reduced to 3,330,030 scf which equals to \$147 saving per year. This value would be \$232.5 saving per year

[1] Standard Cubic Feet per Minute

[2] Standard Cubic Feet

for a single 5-inch-bore cylinder.

Since pneumatic cylinders are often used in applications such as "pick and place" or compression of workpieces, the diameter of the cylinder has a direct relationship with the payload. Given the fact that the cylinder size has a direct effect on the air volume consumption [50], careful sizing of actuators based on the load conditions can be one of the solutions toward energy saving. Elimination of air leakage, effective use of exhaust air, pressure reduction in pressure sources, and the application of shorter connection tubes in the distribution systems are other approaches to save energy in pneumatic systems. Recapturing the pressurized air, which is discharged to the atmosphere in each cycle of operation, is another solution to reduce air consumption in these systems.

The research on the effective usage of pressurized air has led to a moderate volume of published work. The idea of using a reservoir has been proposed by some researchers like Sanville [51], Pu et al. [52] and Li et al. [50].

In Sanville [51] model, exhaust air is collected in a secondary reservoir serving as an auxiliary power supply. He estimated that his method will increase overall efficiency by a factor of two compared with the equivalent conventional systems. However, experimental results and the amount of reduction of compressed air consumption were missing in his analysis.

In Pu et al. [52] configuration, a cross flow path between the chambers of a double-acting cylinder helped to reuse the low-pressure compressed air. Using this structure, the captured air could pressurize faster and the system bandwidth was improved. They added a PID controller to their system and presented the simulation and experimental results, although air saving rate was not provided in their results.

Li et al. [50] utilized an air charge accumulator to absorb the exhausted air and a boost valve to increase the pressure air reuse. They showed that approximately 40% of compressed air can be saved by the direct use of cylinder exhaust air; however, the forward and the backward velocity in the system was about 17% lower because

of the back pressure. Figure 2.3 shows the structure of their system.

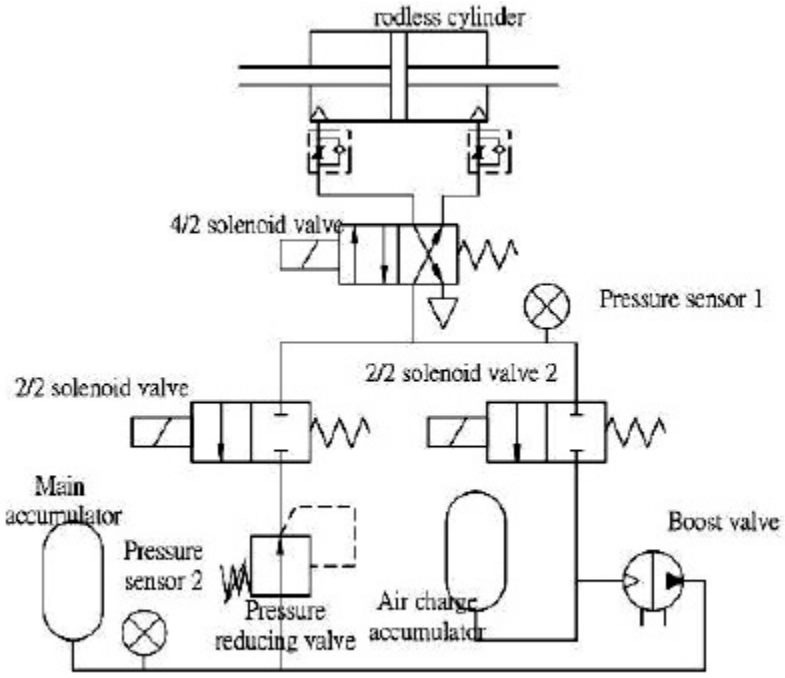

Figure 2.3: Structure of Li's energy-saving system, ©2006 Journal of Physics.

Some researchers have achieved energy saving in their control strategies. Granosik and Borenstein [53] introduced a control method for pneumatic actuators, called "Proportional Position and Stiffness (PPS)" controller. In their four-valve arrangement, when the cylinder reached the reference position with the desired accuracy, both chambers are closed to stop airflow and thus air consumption. The controller was time dependent and was based on considering nonlinear characteristic of airflow, the dynamics of the cylinder, and exact times and sequences of solenoid valves. Through this PWM-based control strategy, the air consumption was reduced to 0.11 litres per cycle. Figure 2.4 shows the structure of their system. Wang et al. [54] analyzed the effect of different velocity profiles on a pneumatic system. Comparison of three different profiles and the simulation results showed that the efficiency of the system can be improved by considering a proper profile of velocity. Kawakami et al. [55] presented a meter-in and meter-out circuit to reduce

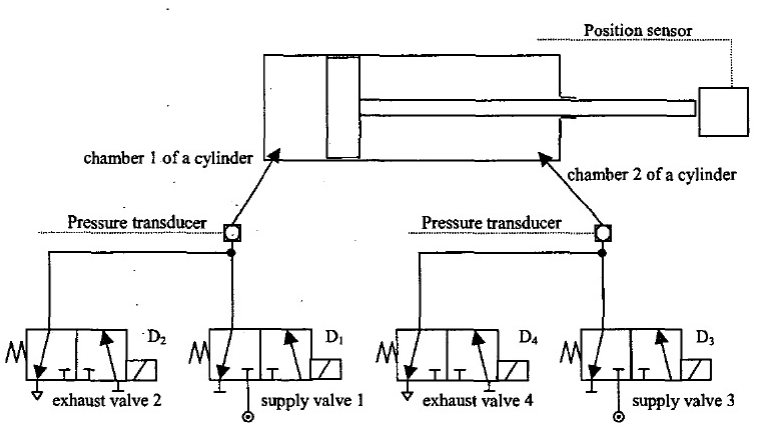

Figure 2.4: Pneumatic circuit of Granosik's energy-saving system, ©2004 IEEE.

the air consumption. Terashima et al. [56] combined the metering circuits with another strategy to save more energy. In their strategy, the supply pressure was disconnected when the piston was at the end of the stroke.

According to Margolis's work [57], although servo valves produce the needed pressure for the actuator to move to the desired position in the pneumatic system, they dissipate a considerable amount of pressurized air across their flow ports. In his design, a servo valve was switched at high frequencies between two extreme flow area positions. The source of pressure was an accumulator, which sent and received flow, as dictated by the control action. Margolis chose the flow area so that low resistive loss occurred. Pressurized air was recovered in the accumulator whenever the load was decelerated. Although he added a position and force controller to the system and presented an acceptable system response, the rate of air saving was not clear. In addition, they did not mention anything about the motion of the piston, which might not be smooth because of the switching nature of the system. Figure 2.5 depicts the structure of the actuator design with an accumulator. Margolis patented his work in 1996 [58]. Al-Dakkan et al. [59] [60] proposed an energy-saving approach to control a pneumatic servo systems. They decoupled the standard four-way spool valve used for pneumatic servo control into two three-way valves. Utilizing a sliding mode control approach, they controlled

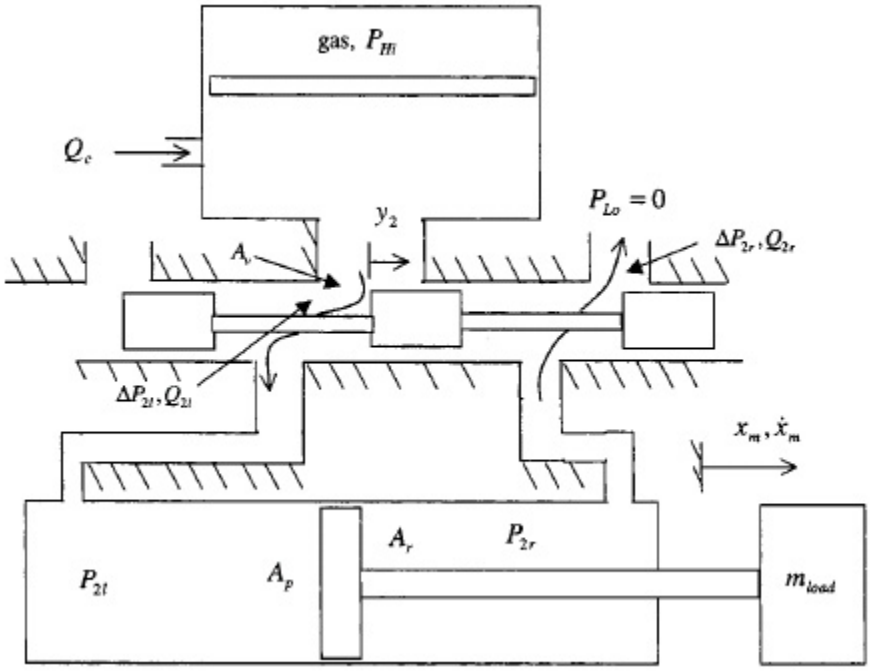

Figure 2.5: Schematic of Margolis's energy storage position control actuator, ©2005 ASME.

a two-degree-of-freedom pneumatic system to minimize the air consumption and get a high tracking performance. The presented experimental results indicate a savings rate of 10 to 46% (depending on the desired tracking frequency), relative to standard 4-way spool valve pneumatic servo actuator control. Figure 2.6 shows the structure of their system. In 2007, Shen et al. [61] proposed a structure and control approach for the energy-saving servo control of a pneumatic servo system. In their structure, a standard four-way spool valve controlled a pneumatic actuator. An additional two-way valve, called the cross flow valve, enabled the flow between the cylinder chambers, recirculation of pressurized air, and thus saved a part of the flow that otherwise would be exhausted to the atmosphere. Sliding mode theory was their control approach. Their experimental results indicated a savings rate of 25 to 52% compared to a standard four-way valve configuration. Figure 2.7 presents their structure. Due to the switching nature of the sliding mode method, the motion of the cylinder might not be completely smooth, but they did not mention anything

about the movement of the cylinder.

As stated before, although some researchers have proposed various methods, such as using a secondary reservoir or an accumulator, incorporating multiple cylinder chambers, connecting the two chambers of a double-acting cylinder by a direct flow path, and using point-to-point motion control, saving energy in pneumatic

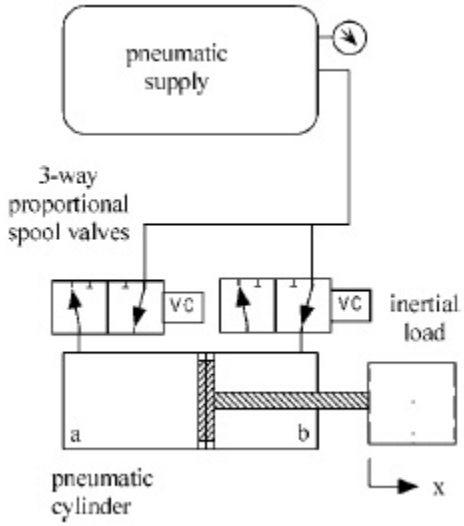

Figure 2.6: Structure of Al-Dakkan's energy-saving approach to control of pneumatic servo systems, ©2003 IEEE.

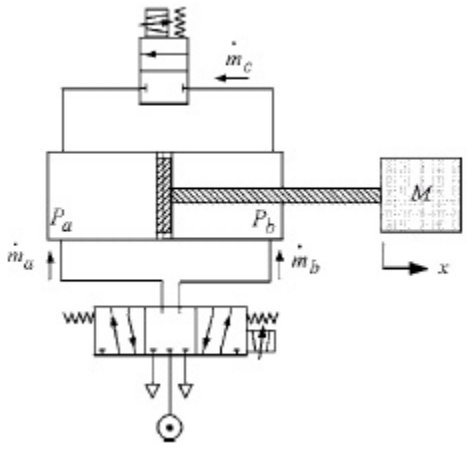

Figure 2.7: Structure of Shen's energy-saving system, ©2007 ASME.

systems still poses a challenge in achieving a commercial and simple solution.

2.9 Summary

In this chapter several control methodologies applied to pneumatic systems were reviewed. It is noted that the cylinder motion smoothness is not reported in the literature related to fuzzy based, PWM-based, and energy-saving controllers. In general, a system with motion performance close to that of conventional pneumatic systems, that can achieve a reasonable air saving rate using a knowledge-based PWM method, has not been reported in the literature.

Chapter 3

PWM and Accumulator-based Approaches to Energy-Saving

The importance of saving energy in pneumatic systems was outlined in the previous chapter. In this chapter, the possible strategies which can be utilized in order to achieve saving energy, will be discussed.

3.1 Pneumatic Systems' Efficiency Issue

From an economic point of view, a pneumatic system is about 50% cheaper than its electronic counterpart with the same performance, and is about 25% to 35% cheaper than a hydraulic system with equal capabilities. However, in comparison with electric and hydraulic systems, pneumatics are not very efficient. The efficiency of electric servo systems is 70% to 90% and hydraulic systems have the overall efficiency of 60% compared with less than 30% efficiency of pneumatic systems [62].

In traditional pneumatic systems, the pressurized air is exhausted to the atmosphere after passing through the valves and the actuator. The efficiency of the pneumatic systems can be improved by finding ways to recapture the exhausted air

and reuse it. In addition, instead of using continuous supply of pressurized air, the source of air can be disconnected at times. This chapter proposes some methods and strategies to save pressurized air in pneumatic systems, without compromising the overall performance of the system.

3.2 Proposed Strategies

The main objective in this research is to reduce the consumption of compressed air as a source of energy and decrease the operational cost. To achieve these goals, several methods are proposed, evaluated and developed on a pneumatic system. In the proposed techniques, two major strategies were combined together to achieve the ultimate goal:

- Accumulator-Based Equalization (ABE) method
- Pulse Width Modulation (PWM) method.

Each of these techniques will be explained in the following sections. The results of applying the proposed methods to the developed test rig are provided in Chapter 5. Also, a fuzzy-expert system is developed to prevent the pneumatic actuators from non-uniform (jerky) motion. The duty cycle patterns obtained from the developed fuzzy-expert system, are then used in an open-loop fashion.

3.2.1 Accumulator-Based Equalization (ABE) Strategy

When the source of pressurized air is connected to the system, the air passes through the main valve and flows into the chamber of the cylinder. In the extending state, a considerable volume of air should travel to the chamber in order to increase the pressure of chamber and to apply enough force to overcome the existing static friction. Therefore, pneumatic systems do not have quick response and are usually activated with time delay. The main cause of this phenomenon is compressibility

of the air which is one of the major factors considered in most of pneumatic control applications.

Traditionally, the exhausted air in pneumatic systems is discharged to the atmosphere. The air that is left in the chamber of the cylinder at the fully extended and fully retracted positions is still pressurized, and can be used again to increase the velocity of the cylinder at the beginning of each motion.

"Equalization" is a method that not only accelerates the initial response of the pneumatic systems, but also provides the ability of saving energy in such a system. In this method, two sides of the cylinder are connected at the end positions through a "regenerative line". Therefore, an effective pressure can be obtained by regularly equalizing the pressure in the two chambers of the cylinder before starting extension or retraction. In this case, after the equalization, the chamber has the equalized pressure, rather than atmosphere pressure. Consequently, both the time delay to start the motion of the piston and the volume of air needed to pressurize the chamber, decrease. Figure 3.2 depicts the Equalization method in a typical pneumatic system.

Although the use of an accumulator or a reservoir has been presented by some researchers, their applications to the pneumatic systems are different. As stated in Section 2.8, in most cases the exhausted air was discharged to an accumulator to be pressurized again.

In the proposed strategy, the accumulator is also charged during the equalization step. As a result, the air pressure inside the accumulator is the same as the equalized pressure in both chambers after the equalization; however, the overall equalization pressure drops. The pressurized air inside the accumulator can be used during the extension to compensate for the required pressure.

3.2.2 On/Off Solenoid Valves and Pulse Width Modulation (PWM) Strategy

In the fluid power industry, valves come in various forms and designs. In terms of classification, they are divided into two categories: continuous or proportional (servo) valves and on/off (solenoid) valves. In the proportional category, the effective area of the valve is controlled continuously while in on/off solenoid valves, there are only two states for the valve: "On" or "Off". In mechanical systems, switching devices come in the form of solenoid valves.

Conventionally, the solenoid valves are used to change the direction of the flow in fluid power systems. As technology progressed, solenoid valves became faster and more suitable for many applications in the industry. Therefore, they can be used instead of proportional valves in servo purposes with advantages including lower cost and simpler, more compact structure compared to proportional valves.

One of the most common methods to control on/off solenoid valves is Pulse Width Modulation or PWM method. In this method, the power supplied to the system is switched "on" and "off" very rapidly; therefore, the full DC supply voltage alters between fully "on" (e.g. 24, 12 or 5V) and fully "off" (zero), giving the system a square-wave signal. During the "on" period, DC supply is applied to the load, and in the "off" period, the supply is switched off. If the width of the pulse changes, the time fraction in which the power is on, changes. As a result, the average power to the system varies depending on the width of the pulses. In other words, PWM can be used to encode a specific level of an analog signal utilizing a pulse train.

Figure 3.1 shows three different PWM signals. As shown in the figure, each PWM signal simulates an analog signal value. For example, if the supply is 24V and the duty cycle is 10%, the resulting output will be 2.4V.

Typically, pneumatic actuators are used to move the load only during extension. Therefore, in both model and experimental tests, the focus was only on the air consumption reduction during the extension.

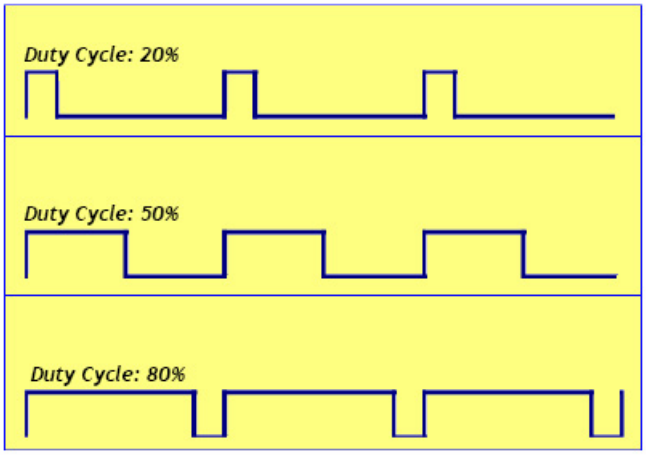

Figure 3.1: PWM with different duty cycle values.

During the extension of the cylinder, the input air to the system is switched between the air coming from the source and the air from the accumulator using PWM method. In higher duty cycle, the source is connected to the system for a longer time, which increases the air consumption.

Under different load values, an effective duty cycle should change. Therefore, with higher payloads, higher duty cycles are needed to move the piston. In conclusion, in this method, instead of having a continuous connection of the source to the system, only the air volume needed to move the load, would be sent to the system and a percentage of the pressurized air is saved. Figure 3.2 illustrates that the volume of pressurized air that goes into the accumulator and increases its inside pressure right after the equalization and before the extension. While extending, the source of the pressurized air is switched between accumulator and the main source utilizing the time-based PWM method. As it has been shown, when the pulse is "on", "A" in the diagram, the power comes from the main source and when the pulse is "off", "B" in the diagram, the air comes from the accumulator. More details have been provided in Section 5.3.1.

In this project, PWM in conjunction with ABE method should be applied to the test rig in a controlled fashion; that is why expert-fuzzy controller will be

considered as a strong tool. The duty cycle patterns obtained from the controller will be applied to the open-loop experimental set-up; then the amount of reduction in air consumption and also the performance of the system will be investigated in the following chapters.

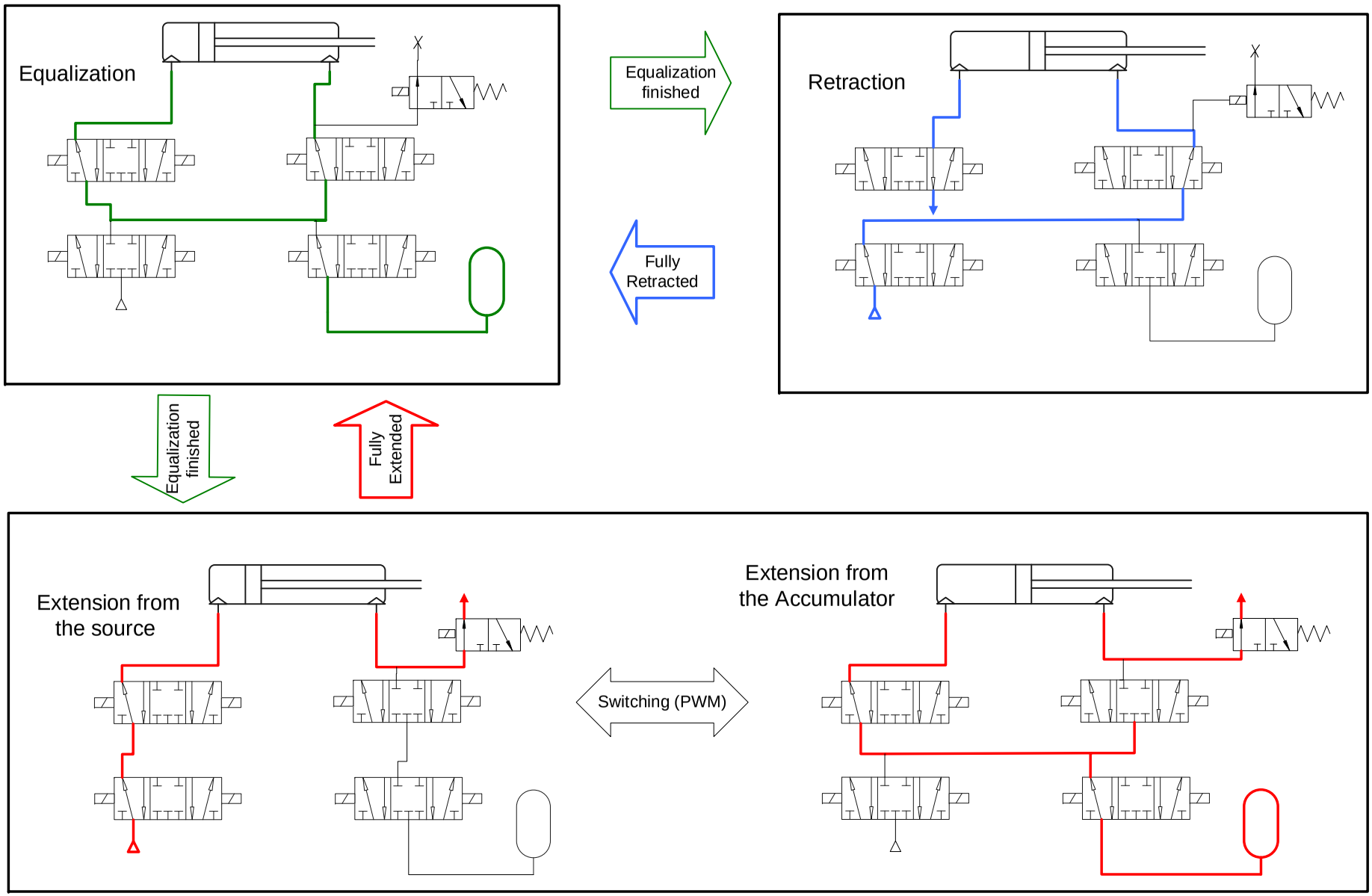

Figure 3.2: PWM and ABE Strategy.

3.2.3 Fuzzy Control Systems

Fuzzy control systems provide the opportunity to apply our knowledge to control a process successfully. A block diagram of a fuzzy control system is shown in Figure 3.3. The main components of fuzzy control systems are "rule base", "interface engine", "fuzzification interface", and "defuzzification interface". The "rule base" component contains the knowledge in the form of a set of rules while "interface engine" picks the best rule, which can be applied to the system given the inputs. In "fuzzification" module, the inputs are converted so that the "interface engine" can interpret them and apply the best rules to the system. "Defuzzification" module converts the final conclusion of the "interface engine" to the actual inputs of the process [63].

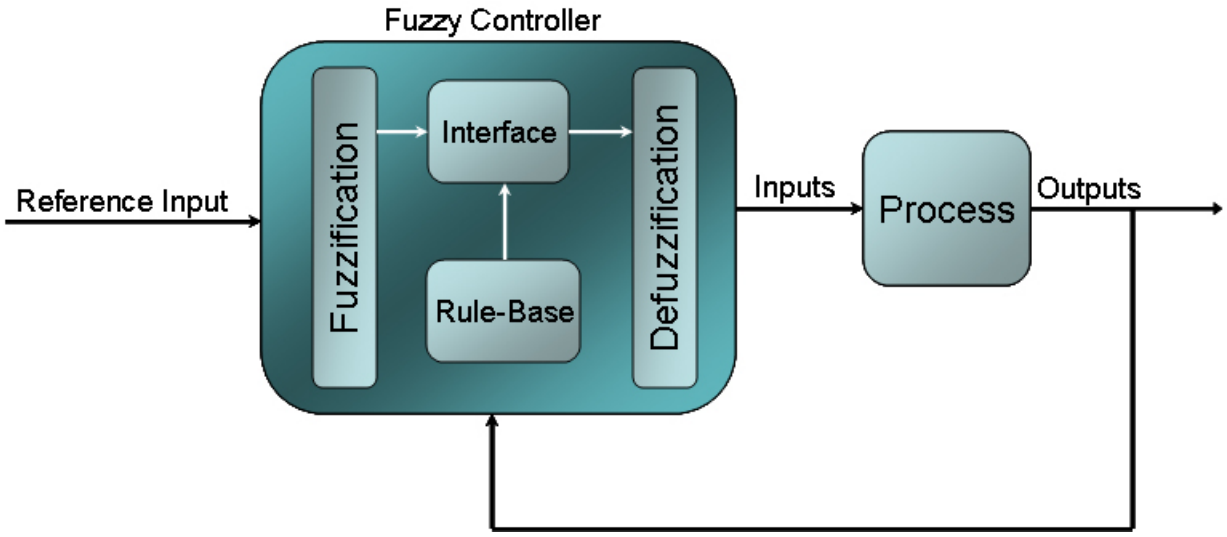

Figure 3.3: Block diagram of a fuzzy controller.

Because of the nonlinear nature of pneumatic systems, which will be discussed in Section 4.2, development of any model-based strategy is difficult and dependent on many different parameters. Therefore, as explained in Section 2.7, fuzzy controllers are good options to tackle the problems involved in these systems. In this research, two methods are recommended in order to apply fuzzy controllers on the developed pneumatic system: a fuzzy-expert system and an error-based fuzzy controller which

are explained below.

Fuzzy-Expert System for Energy-saving

Fuzzy-expert systems are useful tools to apply heuristic knowledge to control systems with nonlinear characteristics. Based on the nonlinear behavior that was observed by performing various tests on the system, an expert fuzzy system was designed and implemented in order to control the velocity of the system, by changing the duty cycle value. Since any change in duty cycle value has a direct impact on the air consumption, saving energy is possible by decreasing the duty cycle value while the performance of the system is kept reasonably consistent. It will be shown in the next sections that the piston does not need a constant duty cycle while traveling the stroke length. In addition, lower duty cycle at the end positions results in reduction of the air consumption. In the proposed fuzzy-expert system, as the Figure 3.4 shows, optimum velocity and position of the piston are the inputs and the duty cycle is the output. In the experimental set-up, an expert system will determine the best applicable duty cycle to the system based on the velocity and the position of the piston in a real time fashion. It is intended to identify optimum duty cycle values generated by the expert system and to apply them to an open-loop system.

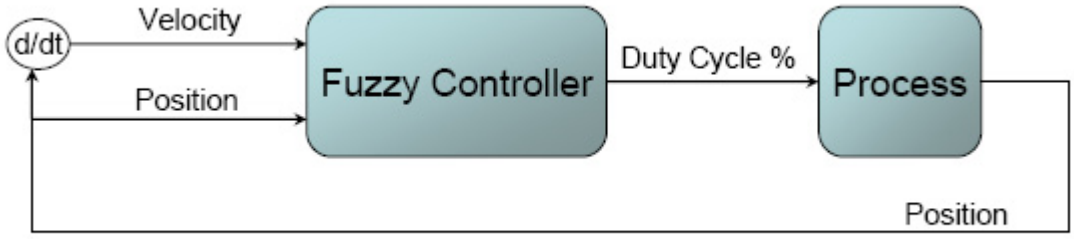

Figure 3.4: Block diagram of the expert fuzzy controller.

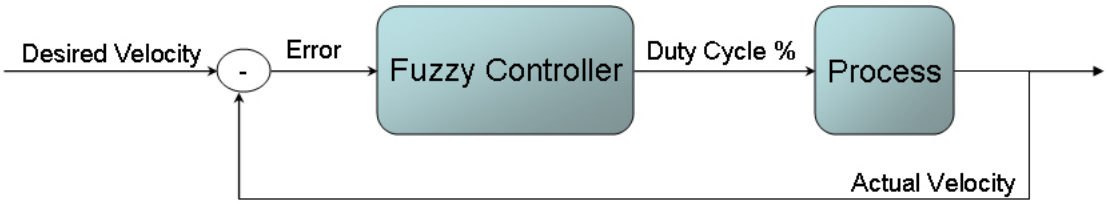

Figure 3.5: Block diagram of the error-based fuzzy controller.

The Error-based Fuzzy Controller

A closed loop fuzzy controller, which controlled the velocity of the piston, was another method that was evaluated experimentally. In this design, the controller should follow a desired velocity profile, which assures a good performance and saving. The difference between the desired and actual velocity is the input to the fuzzy controller and the output to the plant is the duty cycle value. Figure 3.5 depicts the block diagram of the system. The detailed design of the system including the rule table, the membership functions and the final results are provided in Chapter 5.

The final objective of this project is to remove the feedback signal from the sensors and to return back to an open-loop control design. This approach is useful to reduce the overall cost of the system, by eliminating the sensors and feedback signals. In addition, the system benefits from saving energy by applying duty cycle profiles, obtained from the fuzzy-expert controller.

Chapter 4

Plant Modeling

Before implementing the control systems, extensive analyses through simulation revealed some important properties of the system. The data provided the foundation on which the controller designs are based.

4.1 Introduction

Analyzing and evaluating the behavior of a system is one of the necessities to design and implement a proper controller. Since the pneumatic system is highly nonlinear and dependent on parameters, such as duty cycle, load, equalization time, and operating frequency, it was essential to simulate the system and understand the response of the system to different inputs. A simulated model also provides a reference and a basis for comparison when the system is tested, varying other parameters. In this chapter, the analytical equations for the actuator are explained. The behavior of the system in a simulated environment under different conditions is evaluated and the results are provided.

4.2 Modeling Equations for a Pneumatic Valve and Actuator

Figure 4.1 depicts a typical pneumatic valve and actuator. Assuming that x is the piston displacement, M is the mass of the piston and rod assembly plus the mass of the load, b_v is the viscous friction coefficient, A_1 and A_2 are the effective cross-sectional areas of each side of the piston, P_1 and P_2 are the absolute pressure inside each side of the cylinder, and A_R is the cross-sectional area of the piston rod, the dynamic model of the system considering a combined inertial and viscous load is presented in Equation (4.1).

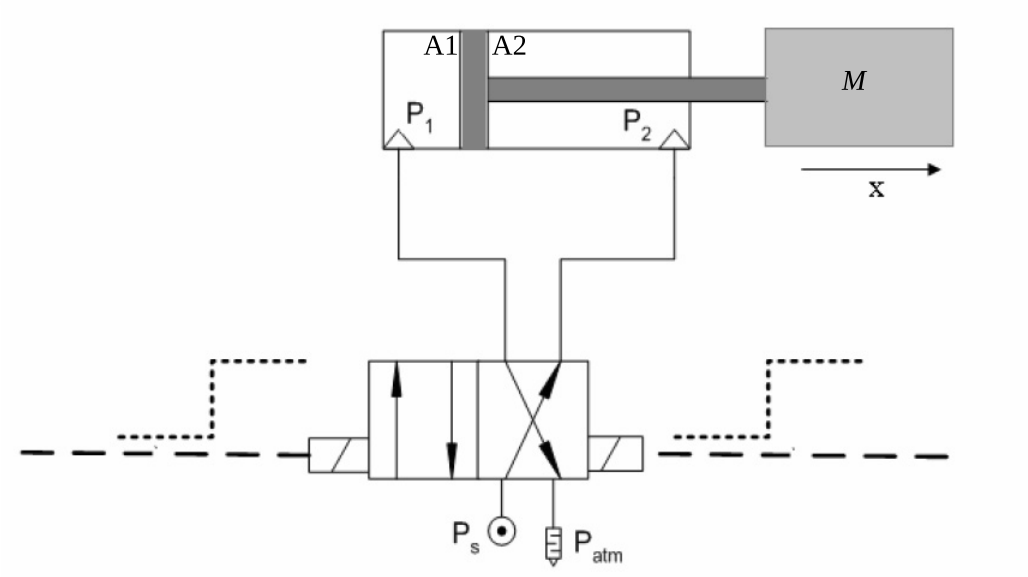

Figure 4.1: A typical pneumatic valve and actuator.

$$M\ddot{x} + b_v\dot{x} = P_1A_1 - P_2A_2 - P_{atm}A_R \tag{4.1}$$

Assuming air to be a perfect gas and the process to be an isothermal process, P_1 and P_2 can be obtained from the following equations.

$$P_1 V_1 = m_1 RT \tag{4.2}$$

$$P_2 V_2 = m_2 RT \tag{4.3}$$

As a result, the rate of change of the pressure inside each chamber of the cylinder can be obtained from the derivative of Equations (4.2) and (4.3), as follows:

$$\dot{P}_1 V_1 = RT\dot{m}_1 - P_1 \dot{V}_1 \tag{4.4}$$

$$\dot{P}_2 V_2 = RT\dot{m}_2 - P_2 \dot{V}_2 \tag{4.5}$$

where T is the gas temperature, V_1 and V_2 are the volume of each cylinder chamber, R is the universal gas constant (R=287 J/kgK), and $\dot{m}_1$ and $\dot{m}_2$ are the total mass flow rate into or out of each side of the cylinder. $\dot{m}_1$ and $\dot{m}_2$ are defined as:

$$\dot{m}_1 = A_v C_f \phi(\sigma_1) \tag{4.6}$$

$$\dot{m}_2 = A_v C_f \phi(\sigma_2) \tag{4.7}$$

where C_f is the discharge coefficient of the valve, A_v is the valve nozzle effective area, $\phi(\sigma)$ is the flow function, and σ is defined as:

$$\sigma = \frac{P_{out}}{P_{in}} \tag{4.8}$$

In Equation (4.8), P_{in} is the absolute input pressure and P_{out} is the absolute output pressure. Therefore σ_1 and σ_2, for two sides of the cylinder, are defined as follows:

$$\sigma_1 = \frac{P_s}{P_1} \tag{4.9}$$

$$\sigma_2 = \frac{P_{atm}}{P_2} \tag{4.10}$$

The mass flow rate traveling through the valve is a function of the upstream and downstream pressures. The ratio of the upstream and downstream pressure is a criteria to specify if the upstream pressure is linearly dependent on the downstream pressure or not. It has been proved that if σ, the pressure ratio, is larger than the critical value of C_r , the flow velocity will reach the speed of sound and is called sonic or choked flow. In this case, the flow rate will be a linear function of the upstream and downstream pressures. If σ is smaller than C_r, the mass flow depends nonlinearly on upstream and downstream pressures and is called subsonic or unchoked flow [16].

In practical calculations, the flow function $\phi(\sigma)$ is divided into two parts based on the type of the flow (sonic or subsonic); therefore, the standard equations for the mass flow passing the orifice area, A_v, assuming k=1.4 as an adiabatic exponent, are[32]:

$$\phi(\sigma_1) = \begin{cases} \sqrt{\frac{k}{RT}(\frac{2}{1+k})^{(1+k)/(k-1)}}\, P_s & \sigma_1 \leq C_r \text{ (sonic)} \\ \sqrt{\frac{k}{RT(k-1)}}\sqrt{1-\sigma_1^{(k-1)/k}}\, \sigma_1^{(1/k)}\, P_s & \sigma_1 > C_r \text{ (subsonic)} \end{cases} \tag{4.11}$$

$$\phi(\sigma_2) = \begin{cases} \sqrt{\frac{k}{RT}(\frac{2}{1+k})^{(1+k)/(k-1)}}\, P_2 & \sigma_2 \leq C_r \text{ (sonic)} \\ \sqrt{\frac{k}{RT(k-1)}}\sqrt{1-\sigma_2^{(k-1)/k}}\, \sigma_2^{(1/k)}\, P_2 & \sigma_2 > C_r \text{ (subsonic)} \end{cases} \tag{4.12}$$

On the other hand, the derivative of Equation (4.1) is:

$$M\ddot{x} + b_v\ddot{x} = \dot{P}_1 A_1 - \dot{P}_2 A_2 \tag{4.13}$$

The dynamic Equation of the system can be presented as Equation (4.14) in which $\dot{P}_1$ and $\dot{P}_2$ were obtained from the Equation (4.5).

$$\dddot{x} = \frac{A_1}{M}(\frac{RT}{V_1}\dot{m}_1 - \frac{P_1}{V_1}\dot{V}_1) - \frac{A_2}{M}(\frac{RT}{V_2}\dot{m}_2 - \frac{P_2}{V_2}\dot{V}_2) - b_v\ddot{x} \tag{4.14}$$

Substitution of V_1 and V_2 with A_1x and A_2x respectively in combination with Equations (4.11) and (4.12) will be ended to the final dynamic equation of the system:

$$\dddot{x} = \frac{1}{M}(\frac{RT}{\dot{x}}A_vC_f\phi(\sigma_1) - \frac{P_1A_1}{x}\dot{x}) - \frac{1}{M}(\frac{RT}{\dot{x}}A_vC_f\phi(\sigma_2) - \frac{P_2A_2}{x}\dot{x}) - b_v\ddot{x} \tag{4.15}$$

The main highlight of Equation (4.15) is presenting the nonlinear nature of pneumatic systems in a way that common linear control methods, like PID controllers cannot easily overcome the nonlinearities existed in the system.

In the actual system, there are many sources of uncertainities and nonlinearitis which make the system more complicated to understand and control. For example, a simple test was performed on the test rig to determine the type of the flow (sonic or subsonic). The upstream and downstream pressures of the cylinder during the extension were recorded and σ was calculated. As mentioned earlier, in subsonic or unchoked flow, the mass flow depends nonlinearly on upstream and downstream pressures. According to the results, which are depicted in Table 4.1, the percentage of subsonic flow is more than sonic flow especially in higher PWM frequencies. 100% subsonic flow at 5 Hz frequency presents the extreme nonlinear behavior of the test rig.

As a conclusion, all the presented work was ended to choose a controller capable of overcoming nonlinearities in this system, when a control action is needed.

Table 4.1: Percentage of subsonic and sonic flow in different PWM frequencies during extension.

PWM Frequency (Hz)	**Subsonic Flow (%)**	**Sonic Flow (%)**
1	67	34
2	83	16
5	100	0

4.3 Simulation of the Proposed System in *AMESim* and Simulink®

Using the *AMESim* to Simulink® interface, constructing a model of a subsystem in *AMESim* and converting it to a Simulink® S-Function is possible. The S-Function can be imported into Simulink® and can be used within a Simulink® mode. Therefore, in order to model the strategies explained before, *AMESim* was connected to Simulink® .

Figure 4.2 presents the *AMESim* model including the Simulink® interface box. Figure 4.3 shows the model in Simulink®. The whole *AMESim* model is presented in Figure 4.3 by a box called "*AMESim* S-Function".

The *AMESim* model of the test rig were created in Simulink® based on two different methods: Regular method and PWM-ABE method. In the Regular model the system reciprocated normally similar to traditional pneumatic systems while in the second method, PWM-ABE strategies explained in Sections 3.2.1, 3.2.2 and 4.4 were modeled.

As stated before, in both simulated and experimental tests, the focus was on the air consumption reduction during the extension only.

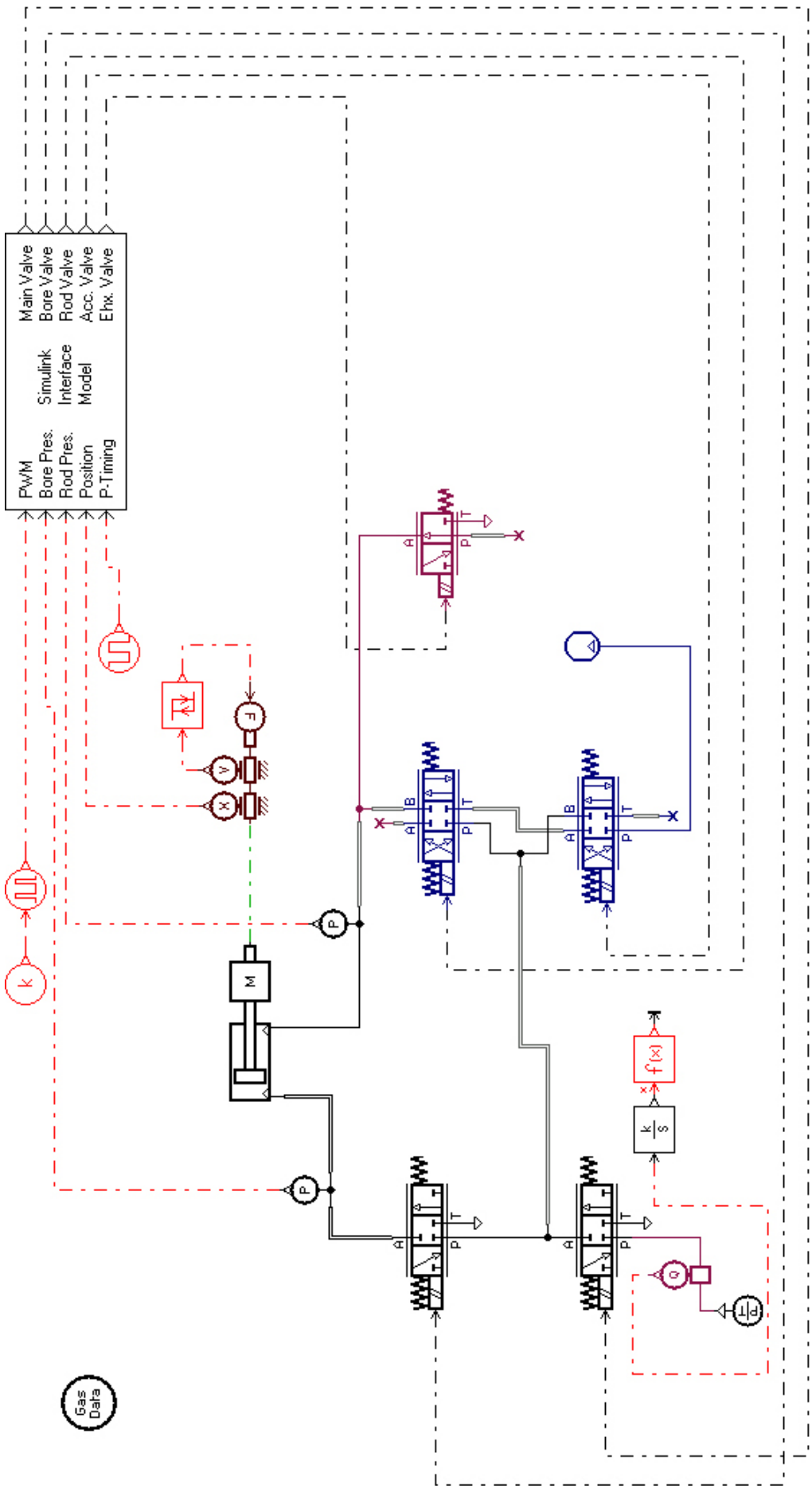

Figure 4.2: The proposed system modeled in *AMESim* environment.

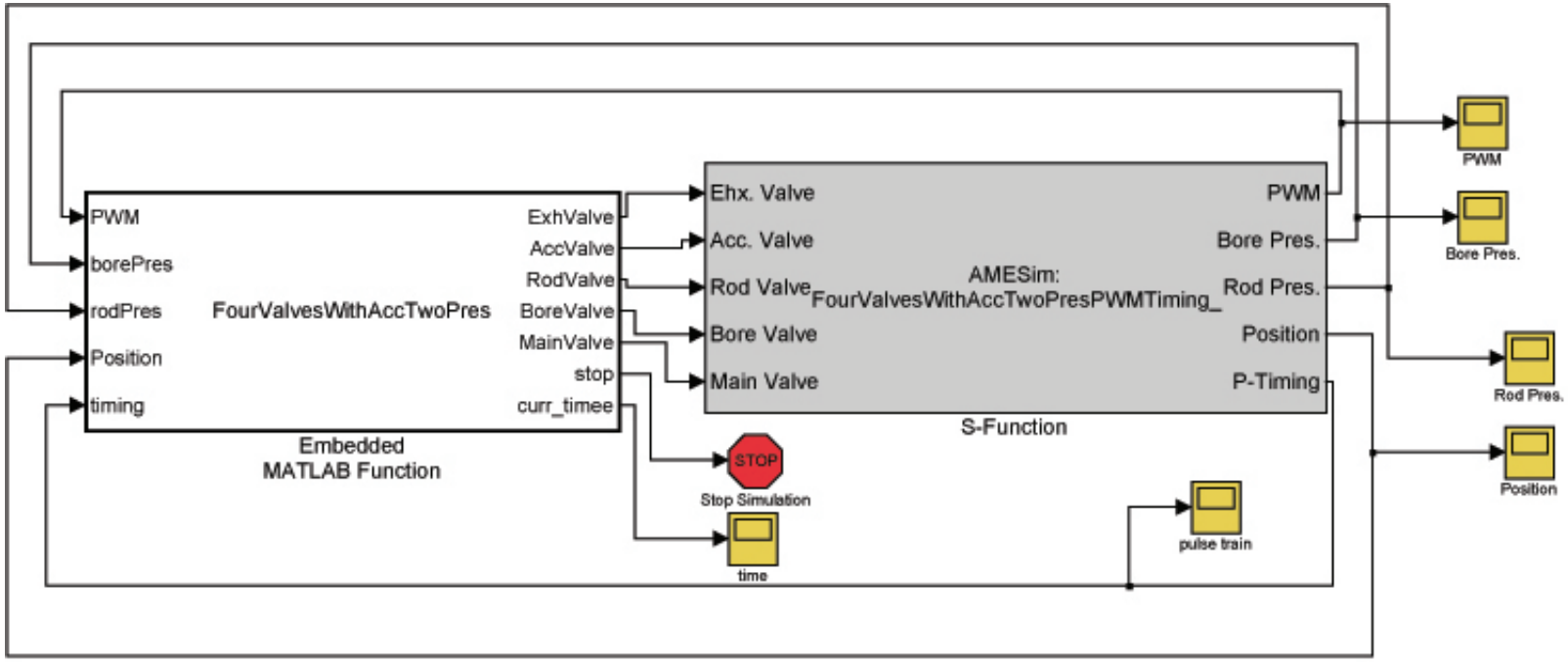

Figure 4.3: The proposed system modeled in Simulink®.

As Figure 4.2 shows, the simulated pneumatic system consists of two three-position-three-port (3/3) solenoid valves with spring offset, two three-position-four-port (4/3) solenoid valves with spring offset, one two-position-three-port (3/2) solenoid valve with spring offset, one double-acting and single-rod cylinder with mass, two pressure transducers, a flow meter, and an accumulator.

The cylinder itself has a bore diameter of 32 mm, a stroke of 300 mm and a rod diameter of 12 mm; these match the dimensions of FESTO actuator in the test rig (see Section 5.2). The mass of the rod and the coupler was approximated to be 5 kg. The flow meter, at the bottom left of the diagram, measures the volume of air flow into the system at standard temperature and pressure. The air consumption is obtained from the integrator attached to the flow meter. Table 4.2 specifies the gas data in the modeling. The volume of the accumulator was set to be 10 cc similar to the test rig.

Table 4.2: Gas data used in the modeling.

Gas Type Index	1
Specific Heat Ratio (Gamma)	1.4 null
Perfect Gas Constant(R)	287 J/Kg/K
Absolute Viscosity (mu)	0.0182 cP
Source Pressure	6 barA
Reference Pressure	1.013 barA
Temperature	293.15 K

In order to model the load mechanism in the test rig, which is explained in detail in Section 5.2, an apposite force is applied to the piston based on the direction of the movement. The value of the force was calculated based on the loading values in the test rig to make the model in agreement with the real system.

All the mechanical parameters of the model, such as the actuator and the valves, parameters, load and mass data; gas properties, such as pressure and temperature

,etc. were set in *AMESim* environment similar to the conditions in the test rig. In order to simulate a reciprocating motion, the commands to the valves had to be changed periodically during the motion which made utilizing Simulink® necessary. In this case, the required feedback from the mechanical model, such as position of the cylinder and pressure in both side of the cylinder were sent to the Simulink® file via S-function in *AMESim*. The collected data from *AMESim* made the basic foundation for the Simulink® model to change the commands of the valve and send them to *AMESim* environment periodically. Therefore, a cycle was created to simulate a reciprocating movement virtually and to analyze the behavior of the system theoretically.

4.4 System State Diagram

As explained before, in order to reduce the flow consumption, pressure in the system can be directed into the accumulator rather than vented to the environment, providing a source of pressure for the remaining reciprocation. Diagram 4.4, presents the system state diagram in each cycle which is implemented in Simulink® and also in the experimental system.

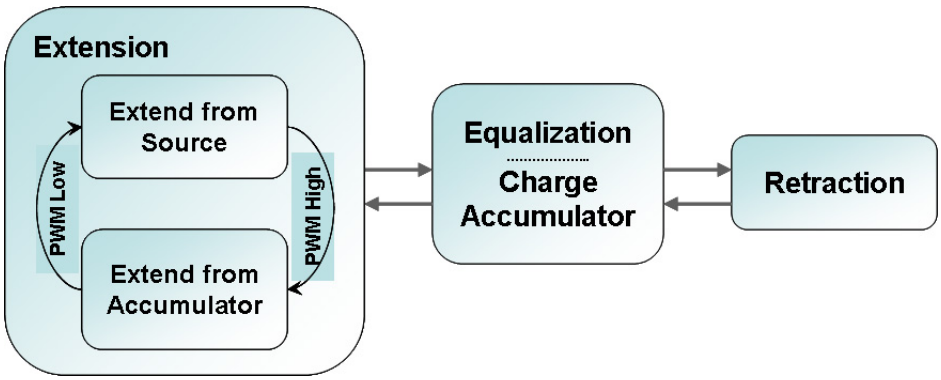

Figure 4.4: The system State Diagram .

At the beginning of the cycle, the pressure inside the accumulator is increased by entering the pressurized air from the both sides of the actuator for a short period

of time during the equalization stage. Following that, the cylinder starts extending while its source pressure is alternating between the line source and the accumulator. Equalization happens at the end positions of the cylinder in each cycle which helps increasing the pressure inside the accumulator.

4.5 Numerical Results

The model in *AMESim* and Simulink® environments was used to analyze the role of all important parameters effective in the performance of the system and saving energy. In other words, the optimum parameters for the algorithm had to be identified. The *AMESim* modeling was performed in PWM frequency of 25 Hz and with a duty cycle varying between 12.5% and 100% where a duty cycle of 100% causes no air to be taken from the accumulator during extension. In this study, a model run with 100% duty cycle is refereed to a "regular model". The source pressure was set to be 6 barA. Figures 4.5, 4.6, and 4.7 present the pressure on both sides of the cylinder for three models: a regular model, a model run with 25% duty cycle, and a model run with 12.5% duty cycle, respectively. All the presented models in these figures were run for five cycles under 220 N load. As the diagram 4.5 shows, PWM and Equalization methods were not applied in the regular system. Figures 4.6 and 4.7 illustrate that the equalization takes place where pressures P_1 and P_2 are the same. The profile of the first cycleof pressure is different in the figures, because the intial pressure of the accumulator was set to be zero in the modeling .

Figures 4.8, 4.9, and 4.10 depict the displacement and velocity profiles of a regular model, a model run with 12.5% duty cycle, and a model run with 25% duty cycle respectively. As the results show, when the duty cycle decreases, the extension time becomes longer; hence the whole process take more time to finish five cycles.

In Figures 4.11, 4.12, and 4.13 the velocity profiles and their FFT (fast Fourier

transform) diagrams are presented. Since the movement of the piston in lower duty cycles is not as smooth as the regular system, FFT profile of the velocity can be considered as a criterion to evaluate the performance of the system in terms of movement. This analysis will be performed on the experimental results in detail.

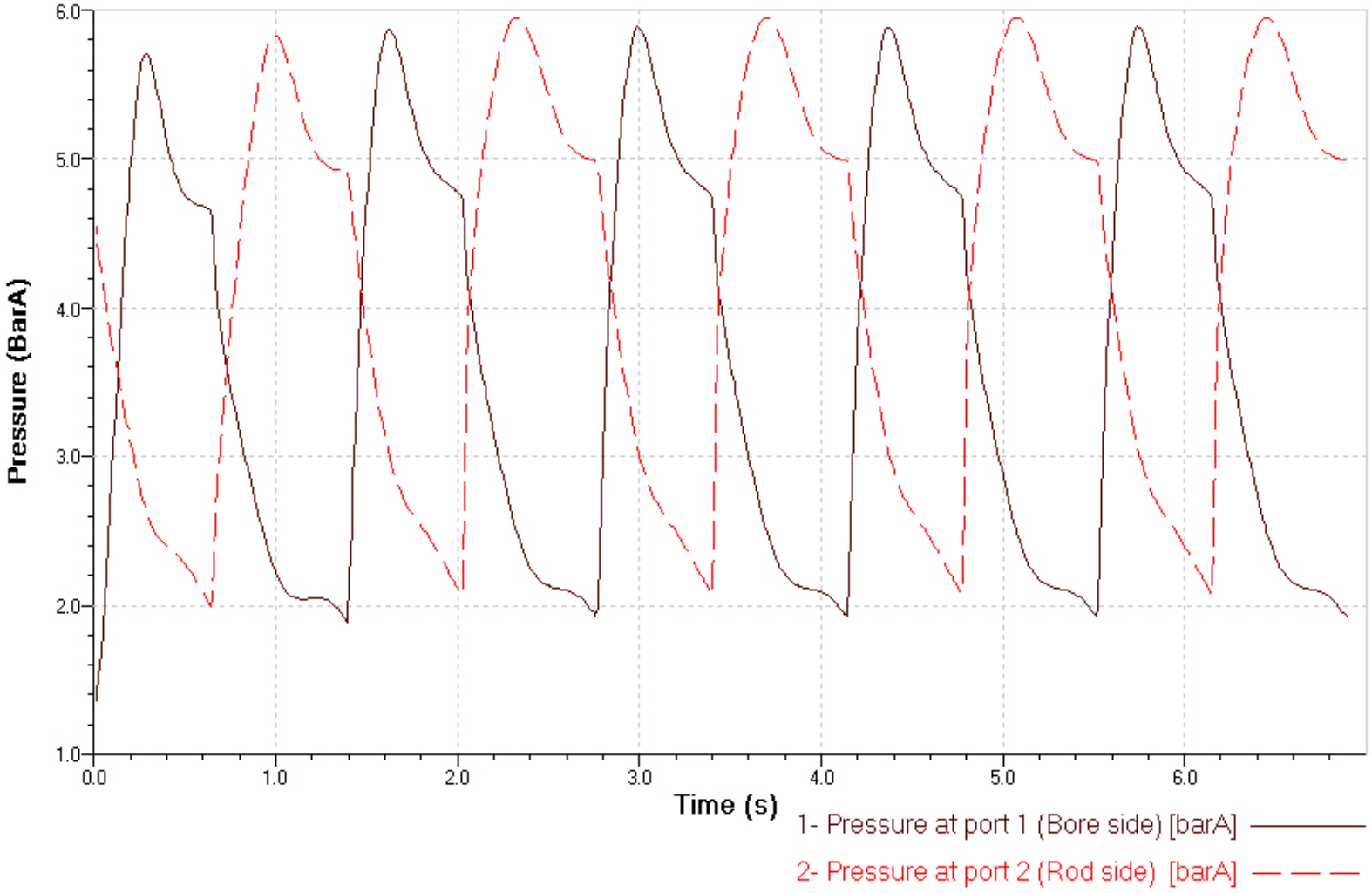

Figure 4.5: Pressure profile of both sides of the cylinder in a regular model with no equalization and PWM.

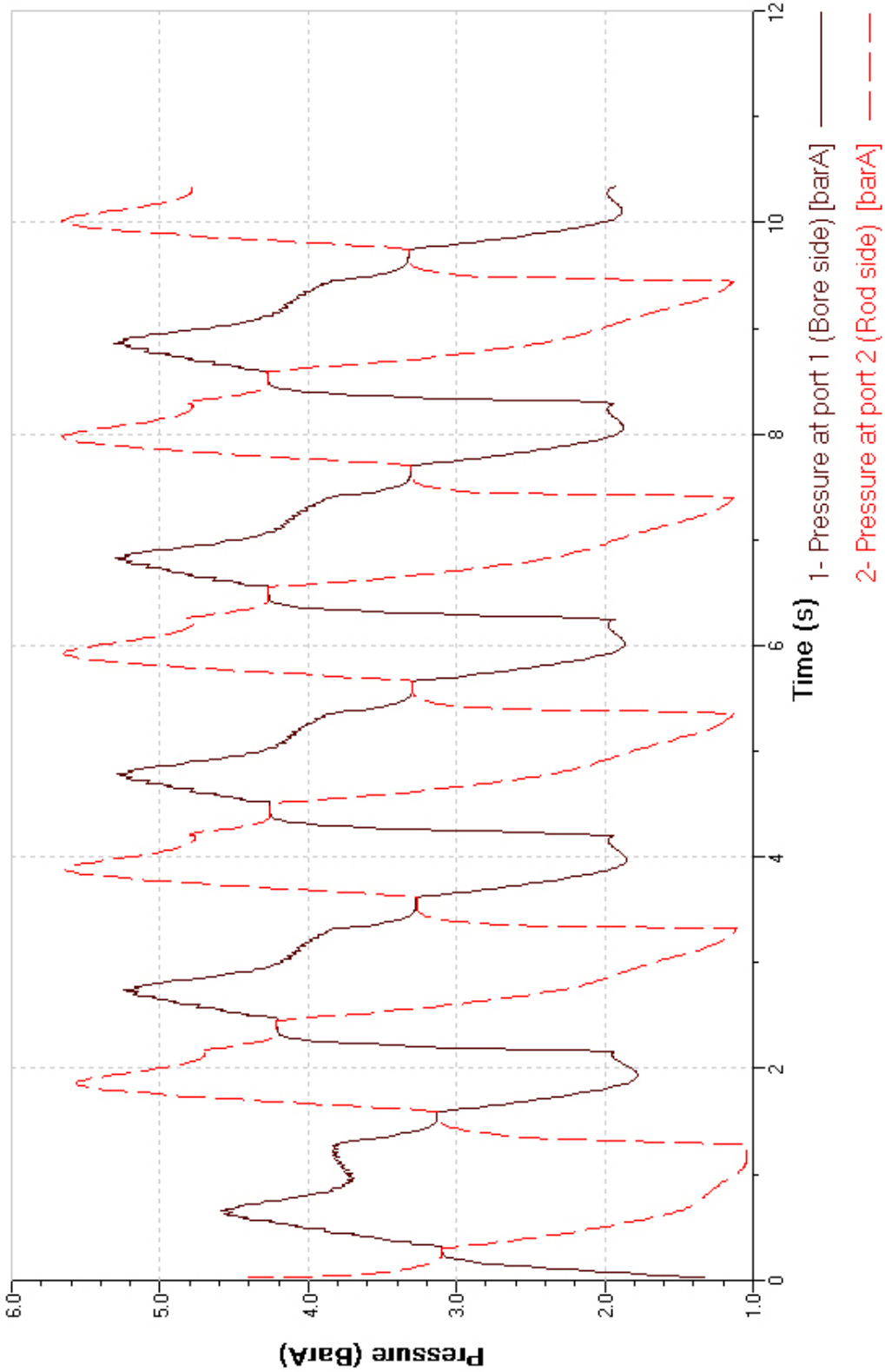

Figure 4.6: Pressure profile of both sides of the cylinder in a model run with 25% duty cycle.

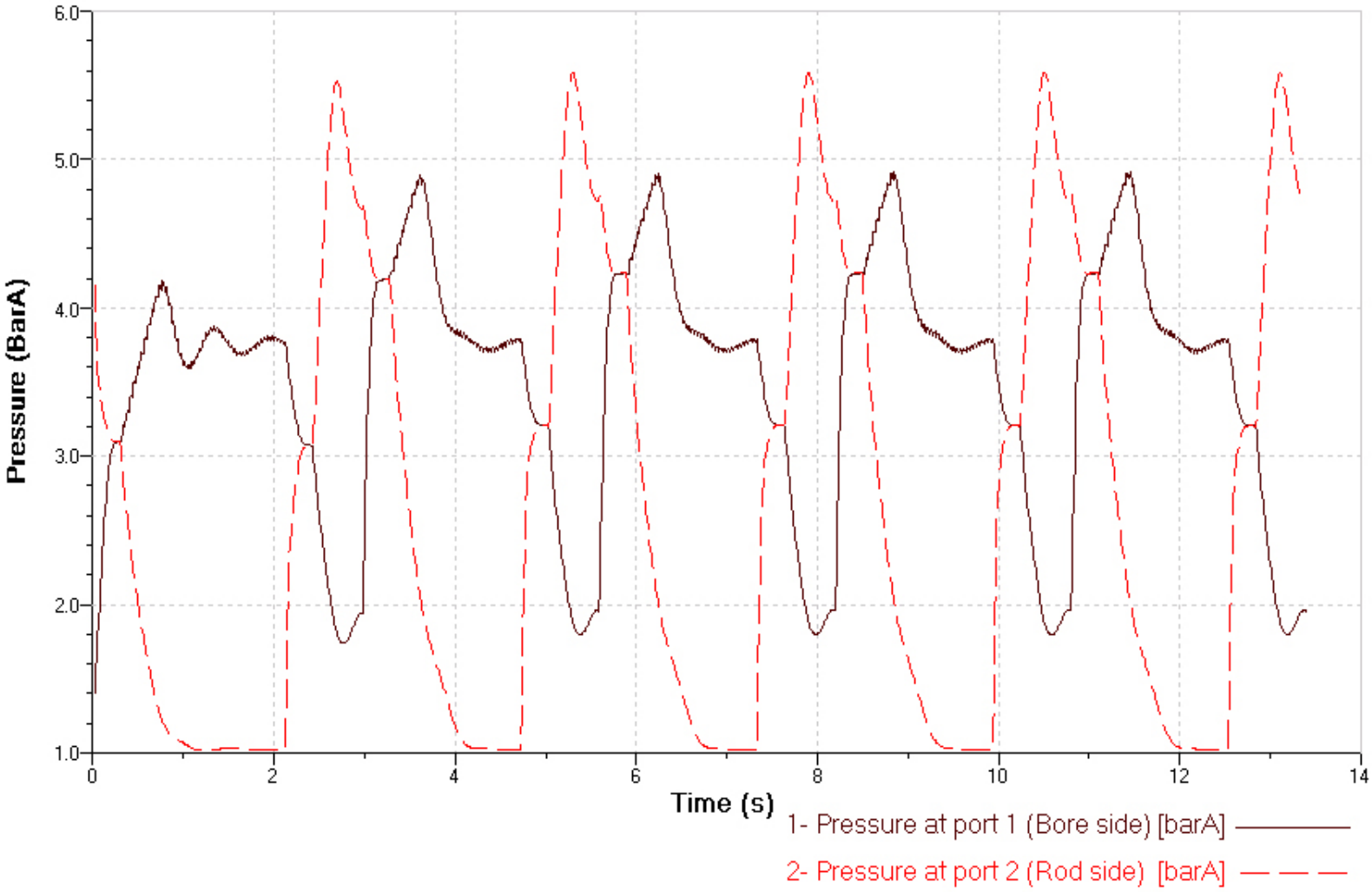

Figure 4.7: Pressure profile of both sides of the cylinder in a model run with 12.5% duty cycle.

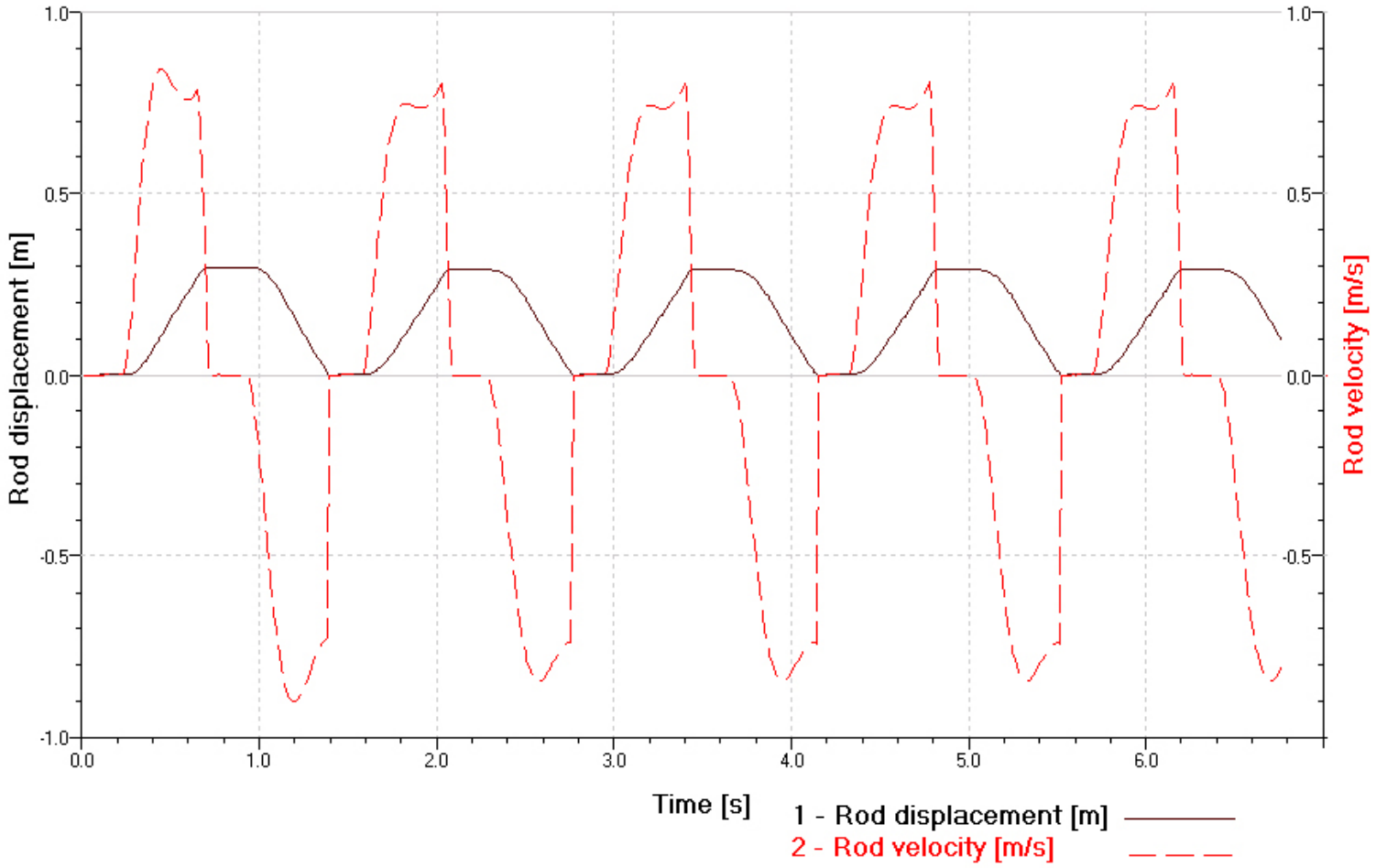

Figure 4.8: Displacement and velocity profile of a regular model with no equalization and PWM.

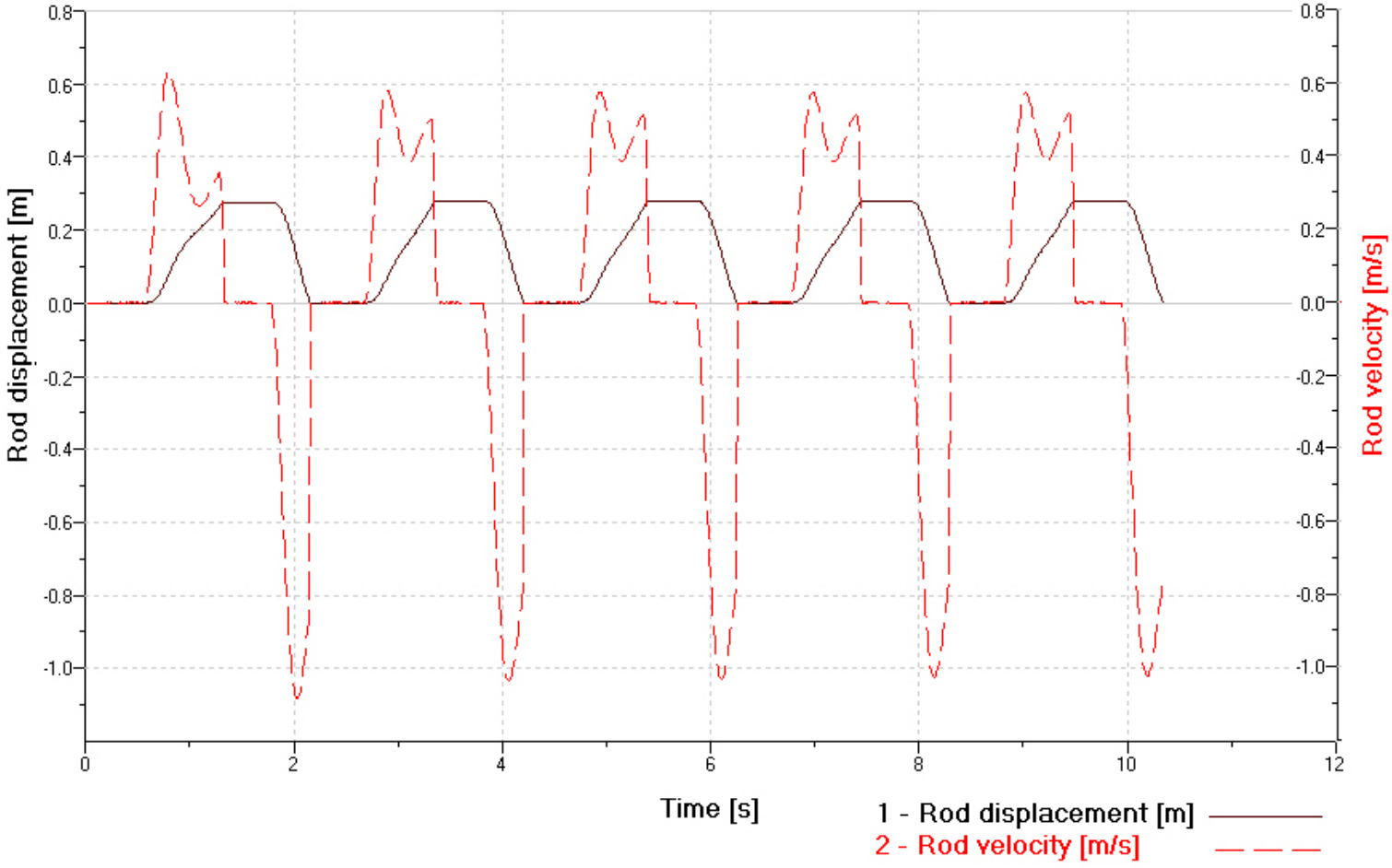

Figure 4.9: Displacement and velocity profile of a model run with 25% duty cycle.

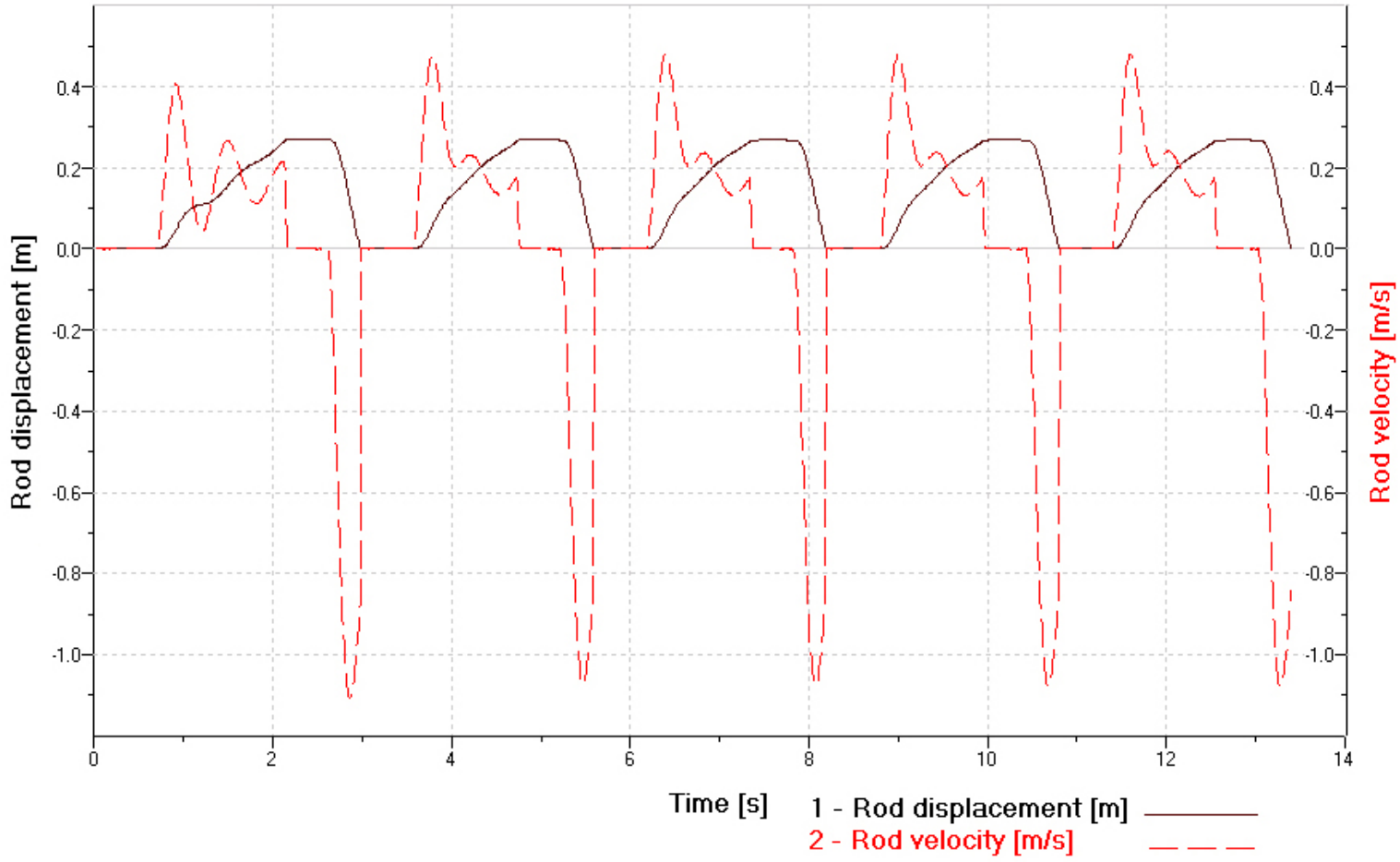

Figure 4.10: Displacement and velocity profile of a model run with 12.5% duty cycle.

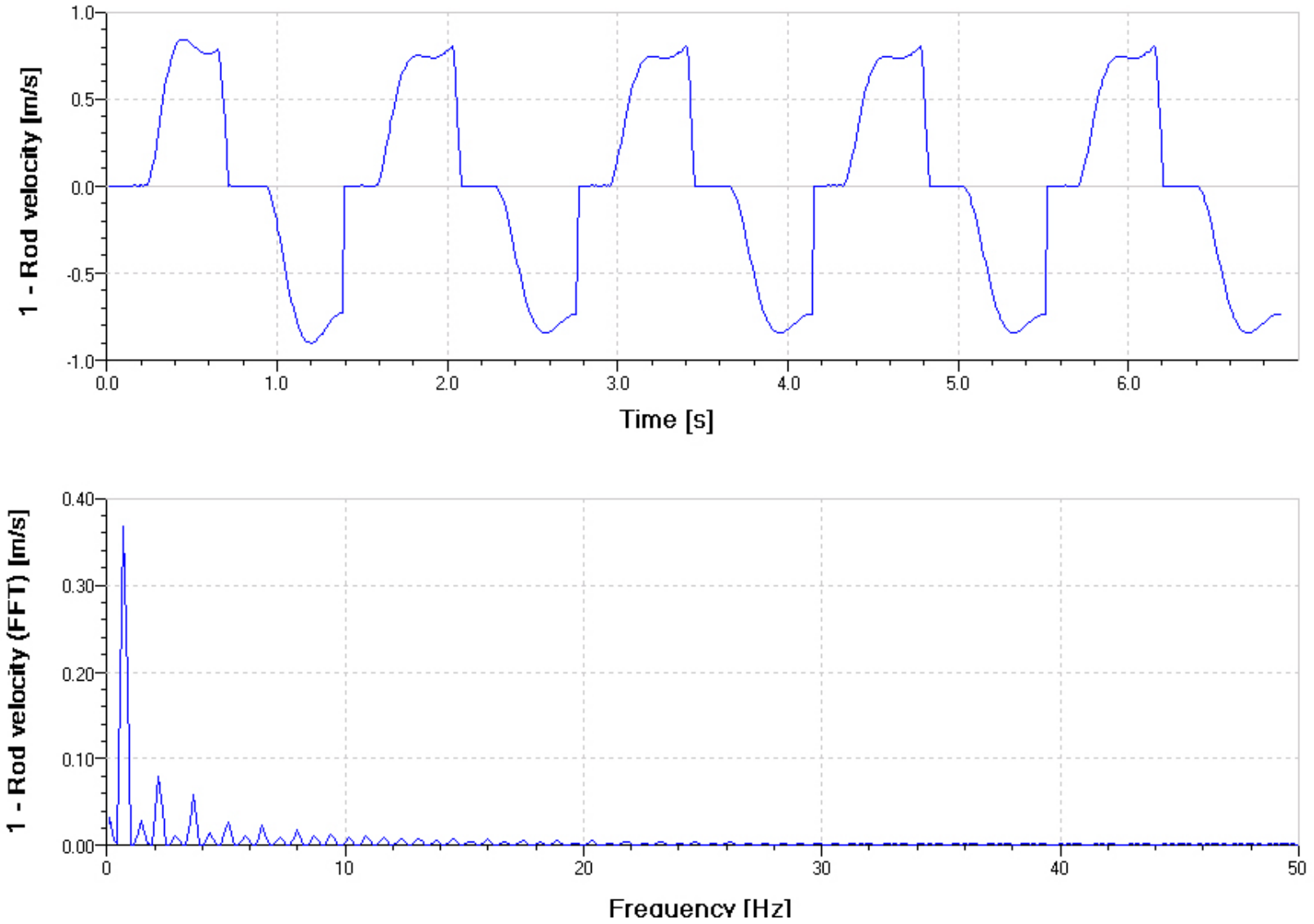

Figure 4.11: Velocity profile and its FFT diagram in a regular model

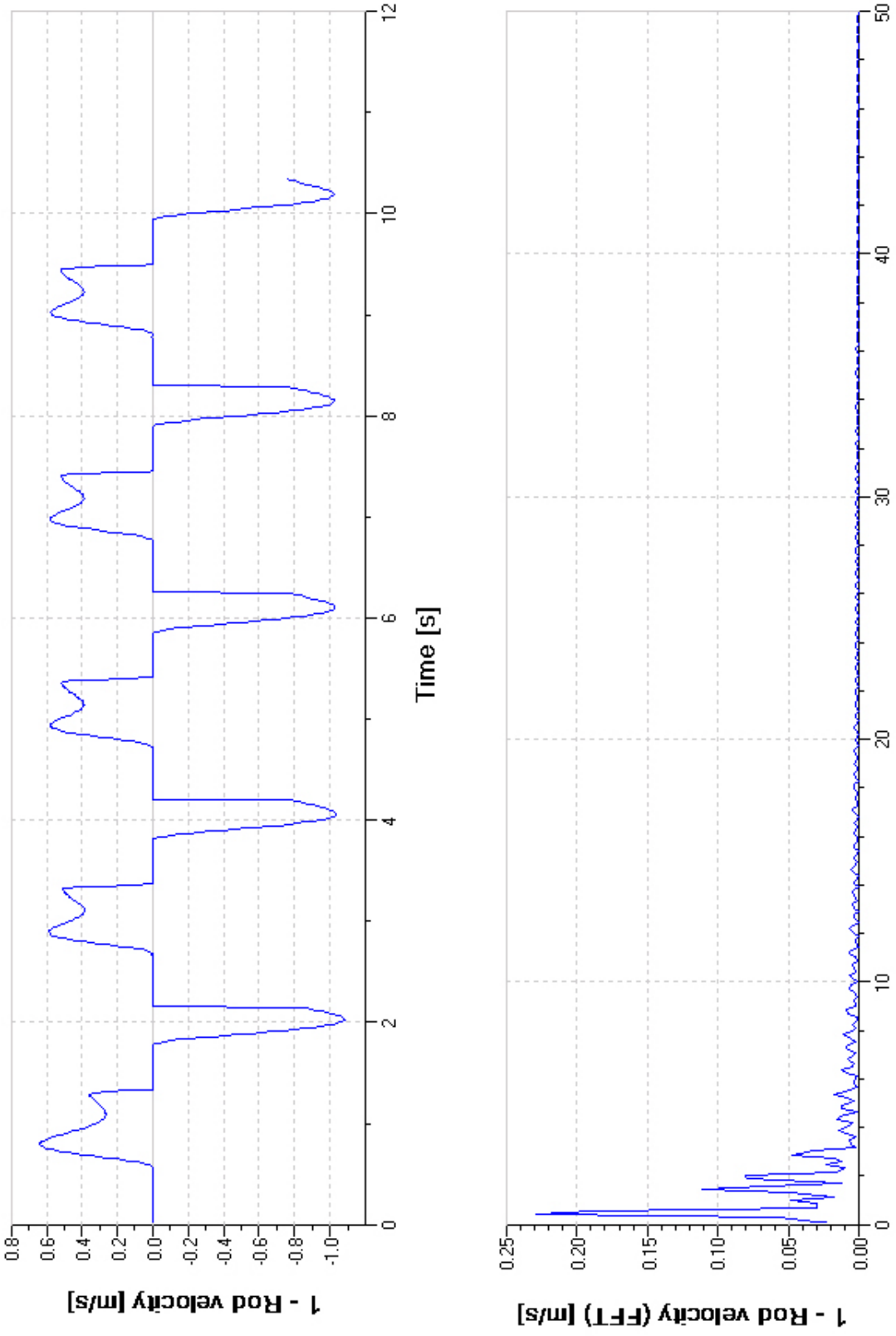

Figure 4.12: Velocity profile and its FFT diagram in a model run with 25% duty cycle.

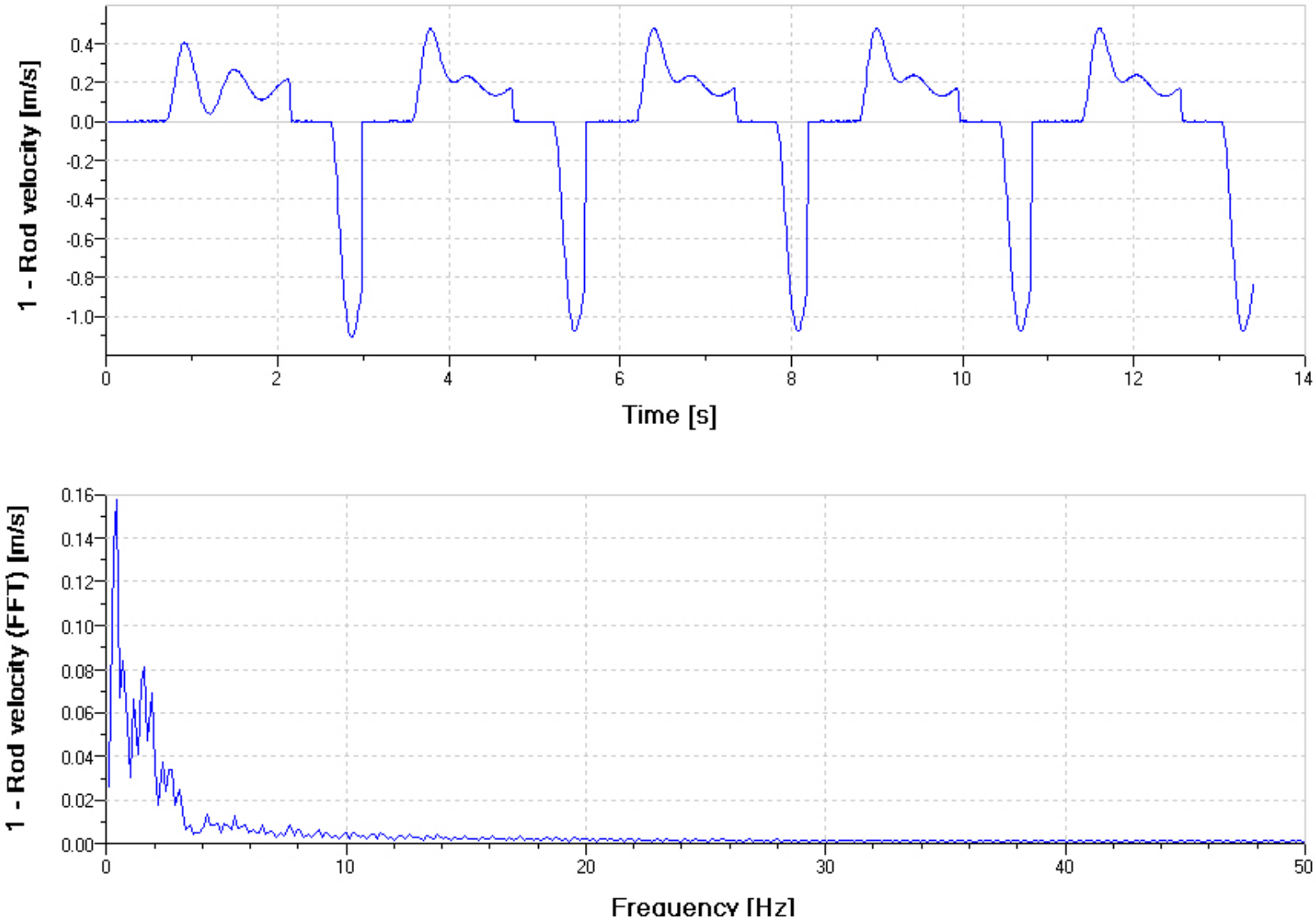

Figure 4.13: Velocity profile and its FFT diagram in a model run with 12.5% duty cycle

The preceding observations do not address the contribution of the proposed model to save pressurized air. In Figure 4.14, the air consumption has been depicted for the regular model, the 12.5%-duty cycle model and 25%-duty cycle model for five cycles. 25%-duty cycle model was run with equalization duration of 50 ms , 100ms, and 300 ms.

Although the diagram shows a longer process for the proposed models, the air consumption value is promisingly less than that of the regular model. For example, a comparison between the air consumption of 12.5%-duty cycle model and the regular model results in 25% saving. The middle profiles in Figure 4.14 present 25%-duty cycle model in different equalization times. As it can be seen, lower equalization time is ended to faster performance but more air consumption.

The above results prove that saving energy is possible; hence, the system performance and air consumption should be evaluated in the experimental system as well. Before starting the work on the test rig, the effective parameters in air consumption in such a system had to be studied. The discussion will be provided in the following sections.

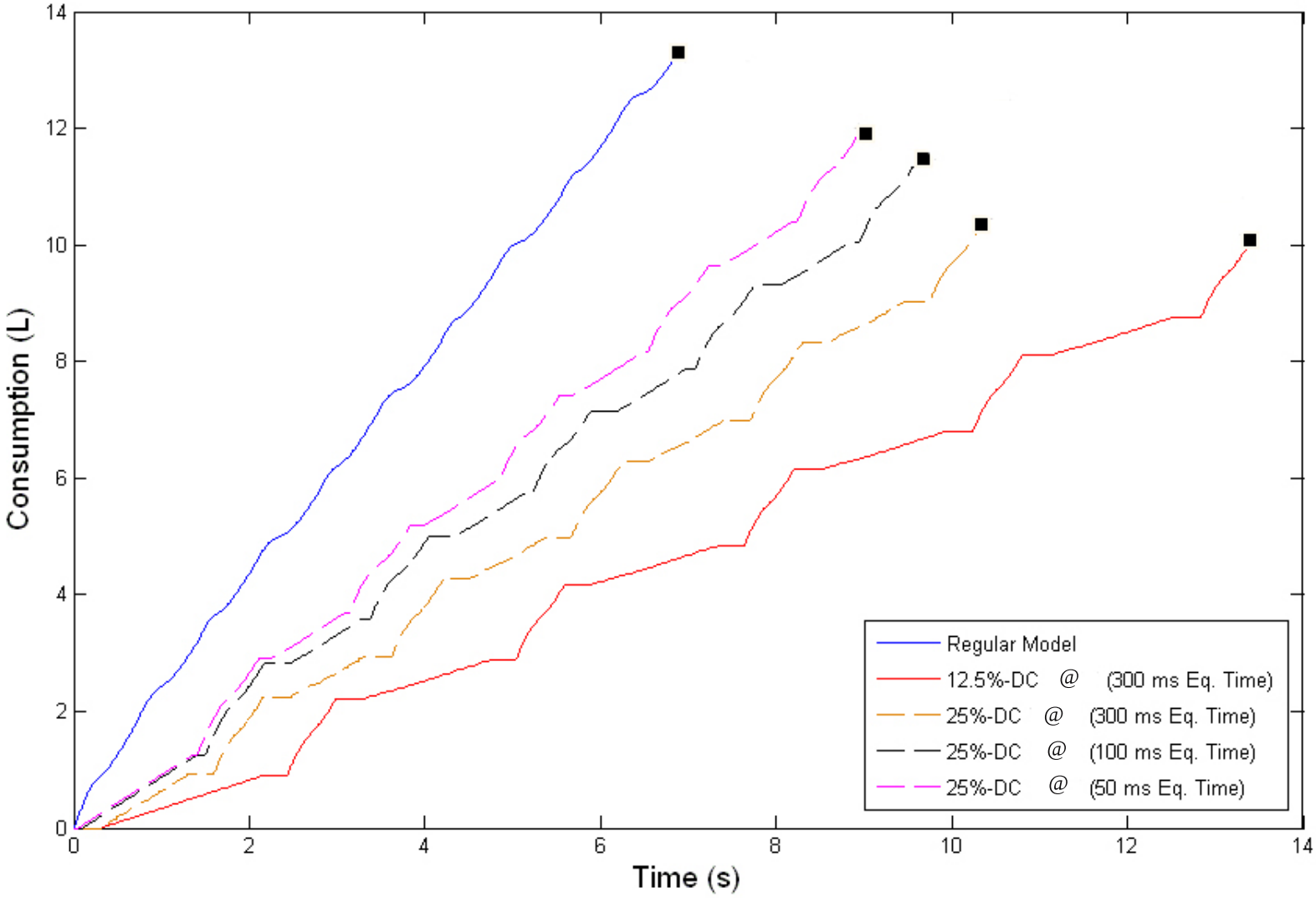

Figure 4.14: Air consumption results in the modeling for five cycles.

4.5.1 The Effect of Duty Cycle

When the duty cycle increases, the duration of "one" in a period of the pulse train increases, which means that the valve connects the source of air to the cylinder longer in a pulse period. Because the cylinder connection to the source results in air consumption, the higher duty cycle values cause more air consumption or less air conservation. Figure 4.15 depicts the saving rate with respect to duty cycle. It shows that the saving rate decreases at higher duty cycles.

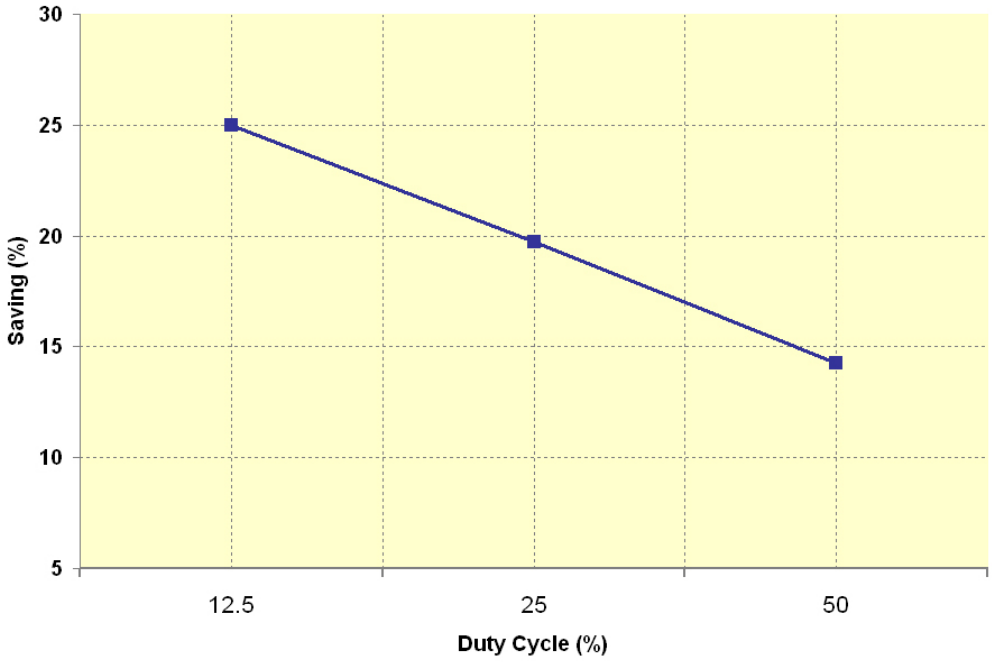

Figure 4.15: Results of air conservation with respect to duty cycle at frequency of 25 Hz.

Despite the above mentioned points, when the cylinder is connected to the source longer, which means a higher duty cycle is applied to the system, it has more power to push the load forward and finally smoother movement. If the smoothness of the movement is called as the system performance, it can be concluded that there is a trade off between saving energy and system performance in such a configuration.

4.5.2 The Effect of Equalization Time

As stated in Section 3.2.1, the equalization happens at the home positions. In these positions, the cylinder ports are connected to the accumulator and the pressure inside the system is equalized; however the question is that for how long the system should remain in the equalization stage and if a longer equalization time has any effect on the air consumption. In order to answer this question, the model was run at different equalization times. As Figure 4.16 shows, air saving starts increasing a little after 20 ms and remains approximately constant after 200ms.

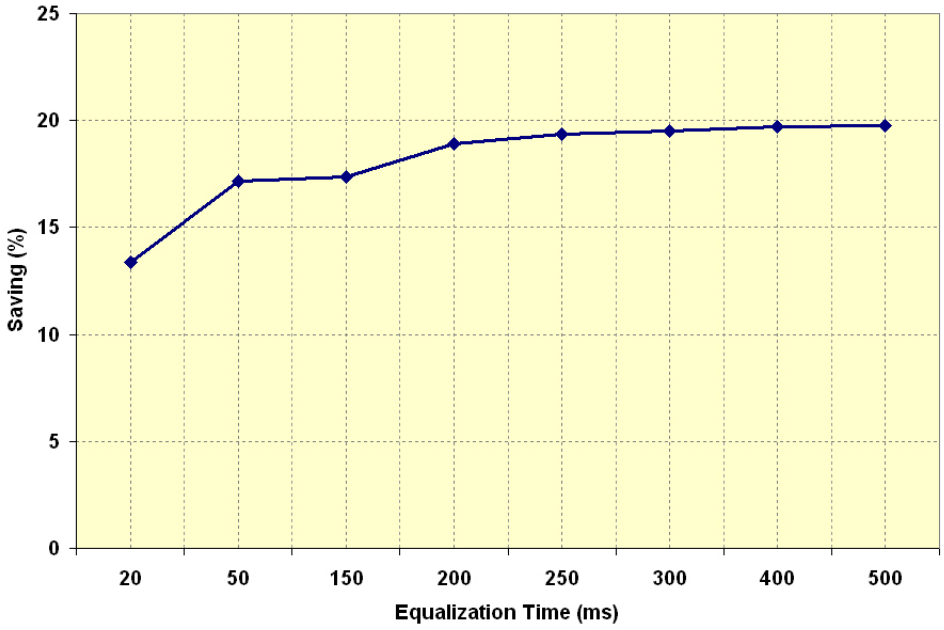

Figure 4.16: Results of air conservation with respect to equalization time in 25%-duty cycle 220N-load models .

The reason for this phenomenon is the fact that when both cylinder chambers volumes are connected together, the cylinder interior pressure has a tendency to be constant after a short period of time. Therefore, increasing the equalization time when the pressure inside the system is constant would not have any effect on the air consumption and final performance of the system. Since a short equalization time results in a lower pressure in one side of the cylinder which will be pressurized by

the supply line subsequently, the level of the flow consumption increases. As seen, an equalization time of 200ms may be the optimum level for the proposed tasks.

As a conclusion, Duty cycle has a direct effect on saving energy in a way that increasing the duty cycle will result in increasing the air consumption. In addition, it was found that equalization time more than 200 ms does not have a considerable effect on saving air in the system.

Chapter 5

Assessment of Proposed Strategies with Experimental Set-up

5.1 Introduction

In this chapter, the actual test rig and its components will be discussed. In addition, the results of expert-fuzzy controller, error-based fuzzy controller, and open-loop controller application on the test rig will be provided in detail. The parameters effective in saving energy in the experimental set-up will be analyzed. A method to calculate the smoothness of the motion will be proposed and the final achievement in saving energy and the performance of the system will be investigated.

5.2 Experimental Set-up

A test rig was created to verify the hypotheses stated in previous chapters. Figure 5.1 shows the diagram of the implemented set-up and Figure 5.2 presents the picture of the test rig.

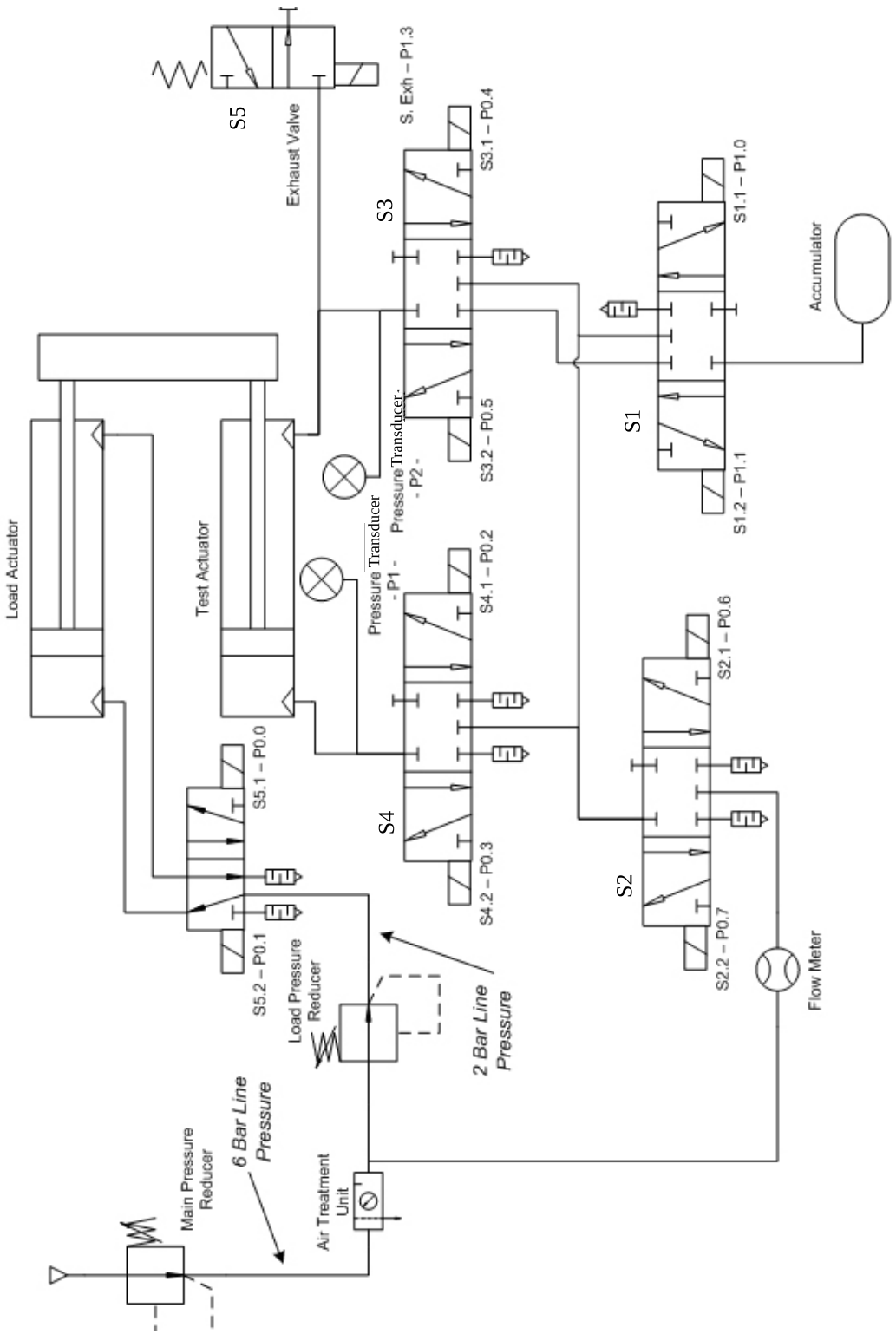

Figure 5.1: Test rig set-up diagram.

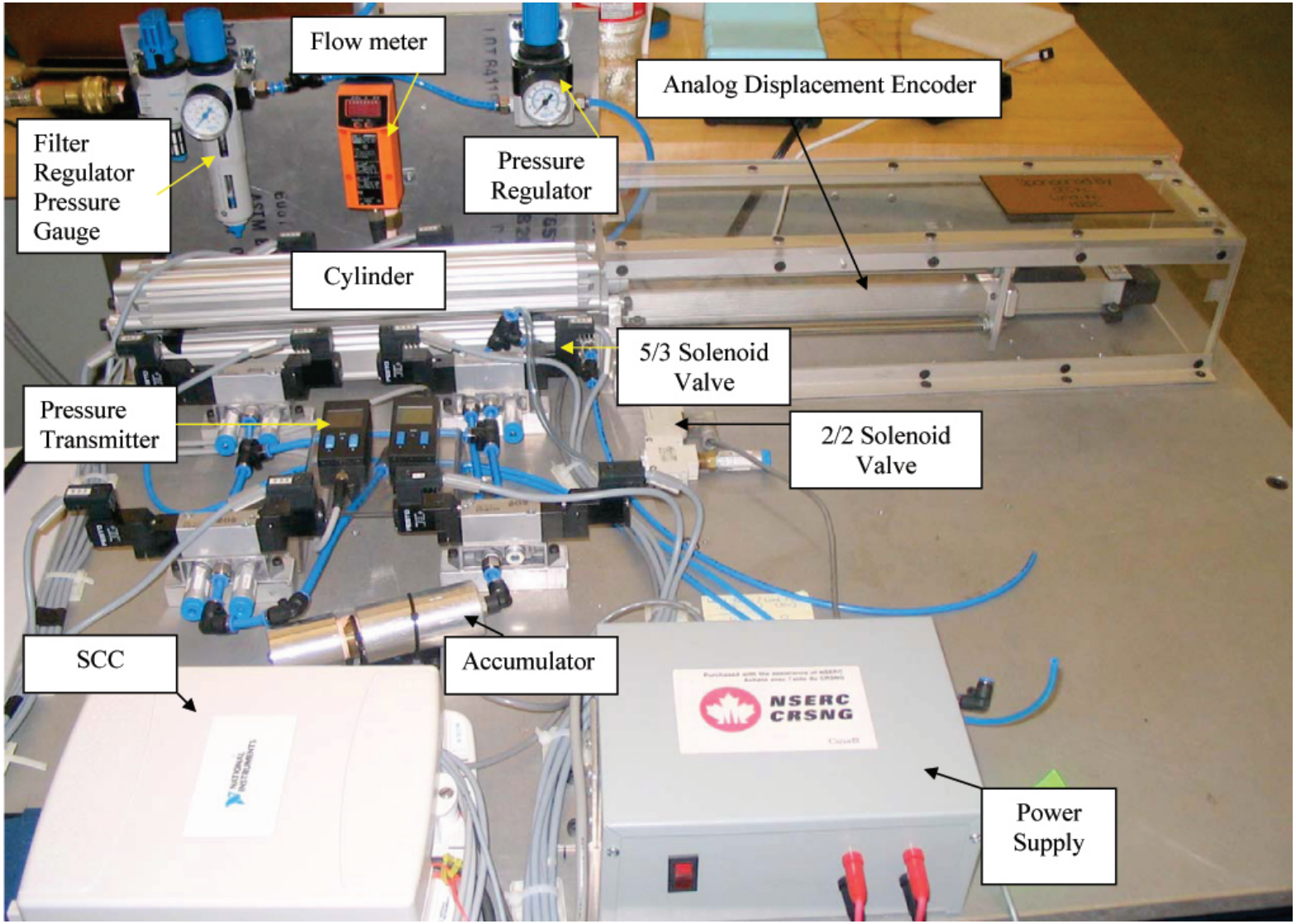

Figure 5.2: Picture of the test rig.

In the test rig, pressure supplied to the main actuator was controlled by a set of electronically controlled valves. Four 5/3 double-solenoid valves, S1, S2, S3, and S4 and one 3/2 single-solenoid valve of S5 had the main role in the implementation of the proposed algorithms on the test rig while they guided the air through different paths in the pneumatic circuit. These four valves were connected together via a regenerative circuit to implement ABE method on the test rig.

A double-acting cylinder with 32 mm piston diameter and 300 mm stroke length was engaged to a linear analog displacement encoder sending the position data of the piston to the DAQ card. A 10-cc accumulator was built and connected to the pneumatic circuit to store a portion of the pressurized air in the system. The pressure on both sides of the main cylinder was measured with two pressure transducers. The air consumption and air flow were measured using a flow meter located in the entrance of the pneumatic circuit.

A data acquisition (DAQ) card , NI PCI-6221, which made the measurement and control of the process possible, provided the interface circuit between the computer and the test rig. A signal conditioning board with terminal blocks, NI SCC-68, collected the analog and digital signals from the test rig and sent them via its 68-pin I/O connector port to the DAQ card. Therefore, pressure, position and flow signals could be monitored and controlled with this structure. This test rig was controlled by real-time operating system available within the LabView 8.4 ® package and all control and measurement was performed by custom LabView® routines.

Table 5.1 provides the part list for the explained pneumatic components. Figure 5.4 shows the code diagrams and Figure 5.3 presents of a part of the front panel in LabView® environment.

Table 5.1: The list of the components utilized in the test rig.

Part	**Manufacturer**	**Model**	**Quantity**
Double-acting Cylinders	Festo	DNC-32-300-P	2
Proximity Sensor	Festo	SME-8F-DS-24V-K2,5-OE	2
Analog Displacement Encoder (Potentiometric)	Festo	MLO-POT-360-TLF	1
5/3 Double-solenoid Valve (S1 to S4)	Festo	MEH-5/3-1/8-P-B-24	4
5/2 Double-solenoid Valve (S5)	Festo	JMEH-5/2G-1/8-P-24	1
3/2 Single-solenoid Spring-return Valve	SMC	VQ110-5M	1
Flow Meter	ifmEfector	SD6001	1
Accumulator	Made in house	N/A	1
Pressure Transducer	Festo	SDE1-D10-G2-R18-M8-G	2
Precision Pressure Regulator	Festo	LRP-1/4-10	1
Precision Gauge	Festo	MAP-40-16-1/8-EN	1
Filter Regulator	Festo	LFR-1/4-D-MINI	1
Filter Cartridge	Festo	LFP-D-MINI-5M	1
Signal Conditioning Board with Terminal Blocks	NI	NI SCC-68	1
Data acquisition (DAQ) device (16-Bit, 250 kS/s)	NI	NI PCI-6221	1
LabView® Real Time software	NI	LabView® Real Time 8.4	1

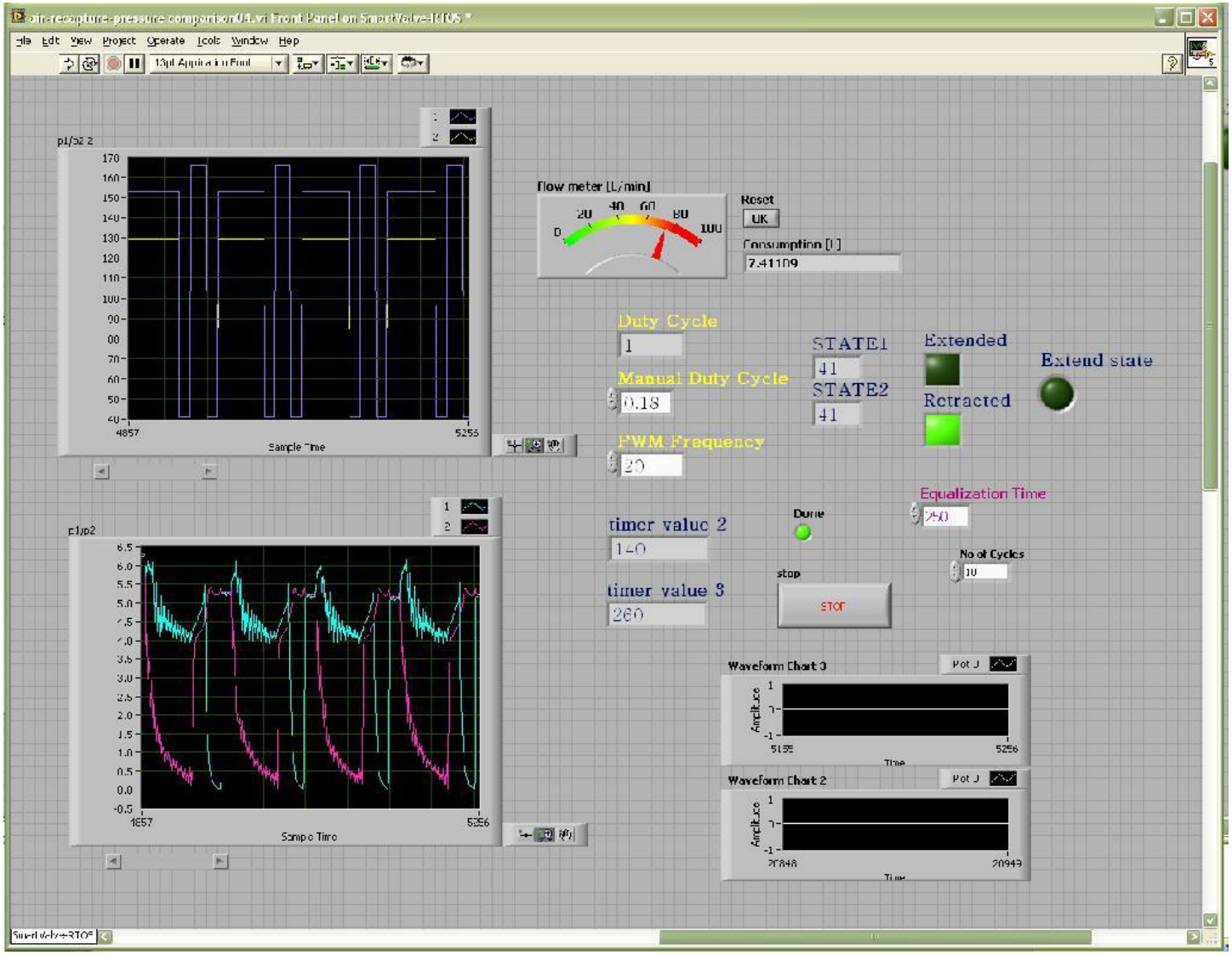

Figure 5.3: Sample front panel of a part of the code in LabView® environment.

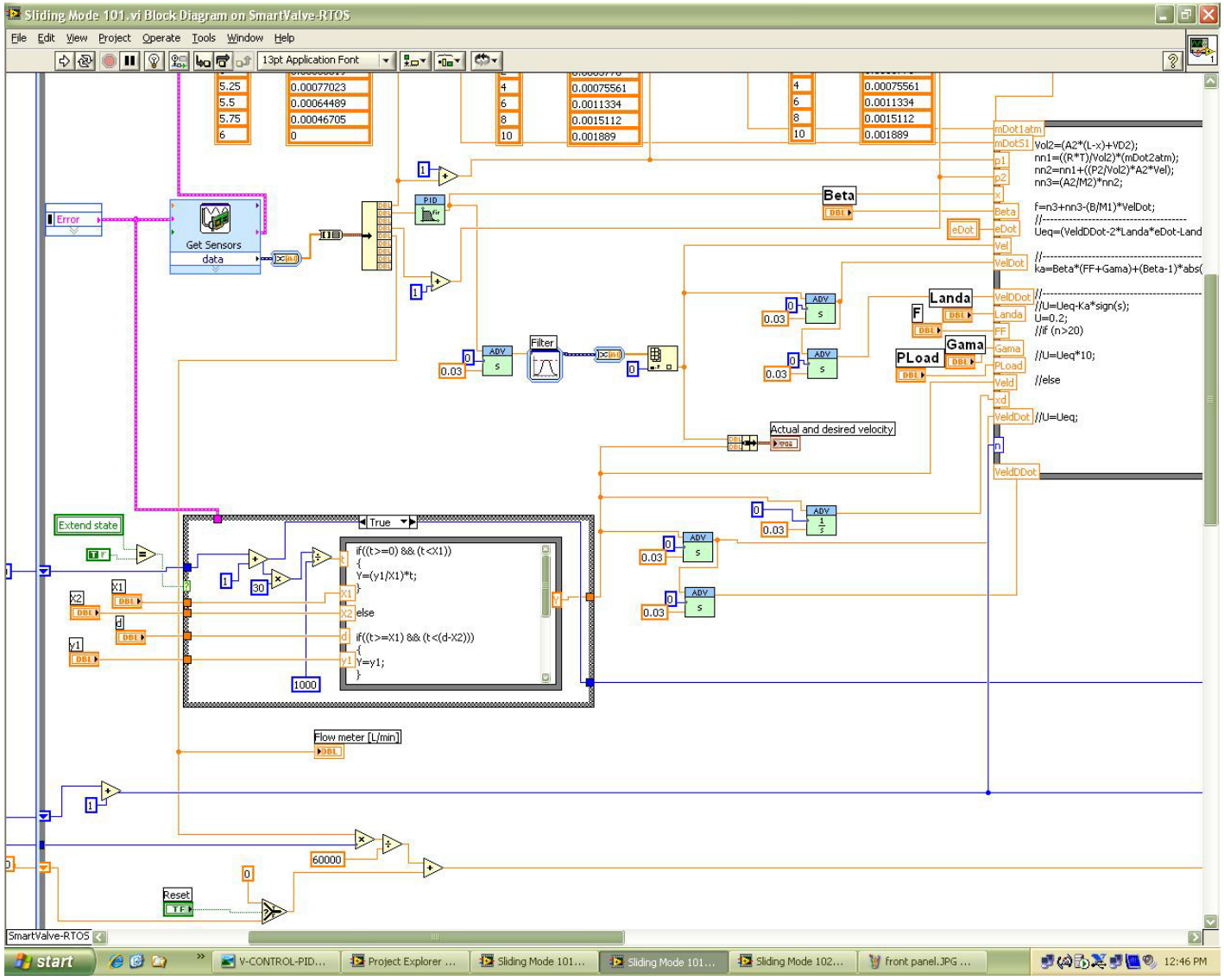

Figure 5.4: Sample code diagram of a part of the codein LabView® environment.

Load Mechanism

For industrial applications, pneumatic actuators are often used to manipulate objects and actuate tools; the load in these applications is usually inertial with some frictional components. It is difficult to conserve compressed air when the load is frictional. The test rig uses a second pneumatic cylinder acting in opposition to the main cylinder to provide a highly frictional load (the mass of the load is approximately 5 kg). In this structure, a load created by an identical cylinder, denoted by load actuator, was applied to the main cylinder, denoted by test actuator, via a coupling bar joining the piston rods of the cylinders. Figure 5.5 presents the mechanism.

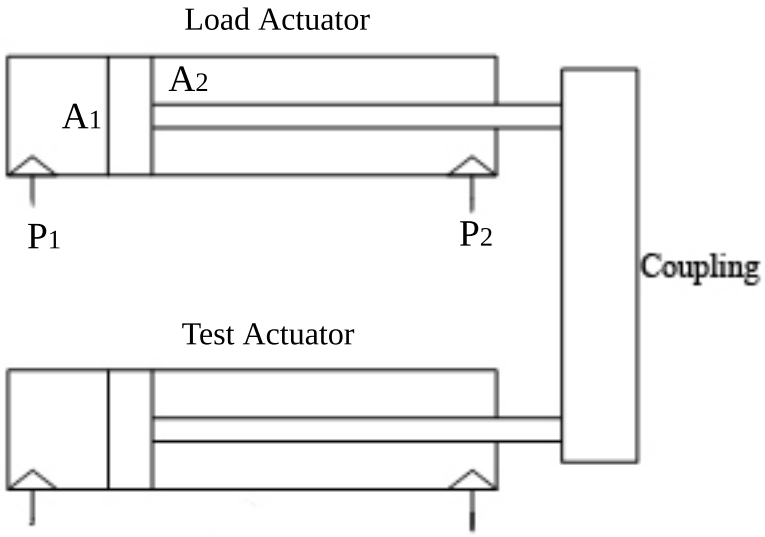

Figure 5.5: Load mechanism in the test rig.

The force generated by the load actuator can be described by the following equation:

$$F = P_1 A_1 - P_2 A_2 \tag{5.1}$$

where A_1 and A_2 are the cross sectional area of the bore-side and rod-side chambers respectively, and P_1 and P_2 are the pressures seen in each chamber. During the extension, when the bore side of the test actuator is connected to the pressure source, the rod side of the load actuator is pressurized to resist against the movement of the test actuator. P_2, which is connected to a pressure regulator, is chosen in a way that the load becomes equal to a certain force value based on Equation (5.1). The direction of the force will be changed during retraction by a 5/2 double solenoid valve; this valve is shown as S5 in figure 5.1.

5.3 Implementation

The strategies explained in the earlier chapter were implemented on the test rig. The structure of each method and the results will be provided in the following sections.

5.3.1 PWM and ABE (Accumulator-Based Equalization) Strategies

As explained in Section 3.2.1, the pressurized air is captured in the accumulator during equalization in ABE method. The air saved in the accumulator is used again in a timely fashion (PWM) during extension in order to reduce the air consumption.

Implementation of these methods in the modeling phase of the project had promising results; therefore, they were developed and evaluated on the test rig. Figure 5.6 depicts the detailed steps of the implementation of the methods on the test rig in one cycle.

The first diagram of Figure 5.6 presents the equalization stage in which both ports of the cylinder are connected to the accumulator. In the second diagram,

equalization has ended and extension has started. PWM signal is activated during the extension in a way that the input air is switched between accumulator and the main source. When the piston reaches the home position, equalization starts right before retraction (diagram 3).

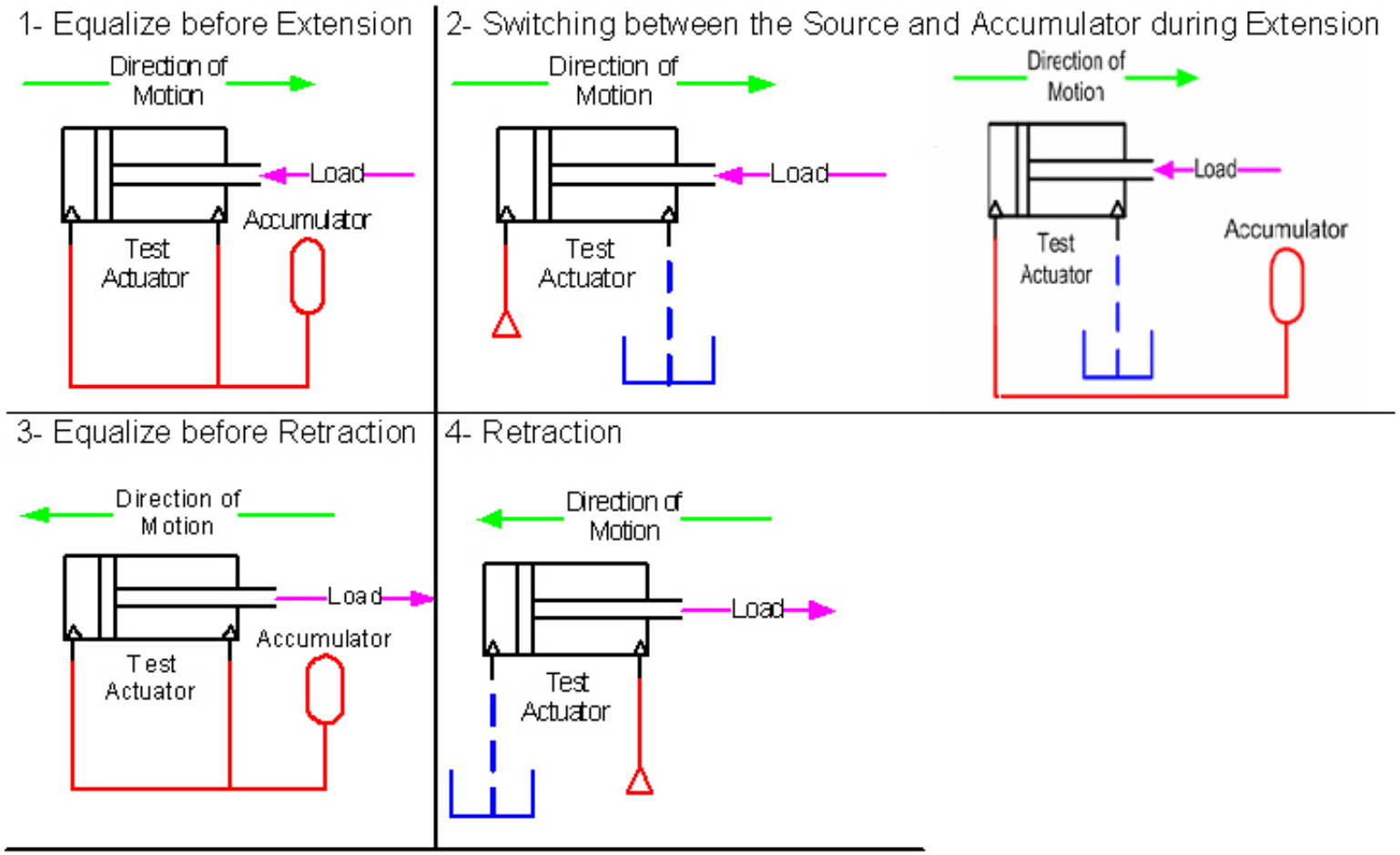

Figure 5.6: Development of ABE method on the test rig.

In the proposed system there were three distinct factors expected to be effective in saving energy: duty cycle, load, and equalization time. The combinations of these parameters in the algorithm were applied on the test rig; therefore, eight tests, were performed for five cyclces at frequency of 25Hz in a random order. The results are presented in Table 5.2.

Table 5.2: PWM and ABE method results on the test rig.

Duty Cycle (%)	**Equalization Time (mS)**	**Load (N)**	**Saving (%)**
25	300	120	25.5
50	300	120	13.8
25	600	120	24.9
50	600	120	13.6
25	300	220	13.07
50	300	220	5.3
25	600	220	12.7
50	600	220	4.9

The Effect of Equalization Time

According to the results provided in Section 4.5.2, an equalization time higher than 200 ms could not be considered as an effective factor in the air consumption in the modeling. As Table 5.2 shows, saving results for 25% duty cycle does not change considerably when load value remains the same and equalization time varies between 300 ms and 600 ms. Similar conclusion can be obtained from the results of applying 50% duty cycle on the system. The main reason is that the equalization happens more quickly. More details have been discussed in Section 4.5.2.

The Effect of Load

According to Table 5.2, air saving under the 220N load is smaller than that of 110 N load, with the same duty cycle value. Under the higher loads, the system must consume more energy to overcome the static friction and the load force; therefore, less air saving is expected in this case. The reason is that the smaller loads require less pressure force to initiate their motion. As soon as the force overcomes the static friction and inertia of the load, the motion starts. At this point, the chamber pressure has not necessarily reached the source pressure. On the other hand, when the piston reaches the end of cylinder, the source pressure is disconnected immediately; hence, the cylinder might not have enough time to reach the source pressure again. As a result, the motion is actuated with an average chamber pressure below the source pressure. Infact, the pressure is regulated by the duty cycle of the PWM.

The Effect of Duty Cycle

The effect of duty cycle was discussed in detail in Section 4.5.1. The consistency between the modeling and experimental results can be seen in the Table 5.2 as well. For example, a smaller duty cycle value of 25% achieves higher saving rate under the same load.

5.3.2 Ramp-Down Strategy

The load applied on the actuator has a significant effect on the performance of the system. As mentioned eariler, large initial forces are required to move highly inertial loads; however, once the load is in motion, only a small force is required to keep the load in motion. In other words, the static friction plus inertia force must be overcome by an applied force at the beginning of the piston movement; once the motion is initiated, piston can continue moving with less pressurized air. This observation provides the basis for ramp-down strategy.

Based on the mentioned fact, a high duty cycle value can be applied to the system to initiate motion. When the system starts moving forward, the duty cycle can be reduced. In this case, the system may consume more air in the first quarter of its displacement and much less air in the last quarter. The above hypothesis was validated by observing the results and comparing them to fixed duty cycle test results.

Figures 5.7 and 5.8 show the sample duty cycle profiles applied to the actual test rig under 110 N and 220 N load, respectively. As the figures show, the highest and lowest duty cycle were adjusted based on the load value. For example, the system under 220 N load started with 45% and reached the end with 20% duty cycle while these values for 110N load were 20% and 15%, respectively.

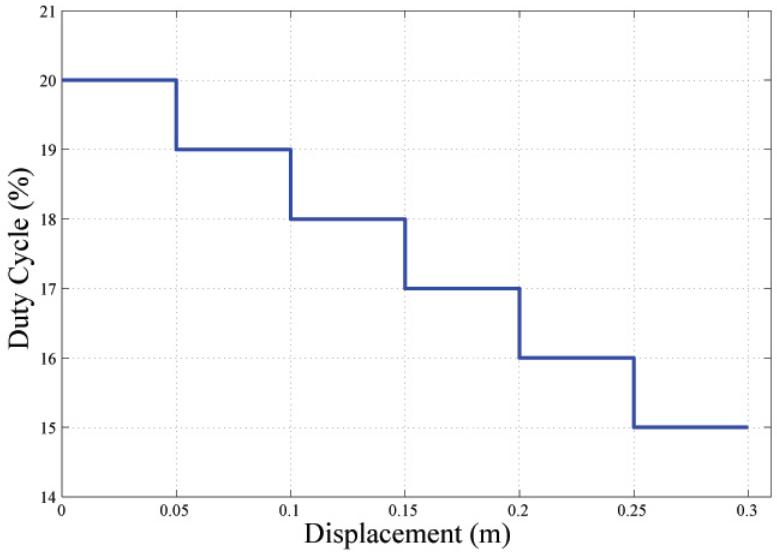

Figure 5.7: The sample duty cycle profile applied to the test rig under 110N.

Figure 5.9 compares the results of the tests performed under 120N and 220 N loads at frequency of 25 Hz. These results illustrate that the saving rate achieved by the ramp down strategy falls between the savings obtained from 25% duty cycle and 50% duty cycle under both 110 N and 220 N load values. The obtained results show that ramp down strategy gave the system the ability to move 120 N load

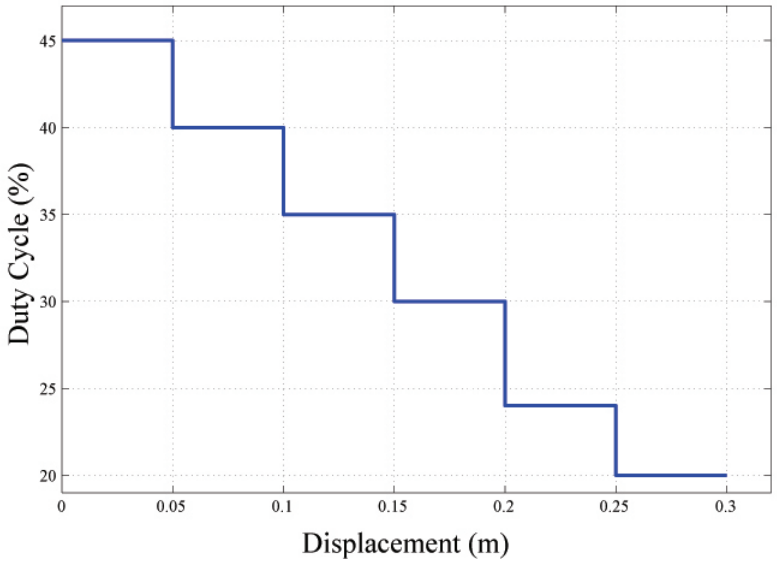

Figure 5.8: The sample duty cycle profile applied to the test rig under 220N.

with the duty cycle value as low as 15% when it is near the end of its motion while the movement could not be started with such a duty cycle value. Therefore, ramp down strategy can save more pressurized air compared to fixed-PWM method.

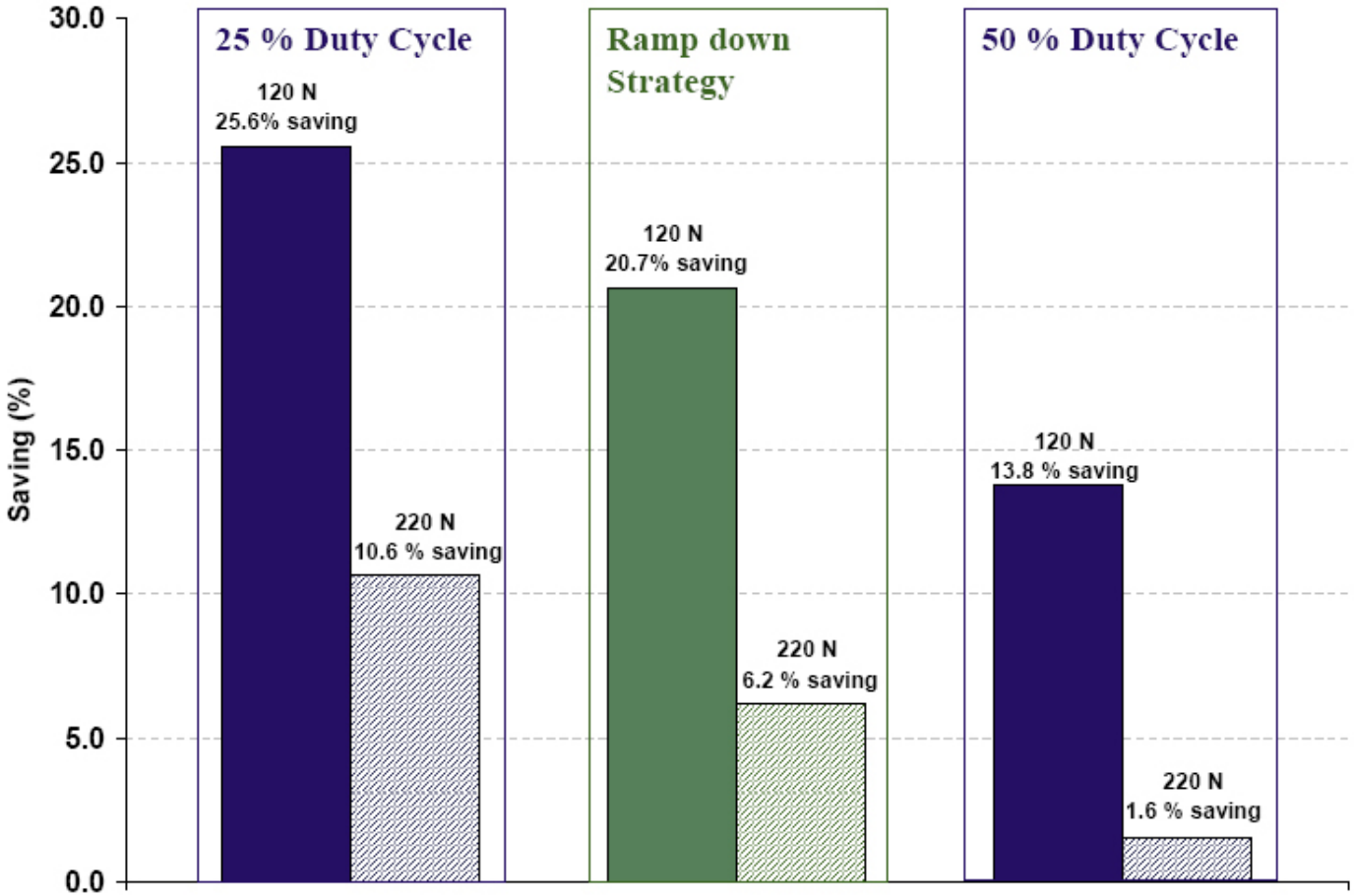

Figure 5.9: The air saving rate of the ramp down strategy compared with saving rates of the system run with fixed duty cycles under 120 N and 220 N load

Another important point observed during the tests was the smoothness of the piston movement during extension utilizing ramp down strategy, compared with the system motion run with fixed duty cycles. The switching nature of pulse width modulation signals, as the input of the system, results in a jerky motion behavior. This issue is more noticeable when the cylinder tries to move forward with low duty cycle under relatively high load value. This observation provides a foundation for designing an expert fuzzy controller presented in the following sections.

5.3.3 Expert-fuzzy System

The results obtained from the ramp down tests proved that applying a suitable duty cycle pattern results in a higher saving rate and a better actuator performance in comparison with the fixed PWM strategy. In order to improve the performance of the system and come up with even more saving, the necessity of designing a controller was felt.

As discussed before, fuzzy controllers are good candidates among many other available techniques because of their ability to control non-linear systems without the need of developing an accurate mathematical model. Considering the real pneumatic system which was highly non-linear and notoriously difficult to model mathematically, fuzzy-logic method was chosen to be the controller of this system. Two important parameters which had to be considered in designing the controller were velocity and duty cycle. Velocity was important because it provided a tool to analyze the smoothness of the movement. Duty cycle was important because it had a direct effect on the saving rate in the system.

In order to design a controller for the system two types of fuzzy controller were defined: fuzzy-expert system and error-based fuzzy controller. It is known that expert systems attempt to mimic the action of an experienced operator in controlling the system. The proposed expert system had to be able to adjust the system input (duty cycle) based on the feedback. In the experimental development the inputs to this controller were defined as position and velocity. The output was

duty cycle. The expert system was to generate the best duty cycle values, based on the real-time position and velocity feedback received from the test rig.

Figure 5.10 presents the membership functions developed for position variable in LabView® real time environment. The functions were presented as Retracted, Nearly Retracted, Middle, Nearly Extended, and Extended. Table 5.3 lists the position membership function bounds.

Figure 5.11 shows the velocity membership functions as Very Low, Low, Medium, High, and Very High. Table 5.4 presents the corresponding membership functions bounds. In addition, the output membership functions of the controller and their bounds are presented in Figure 5.12 and Table 5.5. In Table 5.5, the phrase "Just accumulator" is used for duty cycle values between zero and 4% while "Just Exhausted" is used when the output should be more than 88%.

Table 5.9 demonstrates the rule-base of this controller. The defined rules are based on the ramp down strategy in a way that if the position of the piston increases the input duty cycle should be decreased while the velocity should remain as smooth as possible. The rules are conjunctive. For instance, rule number one is formed as

```
IF Position is "Retracted" AND Velocity is "Very Low" THEN
Duty Cycle="Just Exhausted".
```

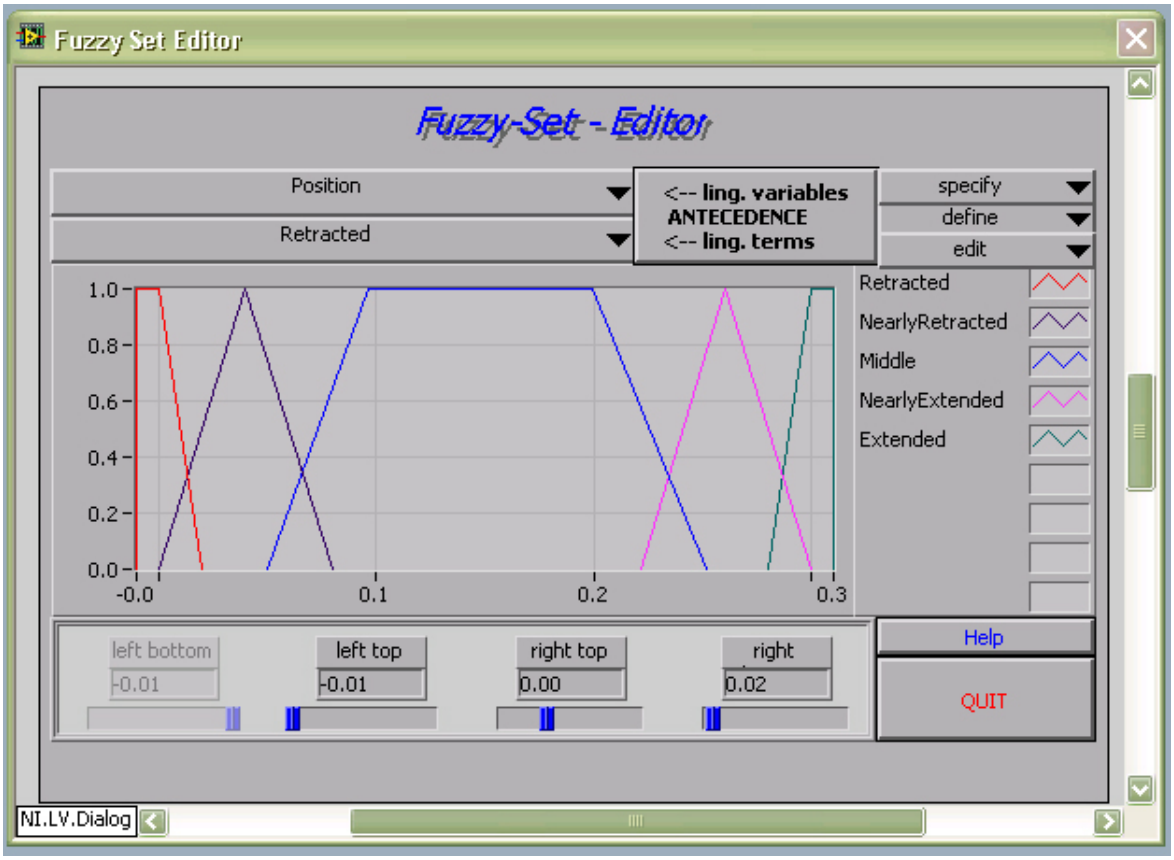

Figure 5.10: The position membership functions for the expert-fuzzy system in LabView® environment.

Table 5.3: The position membership function bounds for the expert-fuzzy system.

Position	**Bounds (cm)**			
	Left Bottomn	Left Top	Right Top	Right
Retracted	N/A	-1	+0.00	+2
Nearly Retracted	+0.00	+4	+4	+8
Middle	+5	+10	+20	+25
Nearly Extended	+22	+26	+26	+30
Extended	+28	+30	+31	N/A

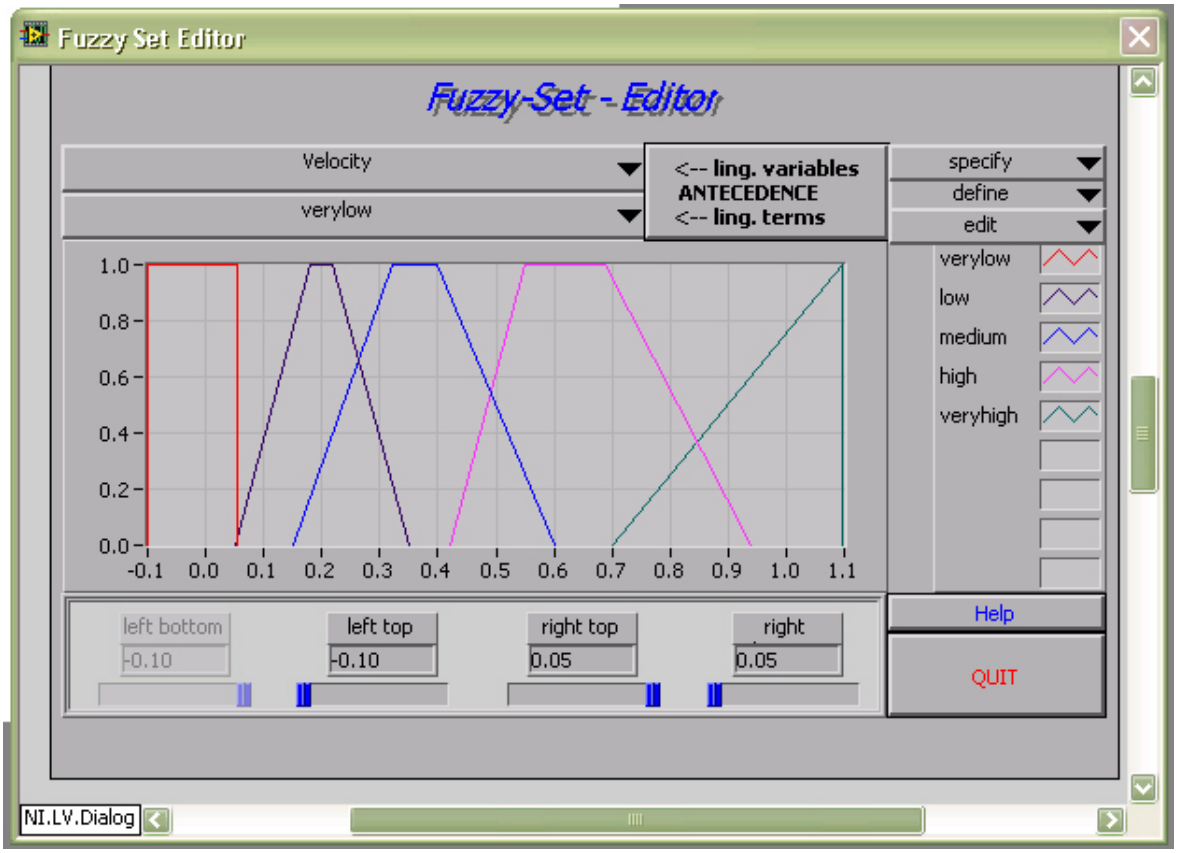

Figure 5.11: The velocity membership functions of the expert-fuzzy system in LabView® environment

Table 5.4: The velocity membership function bounds of the expert-fuzzy system.

Velocity	**Bounds (m/s)**			
	Left Bottom	Left Top	Right Top	Right
Very Low	N/A	-0.10	+0.05	+0.05
Low	+0.05	+0.18	+0.22	+0.35
Medium	+0.15	+0.32	+0.40	+0.60
High	+0.42	+0.55	+0.60	0.70
Very High	+0.70	+0.75	+1.10	+1.10

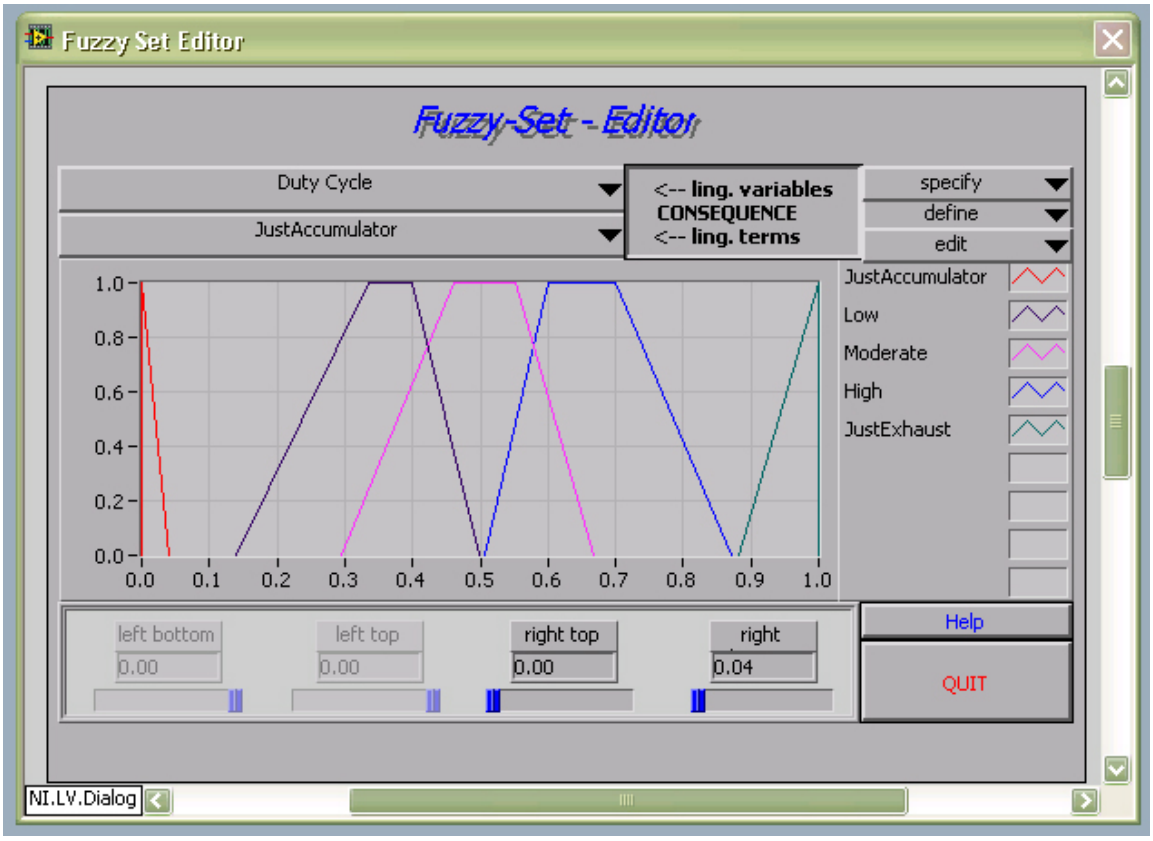

Figure 5.12: The duty cycle membership functions of the expert-fuzzy system in LabView® environment

Table 5.5: The duty cycle membership function bounds of the expert-fuzzy system

.

Duty Cycle	**Bounds (%)**			
	Left Bottom	Left Top	Right Top	Right
Just Accumulator	N/A	N/A	+0.00	4
Low	14	34	40	50
Moderate	29	46	55	67
High	51	60	70	87
Just Exhausted	88	100	N/A	N/A

Table 5.6: The rule-base of the expert-fuzzy controller.

Rule No.	**Position**	**Velocity**	**Duty Cycle**
1	Retracted	Very Low	Just Exhausted
2	Retracted	Low	High
3	Retracted	Medium	Moderate
4	Retracted	High	Moderate
5	Retracted	Very High	Just Accumulator
6	Nearly Retracted	Very Low	Just Exhausted
7	Nearly Retracted	Low	High
8	Nearly Retracted	Medium	Moderate
9	Nearly Retracted	High	Low
10	Nearly Retracted	Very High	Just Accumulator
11	Middle	Very Low	Just Exhausted
12	Middle	Low	Moderate
13	Middle	Medium	Low
14	Middle	High	Low
15	Middle	Very High	Just Accumulator
16	Nearly Extended	Very Low	Just Exhausted
17	Nearly Extended	Low	Moderate
18	Nearly Extended	Medium	Low
19	Nearly Extended	High	Just Accumulator
20	Nearly Extended	Very High	Just Accumulator
21	Extended	Very Low	Just Exhausted
22	Extended	Low	Low
23	Extended	Medium	Just Accumulator
24	Extended	High	Just Accumulator
25	Extended	Very High	Just Accumulator

5.3.4 Error-based Fuzzy Controller

As explained in Section 3.2.3, the error-based fuzzy controller reverts to the more traditional closed-loop control model in a way that it selects the output duty cycle, based on the error between the current velocity and the ideal extension velocity. Therefore, the controller attempts to modulate the PWM signal based on the difference between the desired velocity and the actual velocity. Figure 5.13 shows a sample reference velocity profile in the experimental test. This profile is a common velocity profile used in industry.

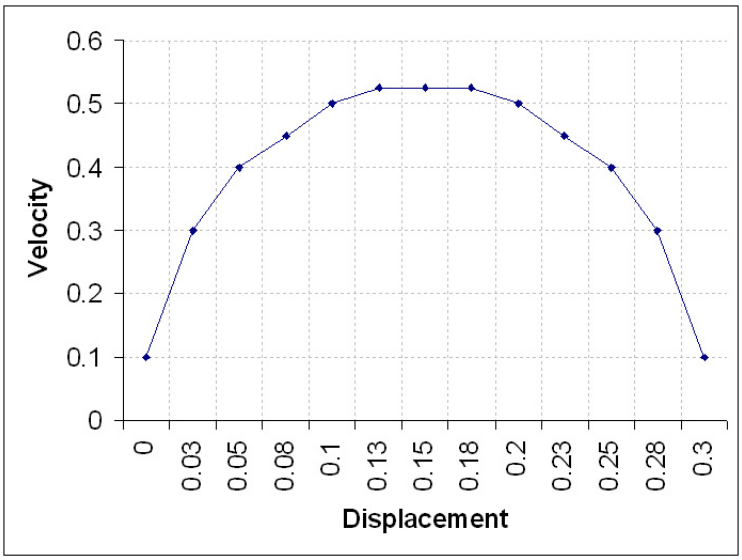

Figure 5.13: Reference velocity profile in error-based fuzzy controller.

Similar to expert-fuzzy controller, the defined input and output membership functions and their ranges are presented in Figures 5.14 and 5.15, and Tables 5.7, and 5.8, respectively.

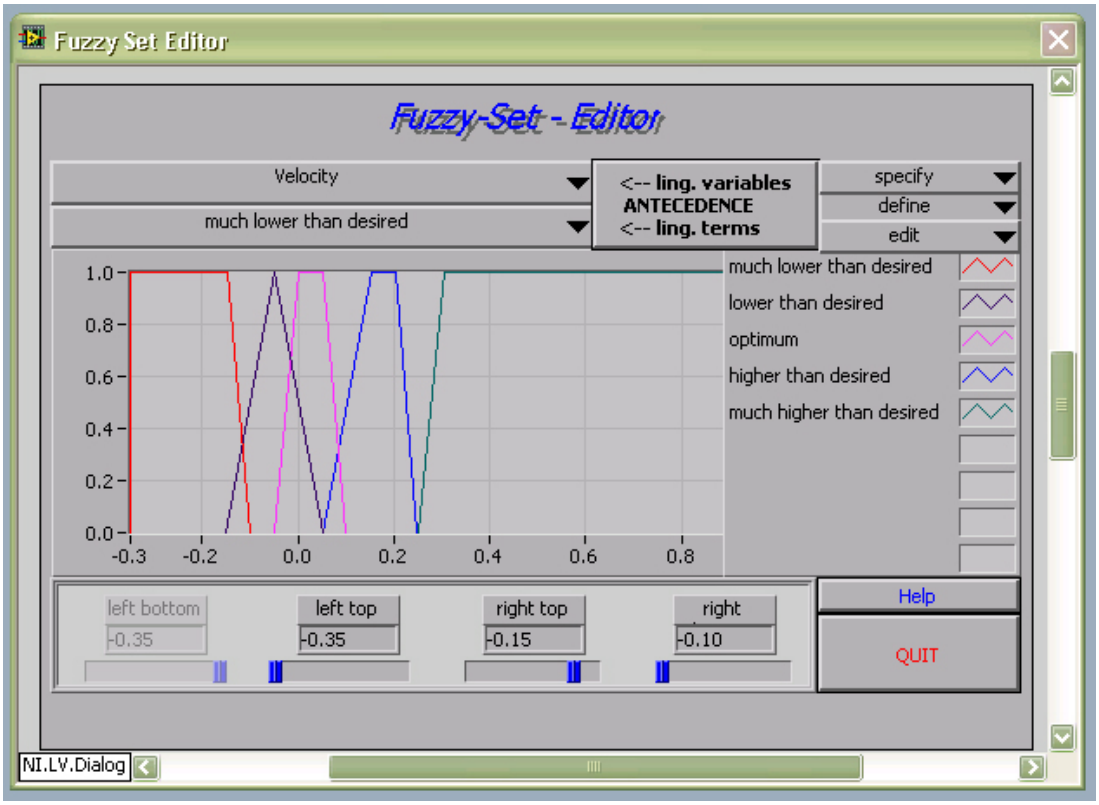

Figure 5.14: The input membership functions of the error-based fuzzy controller in LabView® environment

Table 5.7: The input membership function bounds of the error-based fuzzy controller.

Error	**Bounds (m/s)**			
	Left Bottom	Left Top	Right Top	Right
Much lower than desired	N/A	-0.35	+0.15	-0.10
Lower than desired	-0.15	-0.05	-0.05	+0.05
Optimal	-0.05	+0.00	+0.05	+0.10
Higher than desired	+0.05	+0.15	+0.20	0.25
Much higher than desired	+0.25	+0.30	+1.00	N/A

The duty cycle is again the controller output. The membership functions and their bounds are specified in Figure 5.15 and Table 5.8.

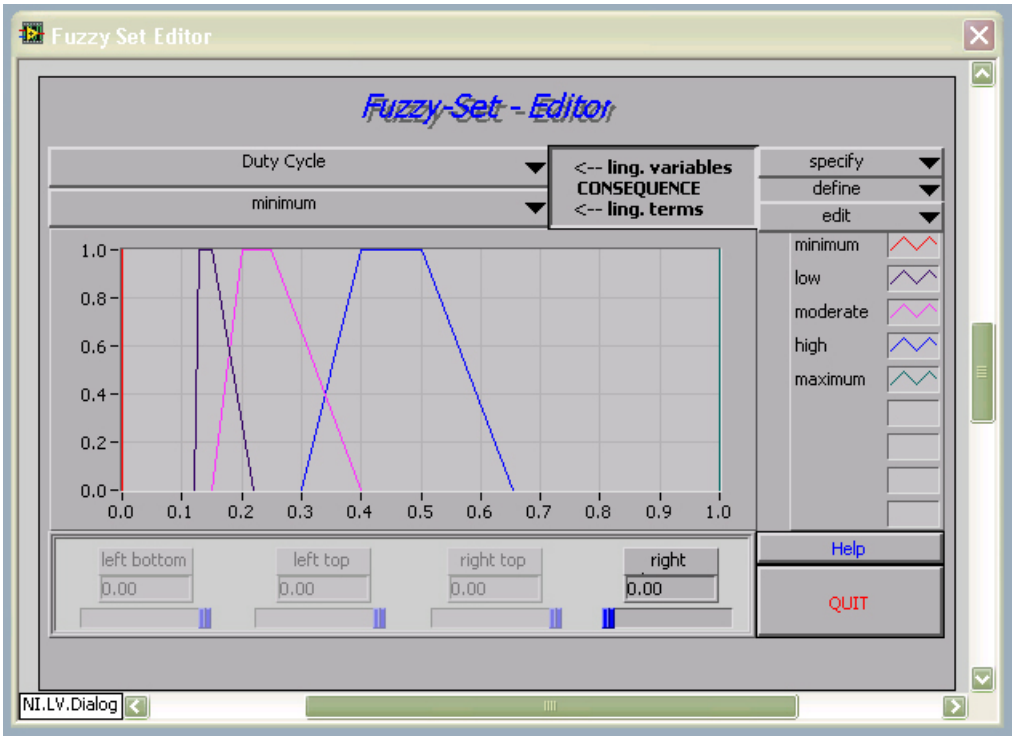

Figure 5.15: The duty cycle membership functions of the error-based fuzzy controller in LabView® environment

Table 5.8: The duty cycle membership function bounds of the error-based fuzzy controller.

Duty Cycle	**Bounds (%)**			
	Left Bottom	Left Top	Right Top	Right
Minimum	N/A	N/A	+0.00	+0.00
Low	12	13	15	22
Moderate	15	20	25	40
High	30	45	50	65
Maximum	100	N/A	N/A	N/A

The rule-base of this controller is presented in Table 5.9. In this rule-base, the output duty cycle is determined, based on the bounds of the error signal. The rules follow the simple IF-THEN format. For instance, rule number one is formulated as

```
IF Error is "Lower than Desired" THEN Duty Cycle="High".
```

Table 5.9: The rule-base of the expert-fuzzy controller.

Rule No.	**Error**	**Duty Cycle**
1	Much lower than desired	Maximum
2	Lower than desired	High
3	Optimal	Moderate
4	Higher than desired	Low
5	Much higher than desired	Minimum

5.3.5 Open-Loop System

After performing all the required tests on the tests rig, an approximate duty cycle profile was obtained from the fuzzy controllers, for different load values. The fuzzy controller proved that the generated duty cycle decreased the air consumption and made the system more robust with less jerky motions. These results will be provided in Section 5.4 in detail. As stated earlier, the elimination of any feedback in the system will result in the reduction in the overall cost of the system. Therefore, if applying the obtained duty cycle profiles to the open-loop system results in a saving energy rate close to that of the fuzzy controllers, an open-loop pneumatic system can be created with the capability of saving energy.

In order to prove the above statement, the duty cycle profiles obtained from the expert fuzzy controller approach were applied to the open-loop system, and the air

consumption and the smoothness of the movement were investigated. These results are discussed in Section 5.4.

Figure 5.16 shows the duty cycle profiles generated by the expert-fuzzy controller under different load values in one cycle. It should be noted cycle duration is longer when the load is heavier because the system needs more time to boost its interior pressure and move the load.

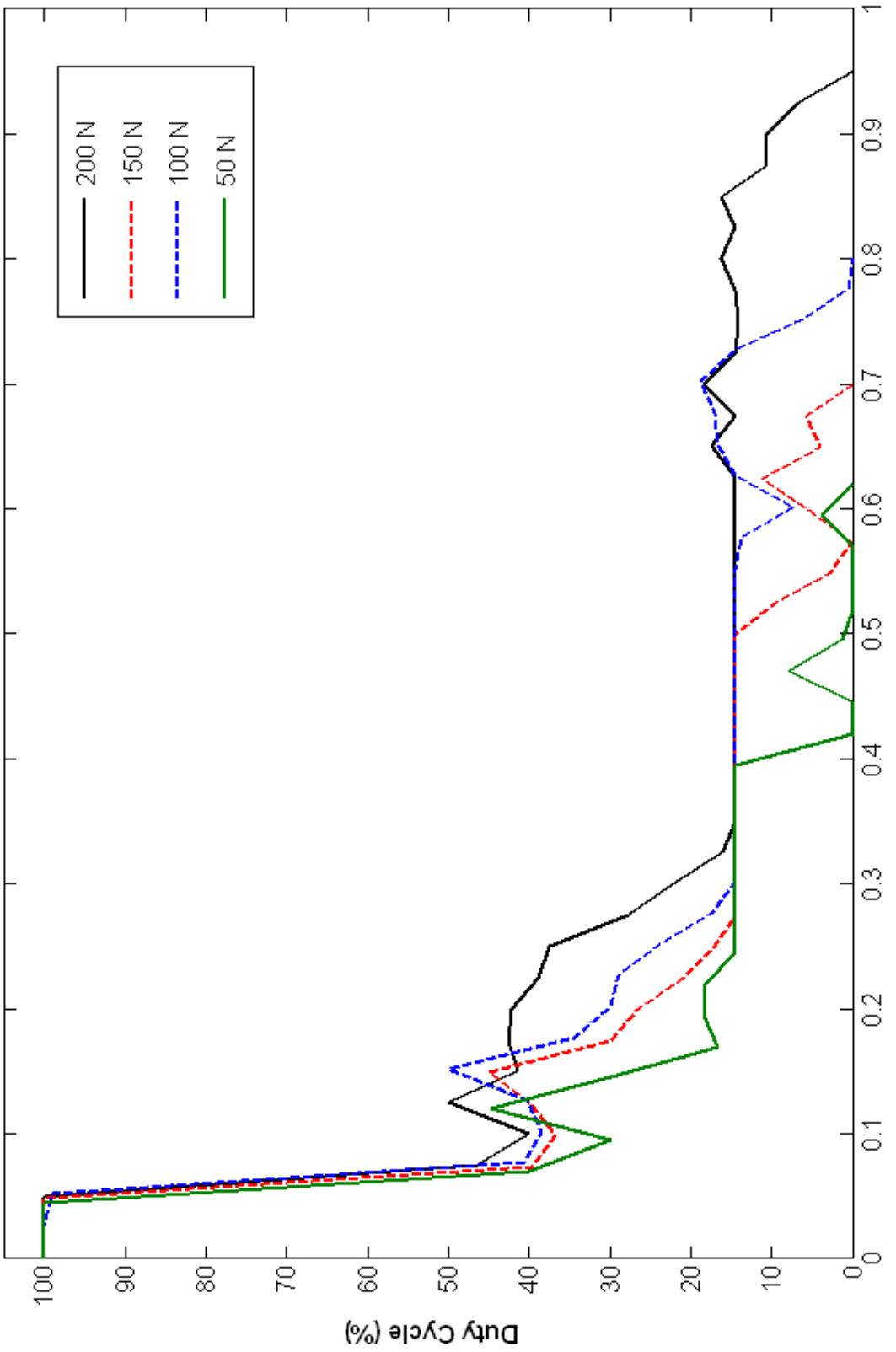

Figure 5.16: Duty Cycle profile of expert-fuzzy controller under different load conditions during extension.

5.4 Results

5.4.1 Air consumption

The air conservation rates achieved by the implemented methods are compared in Figure 5.17. An expected trend common to all the methods is obtained from the results; as the figure shows when the load is increased, less energy is saved. The figure reveals that the fuzzy controllers generally outperform other methods.

Between the two fuzzy controllers, the expert-fuzzy controller accomplished a higher rate of energy saving. That is why the expert-fuzzy method was chosen to collect the duty cycle patterns to be applied in the open-loop control system. The saving rate of the open-loop controller falls below the fuzzy controller, due to the lack of feedback. An interesting result is that the open-loop method exhibits a better performance than the lowest fixed PWM duty cycle of 25% with smoother movement as will be shown in Section 5.4.2.

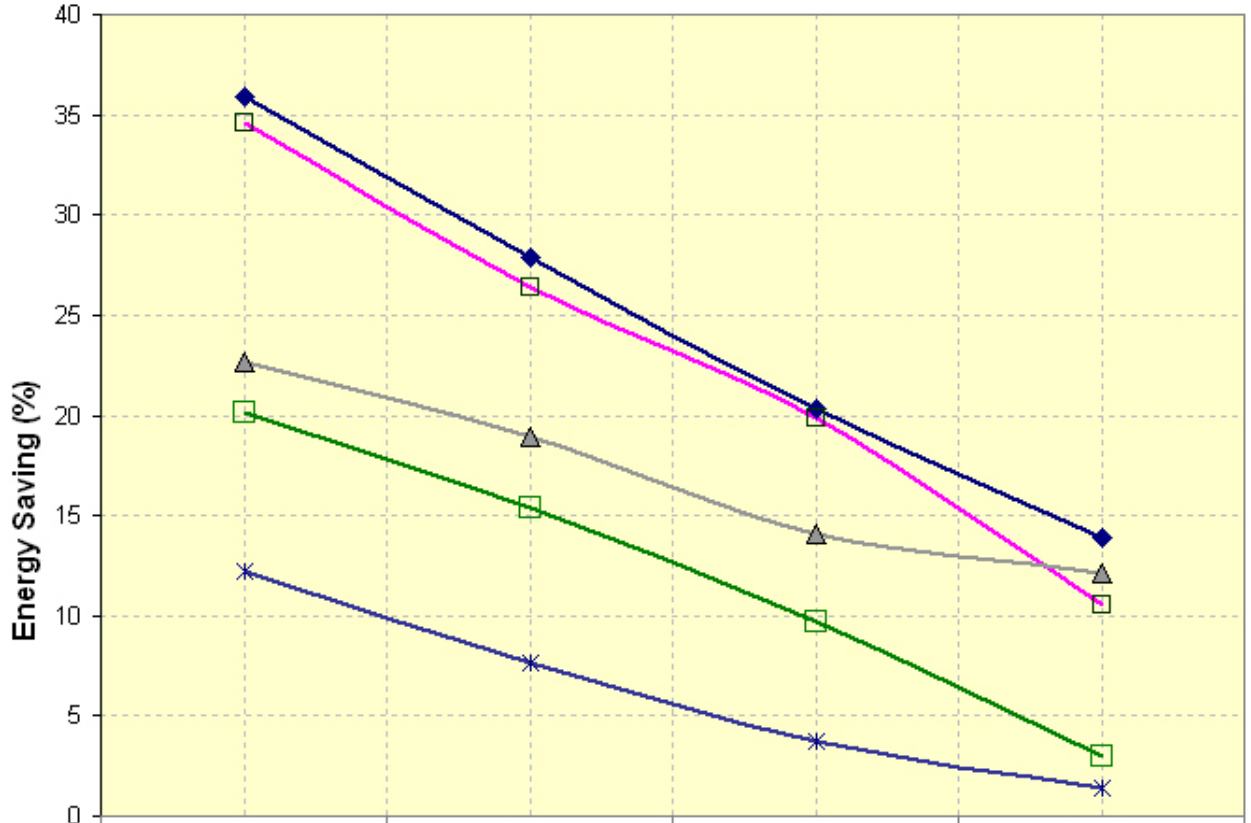

Load (N)	50	100	150	200
Expert-fuzzy Controller	35.89	27.85	20.36	13.89
Error-based Fuzzy Controller	34.61	26.40	19.84	10.57
25% Fixed Duty Cycle	22.63	18.93	14.05	12.13
50% Fixed Duty Cycle	12.19	7.66	3.71	1.43
Open Loop	20.17	15.36	9.72	3.01

Figure 5.17: Energy-saving comparison in the applied method on the test rig for five cycles.

5.4.2 Evaluation of Motion Smoothness

So far, the performance of ABE -PWM-based strategies were evaluated in terms of saving energy. The smoothness of motion is another important factor that should be considered in performance assessment of the methods.

To the best of the author's knowledge, there is no standard method for the measurement of motion smoothness. Therefore, a criterion to measure the smoothness of the movement was defined and called "Smoothness Index". This criterion was utilized to compare the smoothness of piston motion in different scenarios.

The switching nature of PWM signal as the input to the system causes an unsmooth or jerky movement in the system. Intuitively, it is expected that a jerky velocity profile contains several additional vibration modes compared to a smooth velocity profile.

To compare the smoothness of the different velocity profiles, the power spectral density (PSD) function was used which is defined as the distribution of signal power in the frequency domain. The area under PSD can serve as a measure of smoothness since it numerically represents the mean power of the velocity signal in frequency domain.

Unsmooth motion entails rapid changes in the velocity function; therefore, the energy delivered to the system is consumed to induce changes in the velocity in unsmooth motion, i.e. to induce acceleration or deceleration of the rod. This results in a lower average power of the velocity function. Consequently, the area under PSD reduces in jerky motion profiles. Conversely, smoother motion results in a larger PSD area. The area under PSD is called "Smoothness Index" which is formulated in Equation (5.2).

$$\varsigma = \frac{1}{f_{max}} \int_0^{f_{max}} |DFT(V(t))|^2 df \tag{5.2}$$

where ς is the smoothness index, f_{max} represents Nyquist frequency, and DFT is the Discrete Fourier Transform of piston velocity function $V(t)$.

In order to analyze the smoothness of the motion in the system, the velocity profile of various tests under different conditions were saved and evaluated and the area under their PSD profiles was calculated. Figure 5.18 presents the sample PSD profiles of the velocity of 50%-duty cycle method under 50N and 100 N loads. As seen, the area under PSD profile of 50N is higher than that of 100N which means the velocity profile of 50N has been smoother than that of 100 N.

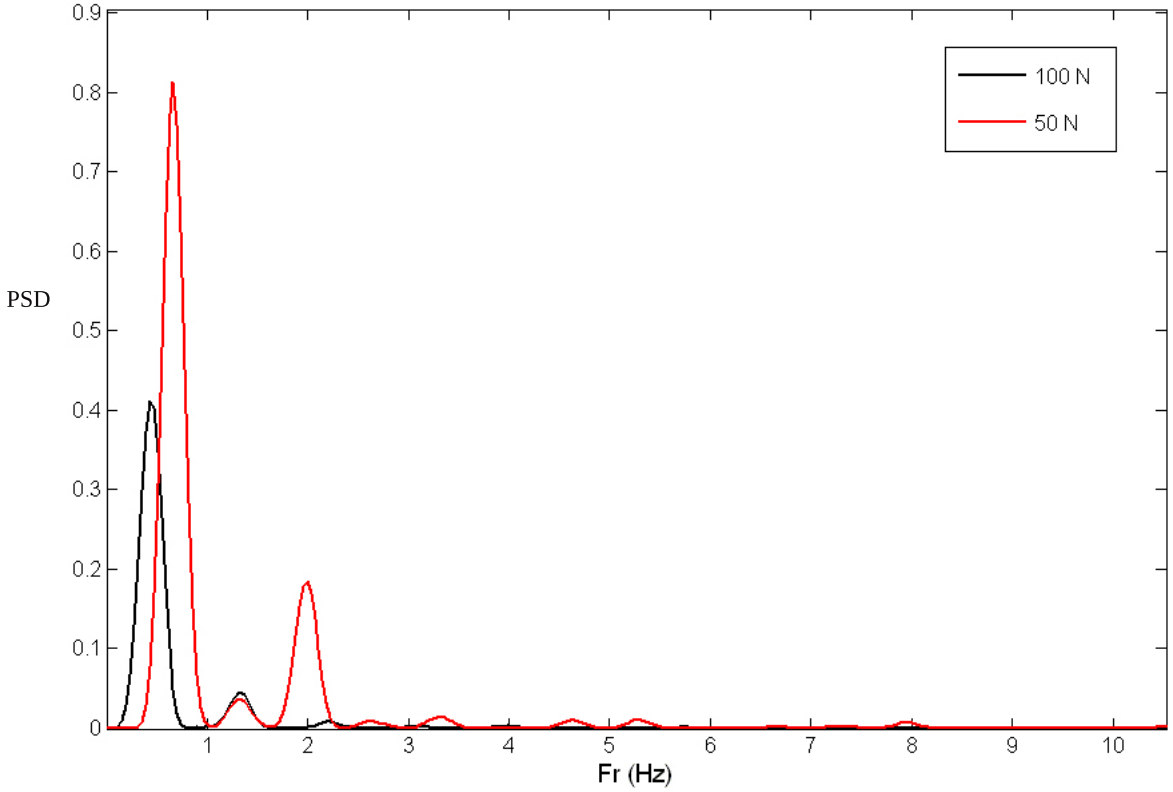

Figure 5.18: Power Spectral Density of the velocity profiles under 50N and 100 N load.

Figure 5.19 compares the smoothness index profiles obtained from different methods on the test rig. As seen in the figure, the smoothness index decreases under heavier loads. The "on and off" nature of PWM signal creates an intermittent force buildup to push the load. This means the movement under heavier loads cannot be as smooth as that of lighter loads because the system pressure should reach a certain pressure value to start moving.

Figure 5.19 also reveals that the movement is smoother when the duty cycle is higher. As explained in Section 5.3.1, when the duty cycle increases the system can connect to the source of pressure longer in each pulse period. Although in this case the system consumes more pressurized air, its movement is smoother because its chamber pressure has gained more pressurized air to push the load.

Investigation on the smoothness profiles of the two proposed methods, error-based and expert-fuzzy controller, shows that the error-based controller has smoother profile than the expert-fuzzy system. The main reason for this behavior could be the fact that in the error-based fuzzy controller, there is a reference velocity profile which the system is obliged to follow while in the expert fuzzy controller, the system is designed by the defined rules based on the feedback of position and velocity. In the expert-fuzzy controller, the velocity feedback was considered just to prevent the system from sudden stops in the middle of the motion.

The open-loop profile's smoothness is higher than that of 15% duty cycle, which is a promising result. From the author's point of view, by fine tuning of the open-loop system, the higher smoothness index is even obtainable.

As a conclusion, the error-based system cannot save energy as much as the expert-fuzzy controller because it tries to follow a reference profile and to control the velocity, while the expert-fuzzy controller is designed to save more pressurized air.

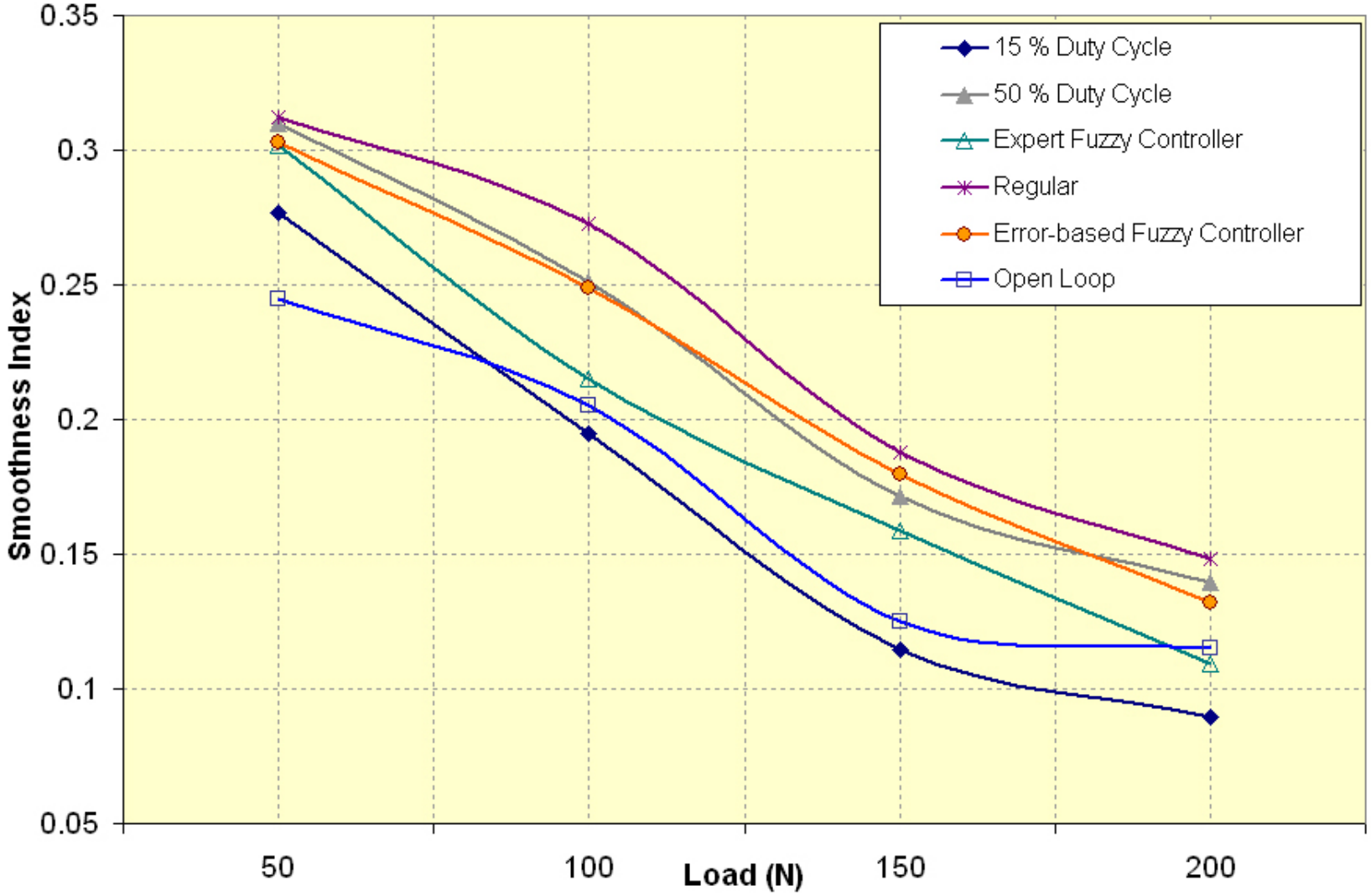

Figure 5.19: Smoothness Index under different load conditions in different controllers.

5.5 Design of an Integrated Valve System

While the test rig previously described serves well for the purposes of research and development, it was necessary to develop an integrated package that can be used in commercial applications[1]. This valve system is designed as a direct replacement for the valves that would normally control common pneumatic linear actuators.

The integrated package has two output ports that connect to the actuator and vents to bleed off unrecoverable air. A single potentiometer control allows operators to tune the PWM duty cycle once the system is installed. The system also takes inputs from two limit switches mounted at the home and limit positions.

As Figure 5.20 shows, the valve system itself consists of four elements: an accumulator, a rapid switching valve enabling PWM control during extension, a basic switching valve that controls the extension and retraction cycle to drive the actuator, and a logic controller which executes the energy-saving algorithm. Based on the testing, an accumulator of 4 cc is required. The rapid switching valve should toggle between the source pressure and the accumulator to drive the extension of the actuator given a PWM signal.

The minimum acceptable switching speed is 30Hz although higher frequencies offer smoother motion, quieter operation, and greater control bandwidth; this minimum was chosen because it was the fastest frequency possible on the test rig and the actuator motion was relatively smooth at this frequency. The basic switch component need only operate at 1 to 2 Hz as standard linear actuators usually require a least half a second to fully extend. This component redirects the source pressure between the two chambers of the actuator to enable retraction, extension, and equalization which occurs at the end of the actuators stroke.

Finally, a simple microcontroller as a well as some supporting electronics are needed to control both the basic and rapid switching elements using feedback from the limit switches to execute the energy-saving algorithm. The open-loop algo-

[1]This section was prepared by Ash Charls and Mihaela Vlasea

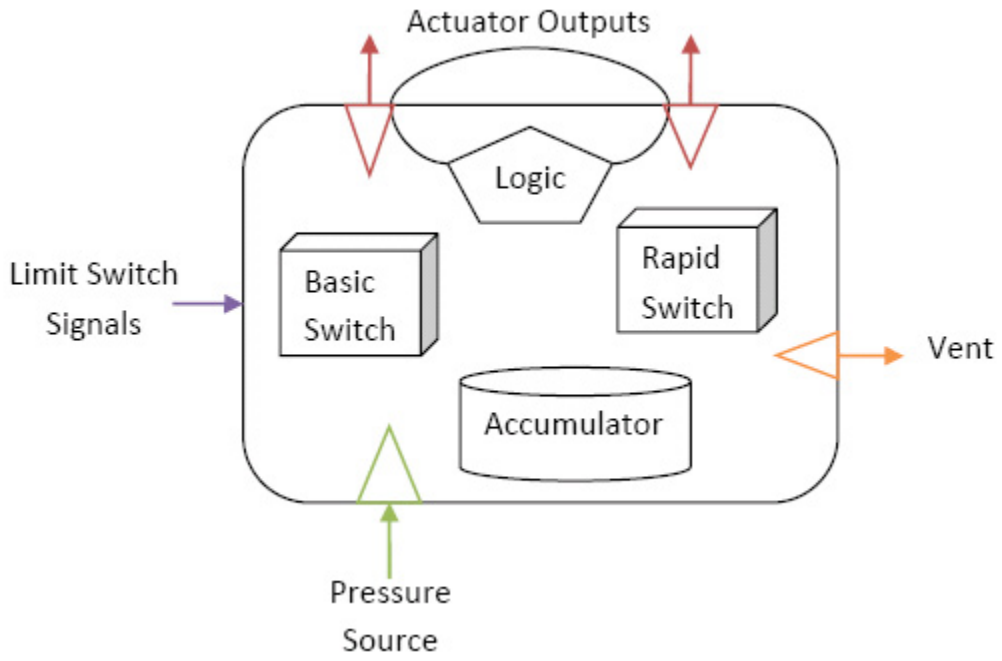

Figure 5.20: Valve system elements.

rithms described before still required feedback from the limit switches as well as user input that describes the degree of loading; this input should be provided via a tuning dial. The microcontroller would also be able to accept input from industrial PLCs etc. although this has not been implemented at this stage of development. Lastly, if the power or pressure supply were to fail, designs must return to an equalization state. This state is safe because the actuator can be freely moved and will not move if the power unexpectedly returns. Figure 5.21 shows the valve diagram.

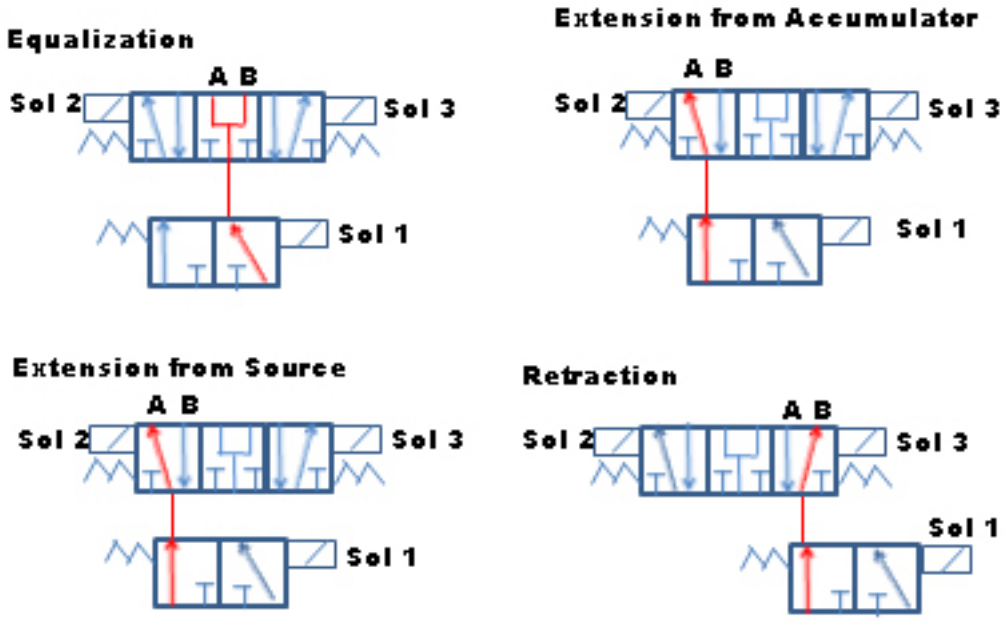

Figure 5.21: Valve diagram.

5.5.1 Integrated Valve

An integrated valve was proposed that packages off-the-shelf valves into a monolithic package alongside an accumulator and a microprocessor prototyping board. Specifically, a high-speed 3/2 valve provides the rapid switching capability to implement the PWM signalling while a standard 5/3 valve acts as the basic switching element. Each valve is selected specifically for its application which eliminates the problem of actuating a combined switching element. Table 5.10 presents the parts of the prototypical system.The user display listed is used to display the current load level however this is not an essential component. The switches on the microcontroller board are used for debugging and testing purposes. The performance of this valve is under investigation by other research team members. Figure 5.22 shows the system layout.

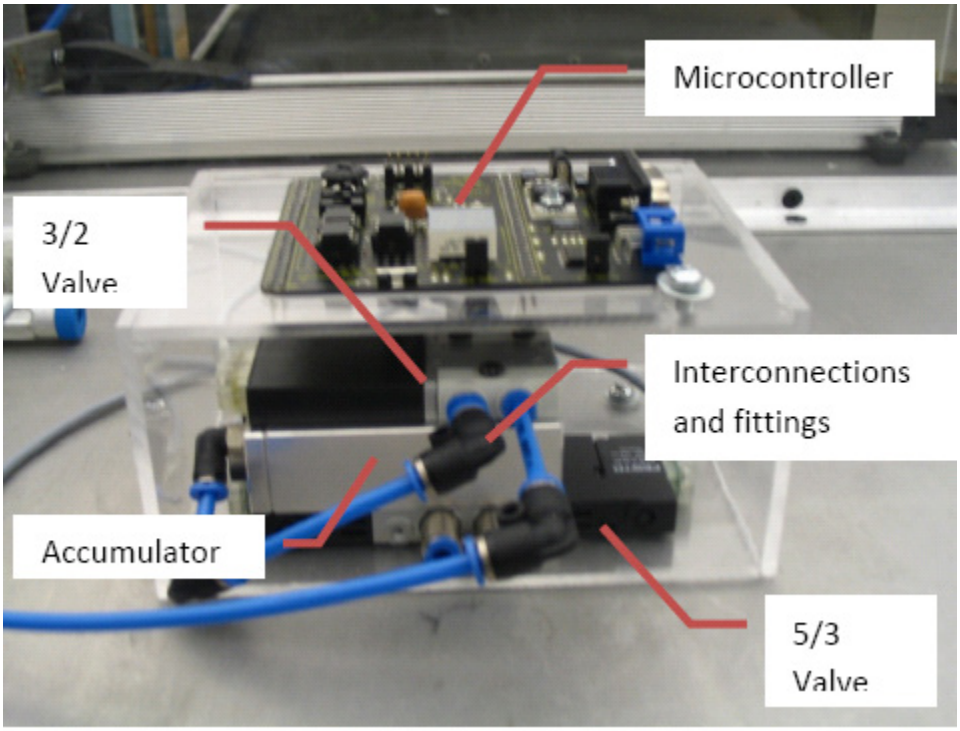

Figure 5.22: The system layout.

Table 5.10: The parts of the prototypical system.

Component	**Supplier**	**Part No.**	**Description**
Basic Switching Element	Festo	CPE10-M1BH-5/3B-M5-B	5/3 valve, centre position open, two solenoid with centring springs.
Rapid Switching Element	Festo	MHE2-MS1H-3/2O-QS-4	3/2 valve, Normally closed, 300Hz max., spring return.
Accumulator	custom part	N/A	4.5 cc volume, 4mm standard pneumatic connection.
Logic Controller	Zilog	Z8FMC16100	Motor controller prototyping board, one trim wheel, two switches, six PWM outputs.
User Display	Lumex	LDD-F304NI	Dual seven segment display, common cathode.
Solenoid Drivers	Panasonic	AQV202	High-frequency, Photo MOS, 40V opto-coupler.

Chapter 6

Conclusions

In this research project, an Accumulator-Based Equalization (ABE) strategy was combined with a knowledge-based PWM (Pulse Width Modulation) protocol and incorporated into an integrated solenoid valve, to increase the energy efficiency of pneumatic systems through the reduction of flow consumption.

The following conclusions can be drawn through this thesis:

1- Modeling and simulations of the proposed strategies were performed to assess the proposed ideas and reduce the cost of system developments. Based on the modeling results the simulated system was able to save almost 26% with 25% duty cycle and 14.5% with 50% duty cycle. These promising results in the modeling phase of the project justified the design and implementation of new strategies to be applied to the real system.

2- An experimental set-up was constructed to evaluate the performance of the proposed methods within the LabView® environment. During the equalization stage of control, the chambers of the pneumatic actuators were momentarily connected to each other to equalize the interior pressure of both side of the cylinder connected to an accumulator before starting the next stage. In addition, during the extension and retraction, a PWM signal was applied to the valves to switch between the accumulator and the supply air. This signal was the output of an expert-fuzzy controller, which was designed to save energy based on position and

velocity profiles of the system. Various tests were performed on the test rig with different duty cycles, loads, and equalization time values. The effect of each parameter was assessed based on the amount of energy saved. The results showed that the equalization time of more than 200 ms does not have a significant effect on the saving rate; therefore, this parameter was kept constant in the subsequent tests. Based on the presented results the system with fixed 50% duty cycle saved about 14% pressurized air under 120 N load while this value increased to almost 25% when 25% duty cycle was applied on the system under the same load.

3- The expert-fuzzy system and error-based fuzzy controller were evaluated based on the amount of energy saved. The saving rate of almost 27% under 100 N load and almost 14% under 200 N showed that the designed fuzzy controllers are capable of saving a reasonable amount of energy compared to the other applied methods. The main advantage of using these systems rather than fixed-duty cycle methods was their performance in terms of the smooth movement.

4- The algorithms performance was also evaluated in terms of motion smoothness. Unsmooth motion was more visible under heavier loads compared to lighter loads. A criterion was defined as "Smoothness Index" to determine the smoothness of the movement in each method. The results showed that 50% duty cycle and error-based fuzzy controller were the best in terms of smooth motion.

5- The last step was to apply the obtained duty cycle profiles from the expert-fuzzy controller to an open-loop system. The energy saving results of the open-loop system revealed that its saving rate was between 50%-duty cycle and 25%-duty cycle systems. For example, it could save 20% pressurized air under 50N load and almost 10% under 150 N load. In terms of smooth movement, this system was located between 15%-duty cycle system and the expert fuzzy controller.

As the final conclusion, the main objective of this research, which was saving energy without compromising the performance of the system, was obtained by step-by-step improvement of the proposed strategies. The fine tuning of the open-loop system is suggested to improve the performance in terms of saving and smooth

movement in the future. In addition, the proposed strategies can be applied to the integrated solenoid valve to effectively move toward the commercialization of the system.

References

[1] W. J. Thayer. Electropneumatic servoactuation – an alternative to hydraulics for some low power applications. *Fluid power National Educational Seminar*, 1:80–91, 1984. 1

[2] JL Shearer. Study of pneumatic processes in the continuous control of motion with compressed air-I. *Trans. ASME*, 78(2):233–242, 1956. 5

[3] JL Shearer. Study of pneumatic processes in the continuous control of motion with compressed air-II. *Trans. ASME*, 78(2):243–249, 1956. 5

[4] JL Shearer. Nonlinear analog study of a high pressure pneumatic servomechanism. *Trans. American Society of Mechanical Engineers*, 5:143–148, 1957. 5

[5] JJ Mannetje. Pneumatic Servo Design Method Improves System Bandwidth Twenty-fold. *Control Engineering*, 28(6):79–83, 1981. 6

[6] S. Liu and JE Bobrow. An analysis of a pneumatic servo system and its application to a computer-controlled robot. *TRANS. ASME J. DYN. SYST. MEAS. CONTROL.*, 110(3):228–235, 1988. 6

[7] D. Ben-Dov and SE Salcudean. A force-controlled pneumatic actuator. *Robotics and Automation, IEEE Transactions on*, 11(6):906–911, 1995. 6

[8] J.E. Bobrow and B.W. McDonell. Modeling, identification, and control of a pneumatically actuated, force controllable robot. *IEEE Transactions on Robotics and Automation*, 14(5):732–742, 1998. 6

[9] J. Wang, DJD Wang, PR Moore, and J. Pu. Modelling study, analysis and robust servo control of pneumatic cylinder actuator systems. *Control Theory and Applications, IEE Proceedings-*, 148(1):35–42, 2001. 6

[10] M. Karpenko and N. Sepehri. Design and experimental evaluation of a non-linear position controller for a pneumatic actuator with friction. *American Control Conference, 2004. Proceedings of the 2004*, 6:5078–5083, 2004. 6

[11] J. Wang, J. Pu, and P. Moore. A practical control strategy for servo-pneumatic actuator systems. *Control Engineering Practice*, 7(12):1483–1488, 1999. 7

[12] L. Guvenc. Closed loop pneumatic position control using discrete time modelregulation. *American Control Conference, 1999. Proceedings of the 1999*, 6:4273–4277, 1999. 7

[13] M. Hamdan and Z. Gao. A novel PID controller for pneumatic proportional valves with hysteresis. *Industry Applications Conference*, 1201:1198–1201, 2000. 7

[14] N. Gulati and EJ Barth. Non-linear pressure observer design for pneumatic actuators. *Advanced Intelligent Mechatronics. Proceedings, 2005 IEEE/ASME International Conference on*, pages 783–788, 2005. 7, 9

[15] AK Paul, JE Mishra, and MG Radke. Reduced order sliding mode control for pneumatic actuator. *Control Systems Technology, IEEE Transactions on*, 2(3):271–276, 1994. 7

[16] E. Richer and Y. Hurmuzlu. A High Performance Pneumatic Force Actuator System: Part INonlinear Mathematical Model. *Journal of Dynamic Systems, Measurement, and Control*, 122:416–425, 2000. 8, 35

[17] E. Richer and Y. Hurmuzlu. A High Performance Pneumatic Force Actuator System: Part IINonlinear Controller Design. *Journal of Dynamic Systems, Measurement, and Control*, 122:426–434, 2000. 8

[18] T. Acarman, C. Hatipoglu, and U. Ozguner. A robust nonlinear controller design for a pneumatic actuator. *American Control Conference, 2001. Proceedings of the 2001*, 6:4490–4495, 2001. 8

[19] SR Pandian, F. Takemura, Y. Hayakawa, and S. Kawamura. Pressure observer-controller design for pneumatic cylinder actuators. *Mechatronics, IEEE/ASME Transactions on*, 7(4):490–499, 2002. 8, 9

[20] P. Bigras and K. Khayati. Nonlinear observer for pneumatic system with non-negligible connection port restriction. *American Control Conference, 2002. Proceedings of the 2002*, 4:3191–3195, 2002. 8

[21] J. Wu, M. Goldfarb, and E. Barth. On the Observability of Pressure in a Pneumatic Servo Actuator. *Journal of Dynamic Systems, Measurement, and Control*, 126:921–924, 2005. 9

[22] N. Gulati and EJ Barth. Pressure observer based servo control of pneumatic actuators. *Advanced Intelligent Mechatronics. Proceedings, 2005 IEEE/ASME International Conference on*, pages 498–503, 2005. 10

[23] T. Noritsugu. Development of PWM mode electro-pneumatic servomechanism. I: Speed control of a pneumatic cylinder. *The Journal of fluid control*, 17(1):65–80, 1986. 10

[24] T. Noritsugu. Electro-pneumatic feedback speed control of a pneumatic motor. II: With a PWM operated on-off valve. *The Journal of fluid control*, 18(2):7–21, 1986. 10

[25] C. Kunt and R. Singh. A linear time varying model for on-off valve controlled pneumatic actuators. *Journal of dynamic systems, measurement, and control*, 112(4):740–747, 1990. 10

[26] N. Ye, S. Scavarda, M. Betemps, and A. Jutard. Models of a pneumatic PWM solenoid valve for engineering applications. *Journal of dynamic systems, measurement, and control*, 114(4):680–688, 1992. 10

[27] M.C. Shih and C.G. Hwang. Fuzzy PWM control of the positions of a pneumatic robot cylinder using high speed solenoid valve. *JSME international journal. Series C, dynamics, control, robotics, design and manufacturing*, 40(3):469–476, 1997. 11, 13

[28] RB van Varseveld and GM Bone. Accurate position control of a pneumatic actuator using on/offsolenoid valves. *Mechatronics, IEEE/ASME Transactions on*, 2(3):195–204, 1997. 11

[29] A. Gentile, NI Giannoccaro, and G. Reina. Experimental tests on position control of a pneumatic actuator using on/off solenoid valves. *Industrial Technology, 2002. IEEE ICIT'02. 2002 IEEE International Conference on*, 1:555–559, 2002. 11

[30] K.K. Ahn, S.M. Pyo, S.Y. Yang, and B.R. Lee. Intelligent control of pneumatic actuator using LVQNN. *Science and Technology, 2003. Proceedings KORUS 2003. The 7th Korea-Russia International Symposium on*, 1:269–266, 2003. 11

[31] A. Messina, N.I. Giannoccaro, and A. Gentile. Experimenting and modelling the dynamics of pneumatic actuators controlled by the pulse width modulation (PWM) technique. *Mechatronics*, 15(7):859–881, 2005. 11

[32] EJ Barth, J. Zhang, and M. Goldfarb. Sliding mode approach to PWM-controlled pneumatic systems. *American Control Conference, 2002. Proceedings of the 2002*, 3:2362–2367, 2002. 12, 35

[33] E.J. Barth, J. Zhang, and M. Goldfarb. Control Design for Relative Stability in a PWM-Controlled Pneumatic System. *Journal of Dynamic Systems, Measurement, and Control*, 125:504–508, 2003. 12

[34] X. Shen, J. Zhang, EJ Barth, and M. Goldfarb. Nonlinear averaging applied to the control of pulse width modulated (PWM) pneumatic systems. *American Control Conference, 2004. Proceedings of the 2004*, 5:4444–4448, 2004. 12

[35] X. Shen, J. Zhang, E.J. Barth, and M. Goldfarb. Nonlinear Model-Based Control of Pulse Width Modulated Pneumatic Servo Systems. *Journal of Dynamic Systems, Measurement, and Control*, 128:663, 2006. 12

[36] E.E. Topçu, İ. Yüksel, and Z. Kamış. Development of electro-pneumatic fast switching valve and investigation of its characteristics. *Mechatronics*, 16(6):365–378, 2006. 12

[37] G. Mattiazzo, S. Mauro, T. Raparelli, and M. Velardocchia. Control of a six-axis pneumatic robot. *Journal of Robotic Systems*, 19(8):363–378, 2002. 13

[38] X. GAO and Z.J. FENG. Design study of an adaptive Fuzzy-PD controller for pneumatic servo system. *Control engineering practice*, 13(1):55–65, 2005. 13

[39] M. Sano and T. Fujita. An effective tuning method of fuzzy controllers in pneumatic servosystem. *Fluid Power, Proceedings of Second JHPS International Symposium on Fluid Power (Ed. T. Maeda)*, pages 731–736, 1993. 13

[40] S. Scavarda. Some theoretical aspects and recent developments in pneumatic positioning systems. *Fluid Power, Proceedings of Second JHPS International Symposium on Fluid Power (Ed. T. Maeda)*, pages 29–48, 1993. 13

[41] T. Matsui, E. Ishimoto, and M. Takawaki. Learning position control of a pneumatic cylinder using fuzzy reasoning. *Journal of Fluid Control*, 20(3):7–29, 1990. 13

[42] T. Raparelli and M. Velardocchia. Fuzzy control of pneumatic servomechanism by on-off and PWM digital valves: a general method. *Proc Int Conf Automation, Milano*, page 263, 1993. 13

[43] M. Parnichkun and C. Ngaecharoenkul. Kinematics control of a pneumatic system by hybrid fuzzy PID. *Mechatronics*, 11(8):1001–1023, 2001. 13

[44] Z. Situm, D. Pavkovic, and B. Novakovic. Servo Pneumatic Position Control Using Fuzzy PID Gain Scheduling. *Journal of Dynamic Systems, Measurement, and Control*, 126:376, 2004. 14

[45] S. Chillari, S. Guccione, and G. Muscato. An experimental comparison between several pneumatic positioncontrol methods. *Decision and Control, 2001. Proceedings of the 40th IEEE Conference on*, 2:1168–1173, 2001. 14

[46] *United Nations Environment Programme*, 1997. 14

[47] Frank Graves and Christian Boucher. Public Attitudes Towards the Kyoto Protocol. *Ekos Research Associates*, 2005. 14

[48] Mich. Farmington. Efficient use of compressed air makes sense and cents. *Hydraulics and Pneumatics*, 59(8):38–43, 2006. 15

[49] WK Clayton. Improving pneumatics bottom line. *Machine Design*, 78(3):80–84, 2006. 15

[50] TC Li, HW Wu, and MJ Kuo. A Study of Gas Economizing Pneumatic Cylinder. *Journal of Physics: Conference Series*, 48(1):1227–1232, 2006. 16

[51] F.E. Sanville. Two-level Compressed Air Systems for Energy Saving. *The 7th International Fluid Control Symposium*, pages 375–383, 1986. 16

[52] J. Pu, JH Wang, PR Moore, and CB Wong. A New Strategy for Closed-loop Control of Servo-Pneumatic Systems with Improved Energy Efficiency and System Response. *The Fifth Scandinavian International Conference on Fluid Power*, pages 339–352, 1997. 16

[53] G. Granosik and J. Borenstein. Minimizing air consumption of pneumatic actuators in mobile robots. *Robotics and Automation, 2004. Proceedings. ICRA'04. 2004 IEEE International Conference on*, 4:3634–3639, 2004. 17

[54] J. Wang, DJD Wang, and VK Liau. Energy efficient optimal control for pneumatic actuator systems. *Journal of Systems Science*, 26(3):109–123, 2001. 17

[55] Y. Kawakami, Y. Terashima, and S. Kawai. Application of energy-saving to pneumatic driving system. *Fluid Power, Forth JHPS International Symposium*, 11:201–206, 1999. 17

[56] Y. Terashima, Y. Kawakami, T. Arinaga, and S. Kawai. An Approach for Energy-saving of Pneumatic Cylinders by Meter-in Circuit. *in Proceedings of the 1st FPNI-PhD Symposium*, pages 49–56, 2000. 18

[57] D. Margolis. Energy Regenerative Actuator for Motion Control With Application to Fluid Power Systems. *Journal of Dynamic Systems, Measurement, and Control*, 127:33, 2005. 18

[58] D.L. Margolis, M.R. Jolly, W.R. Schroeder, M.C. Heath, and D.E. Ivers. Regenerativer system including an energy transformer which requires no external power source to drive same, October 1996. US Patent 5,570,286. 18

[59] K.A. Al-Dakkan, E.J. Barth, and M. Goldfarb. Dynamic Constraint-Based Energy-Saving Control of Pneumatic Servo Systems. *Journal of Dynamic Systems, Measurement, and Control*, 128:655, 2006. 18

[60] K.A. Al-Dakkan, M. Goldfarb, and EJ Barth. Energy saving control for pneumatic servo systems. *Advanced Intelligent Mechatronics, 2003. AIM 2003. Proceedings. 2003 IEEE/ASME International Conference on*, 1:284–289, 2003. 18

[61] X. Shen and M. Goldfarb. Energy Saving in Pneumatic Servo Control Utilizing Interchamber Cross-Flow. *Journal of Dynamic Systems, Measurement, and Control*, 129:303, 2007. 19

[62] Ryan Bachmann. On the dynamics of pneumatic positioning systems. Master's thesis, Queen's University, 1997. 22

[63] K.M. Passino and S. Yurkovich. *Fuzzy control*. Addison-Wesley Menlo Park, Calif, 1998. 29